

Ecomorphodynamic feedbacks and barrier island evolution, Virginia Coast
Reserve, USA

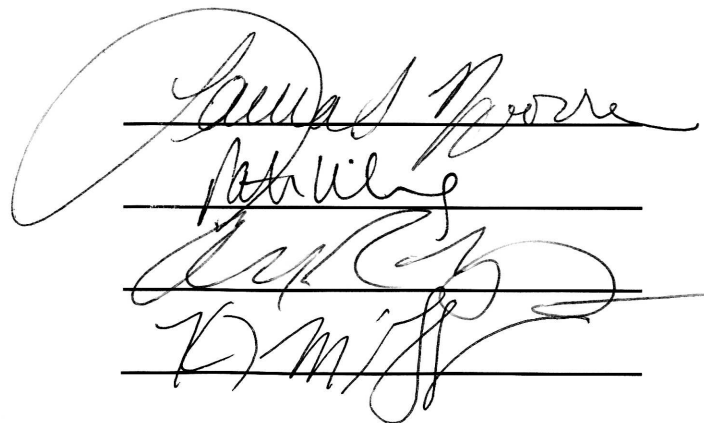
Catherine Wallace Vaccaro Wolner
Columbus, Ohio

B.A., Oberlin College, 2008

A Thesis Presented to the Graduate Faculty
of the University of Virginia in Candidacy for the Degree of
Master of Science

Department of Environmental Sciences

University of Virginia
August, 2011



Four handwritten signatures are written on four horizontal lines. The signatures are: 1. A large, flowing signature that appears to be 'James Moore'. 2. A signature that appears to be 'Phillip'. 3. A signature that appears to be 'John'. 4. A signature that appears to be 'D. Miss'.

ABSTRACT

Ecomorphodynamic feedbacks play an important role in barrier island response to disturbance. Dune-building grasses like *Ammophila breviligulata* can restore areas of high relief after overwash events (resisting disturbance); however, if overwash recurs before dunes have reestablished, overwash-adapted “maintainer” species like *Spartina patens* (upright var.)—which preserve low, flat topography—may preferentially survive, thereby increasing the likelihood of future overwash (reinforcing disturbance). Over time, this positive feedback may lead to overwash persistence. We explore the potential influence of the maintainer feedback on two morphologically distinct islands in the Virginia Coast Reserve (VCR), located on the U.S. mid-Atlantic coast.

Combined topographic and vegetation surveys show that on Hog Island (high-relief, rotating, infrequently disturbed), where dunes dominated by *A. breviligulata* are ubiquitous, overwash is currently limited in extent and related to beach width rather than dominance by *S. patens*. Historical aerial photos and stratigraphic evidence (ground-penetrating radar, cores) indicate that gradual recovery has taken place after overwash events on Hog Island, except where the beach is narrow and eroding. Conversely, on Metompkin Island (low-relief, transgressing, frequently disturbed), overwash is widespread and dominated by *S. patens*, particularly along the rapidly migrating northern half of the island (where shell armoring is also prevalent). Results also suggest that spatially heterogeneous disturbance patterns on Metompkin Island may increase vegetative compositional variability relative to Hog Island. Finally, overwash has generally been more prevalent and persistent over time on Metompkin Island than on Hog Island. In aggregate, our findings suggest that within barrier island systems like the

VCR in which both dune-building grasses and overwash-adapted maintainer species are common, the maintainer feedback is likely to be a more important dynamic on islands that are already susceptible to frequent disturbance due to physical and geological factors. The maintainer feedback therefore has the potential to accelerate large-scale shifts from dune-dominated to overwash-dominated barrier morphologies as overwash becomes more frequent as a result of climate change-induced increases in storm intensity and sea level rise.

ACKNOWLEDGEMENTS

This research was truly a collaborative effort, and there are a number of people without whom it would not have been possible. First, I would like to thank my advisor, Laura Moore, for her invaluable guidance and support throughout the development and implementation of this project. I would also like to thank my committee members, Karen McGlathery, Pat Wiberg, and Don Young, for their helpful advice and feedback. I am especially indebted to Steven Brantley and Spencer Bissett for their crucial collaborative roles in the ecological aspects of this research, as well as to Randy McBride for so generously sharing his vibracoring expertise and immense knowledge of coastal geology. Mike Wilson and Bryan Watts at the Center for Conservation Biology provided the database used in aerial photo analyses.

I am very grateful to the staff of the Anheuser-Busch Coastal Research Center and the staff of the Eastern Shore Laboratory for extensive logistical support in the field. I would also like to thank Owen Brenner, Luke Cole, Dana Oster, Sean McLoughlin, Nick Brockmeier, and especially Meredith Weakley for field and laboratory assistance, as well as Aaron Mills for providing core pipe. Finally, I would like to thank my labmates, officemates, friends, and family for their encouragement and support.

Access to field sites was made possible by the Virginia Coast Reserve Long-Term Ecological Research (VCR LTER) site, The Nature Conservancy, and U.S. Fish and Wildlife Services. Funding for this work was provided by the U.S. Department of Energy's National Institute for Climatic Change Research (NICCR), the Geological Society of America, and the Department of Environmental Sciences at the University of Virginia.

TABLE OF CONTENTS

Abstract	ii
Acknowledgements	iv
Table of contents	v
List of figures and tables	vi
1. Introduction	1
Background	1
Regional setting	7
2. Methods	11
Relating vegetation and morphology: transect surveys	11
Assessing overwash persistence: aerial photo and stratigraphic analyses	16
3. Results	21
Transect surveys	21
Vegetation and morphology	21
Beach width	27
Sediment properties	29
Historical analyses	33
Aerial photos	33
Ground-penetrating radar	37
Cores	47
4. Discussion	59
Vegetation dynamics	59
Physical dynamics	63
Synthesis and implications	67
5. Conclusions	73
References	76
Appendix 1: Study area background	81
1.1 Attributes of common strand species in the Virginia Coast Reserve	81
1.2 Morphological evolution of Hog and Metompkin Islands	82

Appendix 2: Field and laboratory methods.....	87
2.1 GPS surveys.....	87
2.2 Sediment sample preparation and analysis.....	88
2.3 Ground-penetrating radar (GPR) surveys.....	90
2.4 Vibracoring apparatus.....	93
2.5 Core processing and interpretation.....	94
Appendix 3: Supplementary data summaries.....	96
3.1 Spearman correlations.....	96
3.2 Sediment properties.....	97
3.3 Aerial photo features.....	99
3.4 Unedited GPR profile, S. Metompkin Island.....	100
Appendix 4: Core descriptions and interpretation.....	101

LIST OF FIGURES AND TABLES

Figure 1.1	Images of dune and overwash vegetation.....	5
Figure 1.2	Ecomorphodynamic conceptual models.....	5
Figure 1.3	Scenarios for ecomorphodynamic response to disturbance.....	6
Figure 1.4	Map of the Eastern Shore of Virginia.....	9
Figure 1.5	Morphological features of Hog and Metompkin Islands.....	10
Figure 2.1	Map of study sites on Hog and Metompkin Islands.....	15
Figure 3.1	Cross-shore profiles and characteristics of transect sites.....	24
Figure 3.2	Species frequency by morphologic environment.....	25
Figure 3.3	Indicator Species Analysis results.....	26
Figure 3.4	Correlation of beach width and mean elevation.....	28
Figure 3.5	Comparison of sediment properties by island.....	30
Figure 3.6	Grain size distribution by site on Hog Island.....	31
Figure 3.7	Grain size distribution by site on Metompkin Island.....	31
Figure 3.8	Shell gravel content by site on Metompkin Island.....	32
Figure 3.9	Shorelines and overwash zones over time.....	35
Figure 3.10	Overwash area and overlap over time.....	36
Figure 3.11	Example ground-penetrating radar (GPR) facies.....	39
Figure 3.12	GPR profiles from southern Hog Island.....	41

Figure 3.13	GPR profiles from northern Hog Island	43
Figure 3.14	GPR profiles from southern Metompkin Island	45
Figure 3.15	Map of core locations	50
Figure 3.16	Schematic of Hog Island core interpretations	51
Figure 3.17	Photo and interpretation of core HI B-2010-1	52
Figure 3.18	Photo and interpretation of core HI C-2010-1	53
Figure 3.19	Photo and interpretation of core HI X-2010-1	54
Figure 3.20	Schematic of Metompkin Island core interpretations.....	55
Figure 3.21	Photo and interpretation of core MI E-2010-1	56
Figure 3.22	Photo and interpretation of core MI C-2010-3	57
Figure 3.23	Photo and interpretation of core MI C-2010-2	58
Figure 4.1	Expanded ecomorphodynamic conceptual models	72
Table 3.1	Comparison of sediment properties by site.....	30

1. INTRODUCTION

Background

Barrier islands are characterized by low elevations, unconsolidated substrates, and high sensitivity to changes in sea level and storm activity. As a result, these coastal landscapes tend to be disturbance-prone, dynamic systems in which sediment is frequently redistributed and, consequently, ecosystems exhibit considerable variability. Physical parameters such as elevation above sea level and distance from the shoreline determine the frequency of overwash disturbance on barrier islands, which in turn influences the composition and distribution of the ecological communities that these landscapes support (e.g., Fahrig et al., 1994; Hayden et al., 1995). As sea level rise accelerates (Church and White, 2006; IPCC, 2007) and storms potentially become more intense (Komar and Allan, 2007; Bender et al., 2010; Knutson et al., 2010), overwash events on barrier islands will likely become more common, with closely linked morphological and ecological implications.

Overwash typically occurs when storm surge and wave runup combine to overtop the dune or berm crest (Sallenger, 2000), leveling the existing topography and spreading sediment into the backbarrier. The process of overwash is crucial in determining whether barrier islands will survive under conditions of rising sea level: sediment transport by overwash facilitates landward migration, which can help a barrier maintain its elevation relative to sea level (e.g., Hayden et al., 1980). However, if sea level rises too rapidly, sediment supply is insufficient, or topographic recovery is inhibited by recurrent overwash, a barrier island may not be able to adjust quickly enough, ultimately disintegrating as sea level rise progresses.

Barrier islands vary in their susceptibility and response to overwash, depending in part on their morphological and vegetative characteristics. For example, high-relief barrier islands tend to be dominated by dune-building grasses like *Ammophila breviligulata* (Figure 1.1a). Like other dune-building grasses, *A. breviligulata* prefers high topographic roughness and aids vertical accretion by trapping sand, thereby expanding its own preferred habitat in a positive feedback. On the northeastern U.S. coast, for instance, *A. breviligulata* builds characteristically tall, continuous dunes (facilitated by the guerrilla growth style of its vertically- and laterally-propagating rhizomes), restricting large-scale overwash events to only the most severe storm conditions (i.e., resisting disturbance). In the relatively rare event that overwash does occur, recolonization by *A. breviligulata* leads to the reestablishment of the dune horizon (Godfrey et al., 1979; Leatherman and Zaremba, 1987), given sufficient sand supply.

In contrast, barrier islands that are characterized by low, discontinuous, or absent dunes are susceptible to frequent overwash. Where these low-relief barriers occur on the southeastern U.S. coast, the strand grass *Spartina patens* (upright var.) tends to dominate the widespread overwash flats that result from recurrent disturbance (Godfrey et al., 1979; Figure 1.1b). *S. patens* is especially well-adapted for overwash: it can regenerate upwards through thick deposits of overwashed sand (Ehrenfield, 1990), in addition to being tolerant of saline flooding (Silander and Antonovics, 1979) and thriving in wetter soils (i.e., lower elevations on barrier islands). *S. patens* does not contribute significantly to dune building, but rather maintains low, flat topography by stabilizing the sediment surface (e.g., Stallins, 2005; Godfrey and Godfrey, 1976) with its turf-like mat of roots and rhizomes. Godfrey et al. (1979) proposed that while the dominance of *A.*

breviligulata in high-relief barrier systems contributes to disturbance resistance, the dominance of *S. patens* in low-relief barrier systems reinforces frequent disturbance by maintaining low topographic roughness. Similarly, Stallins and Parker (2003) and Stallins (2005) suggested a positive feedback in which overwash-adapted species that do not build dunes may be more successful under conditions of repeated disturbance, promoting the maintenance of low-relief topography by rendering sand unavailable for dune building, and thereby increasing the likelihood of overwash during even moderate storms—which, in turn, further favors the dominance of these overwash-adapted species.

Thus, while physical factors are the primary determinants of disturbance frequency on barrier islands, the two opposing ecomorphodynamic feedbacks described above also contribute to disturbance resistance (via dune building) and disturbance reinforcement (via overwash maintenance), respectively (Figure 1.2). These feedbacks have been compared separately in distinct barrier systems (e.g., Godfrey et al., 1979; Stallins and Parker, 2003) that vary not only physically and ecologically but also in disturbance-forcing conditions (e.g., hydrodynamics, climate). However, they have not been considered within a single barrier island chain where *A. breviligulata* is the dominant dune-building species, but overwash-adapted “maintainer” species like *S. patens* are also common.

In such systems, we hypothesize that the dune-builder feedback is likely to be the primary ecomorphodynamic influence on barrier morphology when disturbance is rare, because dune-building grasses like *A. breviligulata* can effectively create high-relief habitat for themselves in the absence of disturbance. As disturbance frequency increases, however, we hypothesize that the relative importance of the maintainer feedback will

increase as well, because overwash-adapted maintainer species are likely to preferentially survive repeated disturbance events (as long as disturbance frequency does not become so high that *no* vegetation can survive); ultimately, dominance by maintainer species resulting from more frequent disturbance may effectively lengthen the time needed for dune recovery, not only by decreasing the space available for dune-building grasses, but also by limiting the availability of sand for aeolian transport (Figure 1.3). Over time scales of decades to centuries, the balance between these feedbacks will likely influence large-scale morphological characteristics by contributing (along with external physical drivers) to the development or maintenance of topography, thereby modulating or intensifying barrier island response to climate change.

To evaluate our hypothesis that the maintainer feedback is more likely to be playing a role where disturbance occurs more frequently, we assess the relationship between morphology and vegetative species composition, as well as the spatial (100s of m to km) and temporal (decadal to centurial) persistence of overwash zones on two morphologically distinct barrier islands in the Virginia Coast Reserve (VCR), located on the mid-Atlantic coast of the U.S. Establishing a conclusive, quantifiable relationship between vegetation composition and long-term overwash persistence is beyond the power of the techniques employed in this study; however, identifying a relationship between the presence of overwash and the dominance of maintainer species that is spatially consistent with evidence of overwash persistence will allow us to infer where and under what conditions the maintainer feedback is likely to be at work in the VCR, as well as in other, similar barrier island systems.



Figure 1.1. a) Tall, continuous dunes built by *A. breviligulata*. b) Overwash flats stabilized by *S. patens* (photo: R. McBride, 2010).

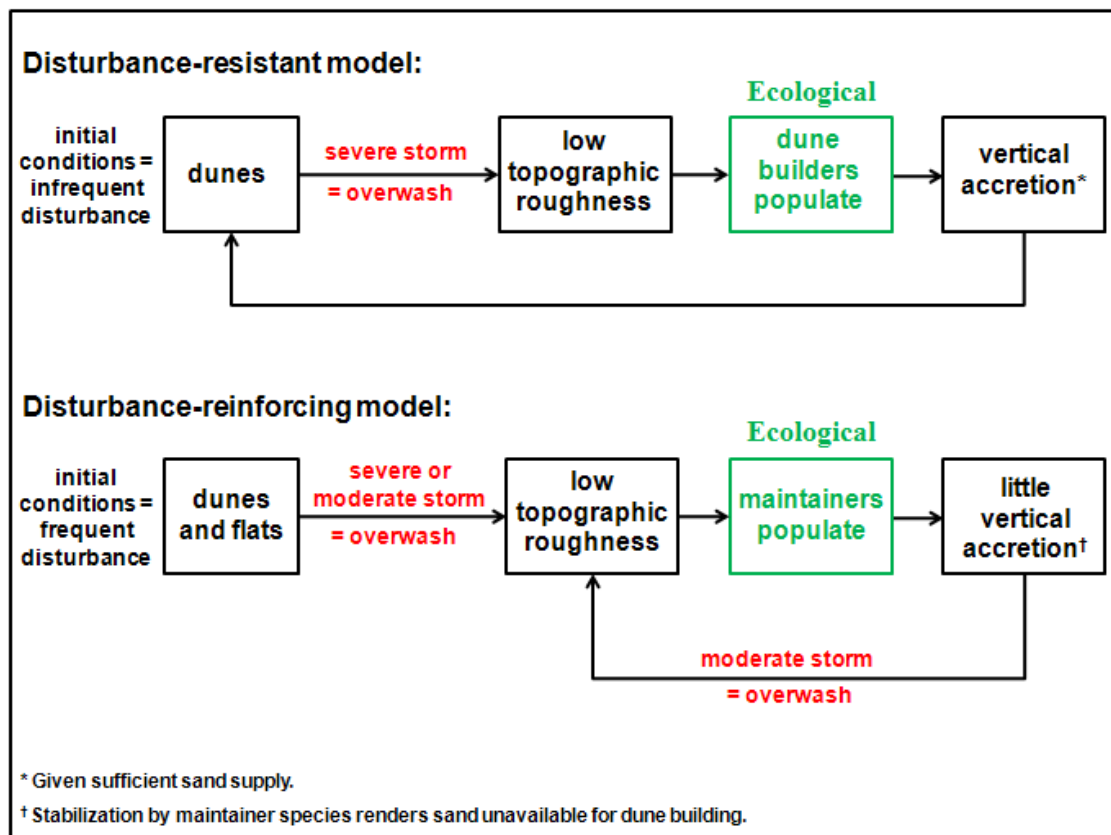


Figure 1.2. Ecomorphodynamic conceptual models of barrier island susceptibility and response to overwash. Initial conditions (disturbance regimes) are set by physical factors such as relative sea level rise rate, antecedent geology and topography, sediment supply, wave climate, shoreline orientation, etc.

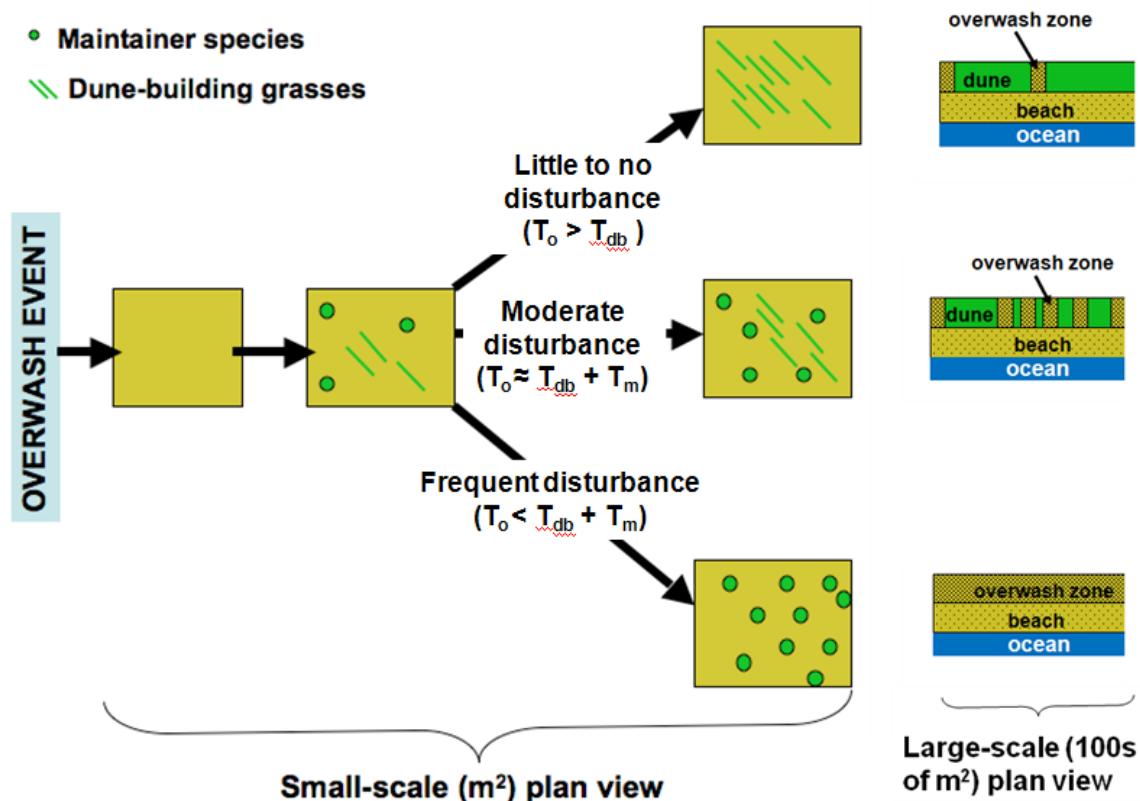


Figure 1.3. Possible scenarios for ecomorphodynamic response to overwash when both continuous dune builders and overwash-adapted maintainer species are present, where T_o = time between overwash events, T_{db} = time needed for dune-building grasses to restore topographic relief, and T_m = time added to topographic recovery by the preferential survival of maintainer species, which stabilize low topography and render sand unavailable for dune building. After overwash (left), both types of vegetation are likely to recolonize the area, but we hypothesize that subsequent disturbance frequency may determine which species ultimately becomes dominant (small-scale plan view). The right-most column (large-scale plan view) shows the implications for barrier island morphology associated with each scenario. Modified from Wolner et al., 2011.

Regional setting

Located on the Eastern Shore of Virginia, USA (Figure 1.4), the Virginia Coast Reserve encompasses a barrier island system in which *A. breviligulata* (as the dominant dune-building species) and *S. patens* are both prevalent (Appendix 1.1). The VCR, currently a Long Term Ecological Research (LTER) site, has been protected from anthropogenic development since the mid-20th century, providing an unparalleled opportunity to observe a mid-Atlantic barrier island chain in its (nearly) natural state. Shoreline dynamics and island morphologies are highly variable within the VCR (Dolan et al., 1979; Leatherman et al., 1982; Kochel et al., 1985). Here, we focus on two morphological end-members, Hog and Metompkin Islands (Figure 1.4).

Hog Island is a high-relief (dune-dominated), drumstick-shaped barrier characterized by multiple accretional dune ridges and a history of rotational shoreline change (alternation between accretion on the northern half/erosion on the southern half and vice versa, with generally clockwise rotation since the late 1800s; Figure 1.5; Appendix 1.2). The northern half of Hog Island is generally dominated by dune/swale topography, although small-scale overwash (10s of m) is evident along the youngest (lowest and seaward-most) accretional dune ridge. Excluding inlet-parallel beaches, large-scale overwash (100s of m) is limited to the island's rotational axis, where shoreline oscillation has exposed a swale to wave action (Harris, 1992) and the beach is narrowest. Relict overwash channels are apparent—now disconnected from the active beach by relatively tall, continuous dune ridges—in the southern half of the island, where the shoreline has switched recently (ca. 40 years BP) from an erosional to an accretional regime. The southern-central portion of the island includes dunes and hummocky, lower-

relief transitional areas. While active overwash is currently absent along the southern half of Hog Island, this part of the island overwashed more frequently during the 20th century than the northern half (Fenster and Hayden, 2007).

Conversely, Metompkin Island (Figure 1.5) is a low-relief (overwash-dominated), linear island undergoing rapid parallel shoreline retreat (between 1.9 and 13.6 m/yr in the late 20th and early 21st century; Byrnes, 1988; O. Brenner, personal communication, 14 June 2011). The southern, lagoon-backed half of the island is separated from the northern, marsh-backed half by an offset in shoreline position at the site of a former ephemeral inlet. The southern half has historically migrated more rapidly than the northern half, but this trend reversed ca. 30 years BP, when the northern half began migrating (largely via overwash) up to 4 times faster than the southern half, thus reducing the magnitude of the shoreline offset (Byrnes, 1988; Byrnes and Gingerich, 1987). Consistent with this heterogeneity in migration rates, the southern half of the island is characterized by a discontinuous single dune line punctuated by overwash fans and channels as well as transitional areas in various stages of recovery, while the northern half consists entirely of coalesced overwash terraces.

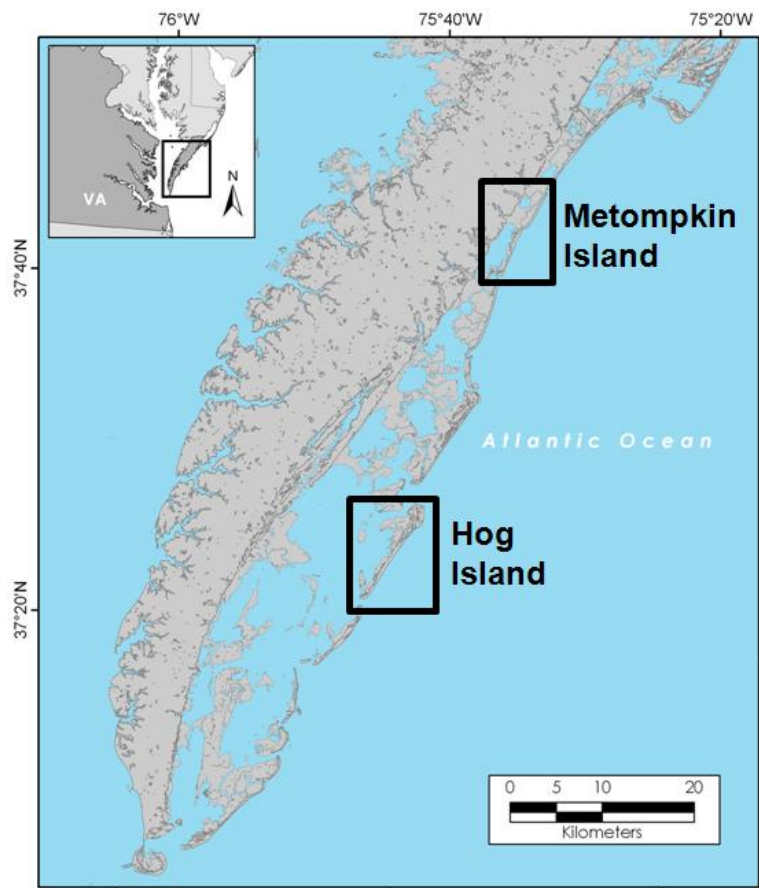


Figure 1.4. Map of the Eastern Shore of Virginia, including the Virginia Coast Reserve (VCR) on the Atlantic coast. Hog and Metompkin Islands represent morphological end-members within the barrier island chain.

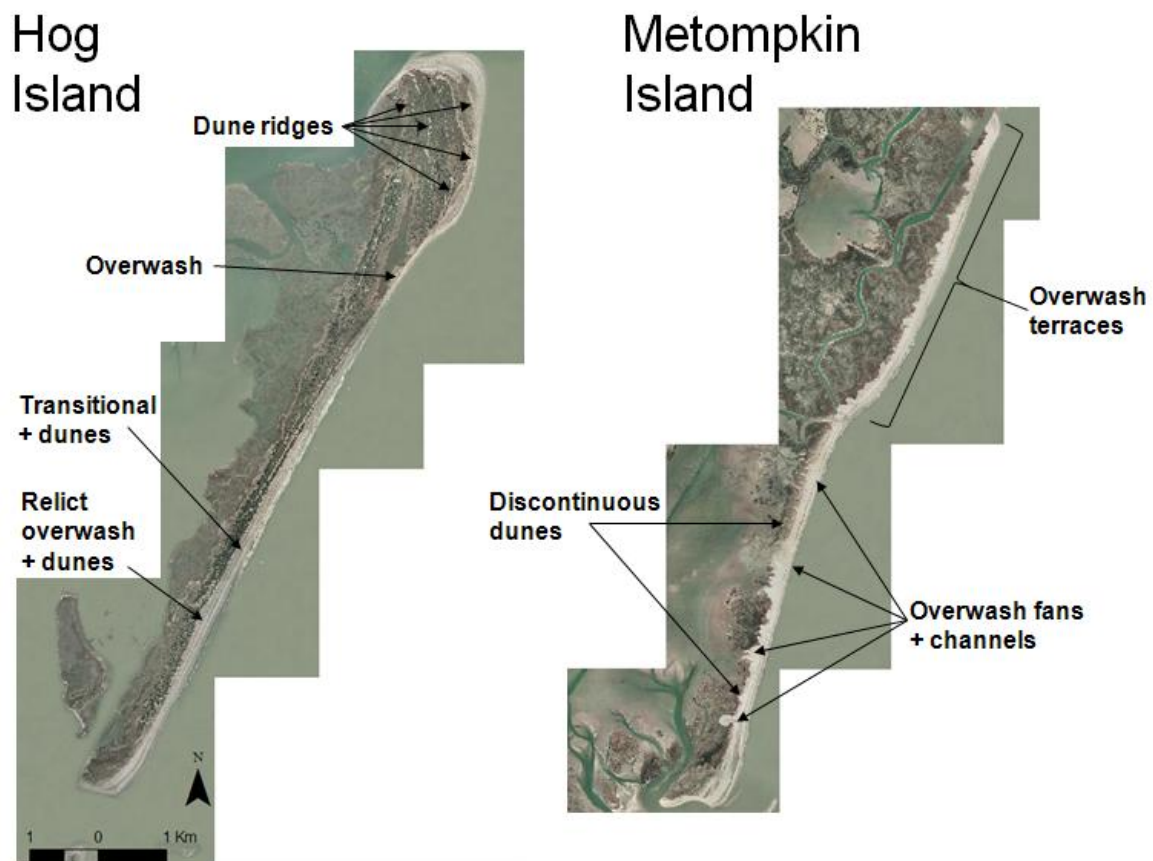


Figure 1.5. 2007 aerial photos of Hog and Metompkin Islands in the Virginia Coast Reserve, with labels from 2009-10 field reconnaissance.

2. METHODS

Relating morphology and vegetation: transect surveys

On each island, we selected a set of morphologically representative sites on which to focus our field campaigns. Because Hog Island and Metompkin Island are both characterized by distinct morphological dynamics in their northern and southern halves (Fenster and Hayden, 2007; Harris, 1992; Byrnes, 1988), we chose 3 sites in the north and 3 sites in the south, for a total of 6 sites on each island (lettered A through F from south to north; Figure 2.1).

In collaboration with the Coastal Plant Ecology lab at Virginia Commonwealth University, we established one cross-shore and two alongshore transects at each site for collection of topographic, ecological, and sedimentological data. Cross-shore transects (extending 50–200+ m) began at the foredune toe or vegetation line—or, if absent, the estimated point where these would be expected to develop—and extended to the start of the stable island interior or backbarrier (e.g., shrub thicket, mudflat, marsh, or water). The two alongshore transects—included to capture more fully the ecological variability that may occur with changing distance from the shoreline—intersected the cross-shore transect at both 5 m and the midway point. Alongshore transects extended 50 m in either direction from the cross-shore transect, or until the stable interior or backbarrier was encountered (whichever was closer).

At 5 m increments along the transects, we paired high-resolution GPS elevation measurements (R7/8 GNSS, Trimble Navigation Limited, Sunnyvale, CA; Appendix 2.1) with observations of vegetation composition and percent cover in a 0.5 x 0.5 m quadrat. All elevations were referenced to the NAVD88 datum. We recorded the morphologic

environment of each paired sampling point as one of the following: overwash, transitional (e.g., partial or recovering overwash, low hummocky topography), dune, swale (either interdunal or backing a single dune), or relict overwash (known instances of past overwash now cut off from the beach by accretional dunes). To capture transect topography in greater detail, we collected additional elevation measurements at any change or break in slope. Elevation measurements on the cross-shore transects also extended seaward to the water line to record the beach profile and location of the wet/dry line. Finally, we collected grab samples every 10 m on both the cross- and alongshore transects in order to characterize the sediment properties at each site.

To streamline the analyses of vegetation and environmental data, we focused on the primary dune-building and maintainer species, *A. breviligulata* and *S. patens*, respectively. Because vegetation cover at our transect sites was relatively sparse, our sampling units were small, and the spatial distribution of species relative to disturbance was our primary interest, we chose frequency of occurrence (as opposed to percent cover or biomass) as the best metric for assessing relative species dominance in each morphologic environment (McCune and Grace, 2002). We then normalized the frequency data (i.e., converted to percent frequency) using the number of observations in each morphologic environment.

For each island (respectively), we used Indicator Species Analysis (ISA) to determine the strength and statistical significance of the observed relationships between vegetation and morphology (PC-Ord, MJM Software Designs, Glendale, OR). ISA is a community ordination technique that considers both presence/absence and relative abundance of different plant species across a range of categories (Dufrêne and Legendre,

1997); in this case, the categories were morphologic environments. Because ISA considers not only the abundance of species within categories but also the fidelity of species to particular categories, it can be more useful for comparing the strength of species-environment associations than considering abundance only. ISA assigns an indicator value (IV) of 0–100 to each species based on the relative strength of the relationship between that species and a given category—i.e., the IV designates how strongly the species “indicates” the category in question (a strong IV is >25 ; Bakker, 2008). The threshold above which the maximum IV for a given species is statistically significant ($\alpha = 0.1$) based on a Monte Carlo test varies by species and between analyses, but was generally ~ 5 in this study for commonly occurring species when all sampling points were included (or ~ 20 on Hog Island and ~ 10 on Metompkin Island when only vegetated sampling points were included).

Because beach width exerts substantial control over the rate of dune growth (i.e., sand supply to the dunes; e.g., Bauer and Davidson-Arnott, 2002), and thus is related to the likelihood of overwash at a given location, it was important to consider beach width along with species composition at each transect site. Using the surveyed cross-shore profile, we calculated beach width for each site as the distance between the wet/dry line and the start of the cross-shore transect (i.e., the actual or inferred pre-overwash position of the foredune toe or vegetation line). We related beach width and mean transect elevation (as an inverse proxy for degree of disturbance) on each island using Spearman correlation, which tests for any monotonic relationship. Where beach width values appeared suspect, we used 2009 aerial photos to correct them or, if aerial photo evidence supported the outlying value, dropped them from a subsequent analysis (Appendix 3.1).

In addition to beach width, surficial sediment properties may also influence dune development (or lack thereof). For instance, fine, cohesive sediments and heavy, coarse sediments are difficult to transport via aeolian processes. Furthermore, post-overwash armoring by coarse shell lag may limit sand transport and thus inhibit dune recovery (e.g., Priestas and Fagherazzi, 2010). We therefore analyzed surficial sediment grab samples from each site for sediment distribution characteristics and shell gravel content using the following procedures: after drying, passing through a 2 mm sieve to separate shells, and removing organic matter using loss on ignition (LOI), we analyzed each sample in sets of 3 sub-samples using an LS 13 320 laser diffraction particle size analyzer (Beckman Coulter, Brea, CA; Appendix 2.2). We averaged the volume-percent size distributions of the sub-samples to obtain a single distribution and a set of arithmetic statistical moments (median, mean, standard deviation, skewness, D10, D90, etc.; Appendix 3.2) for each sample. After reviewing these data, we selected median grain size as a measure of central tendency and standard deviation as a measure of sorting. We calculated shell gravel content as the percentage of the total dry weight of each sample accounted for by shells > 2 mm. We compared medians, standard deviations, and shell gravel weight percent between islands and sites using 1-way ANOVA when the data conformed to parametric assumptions of homoscedasticity and residual normality; when they did not, we employed the Kruskal-Wallis test (non-parametric ANOVA analogue).

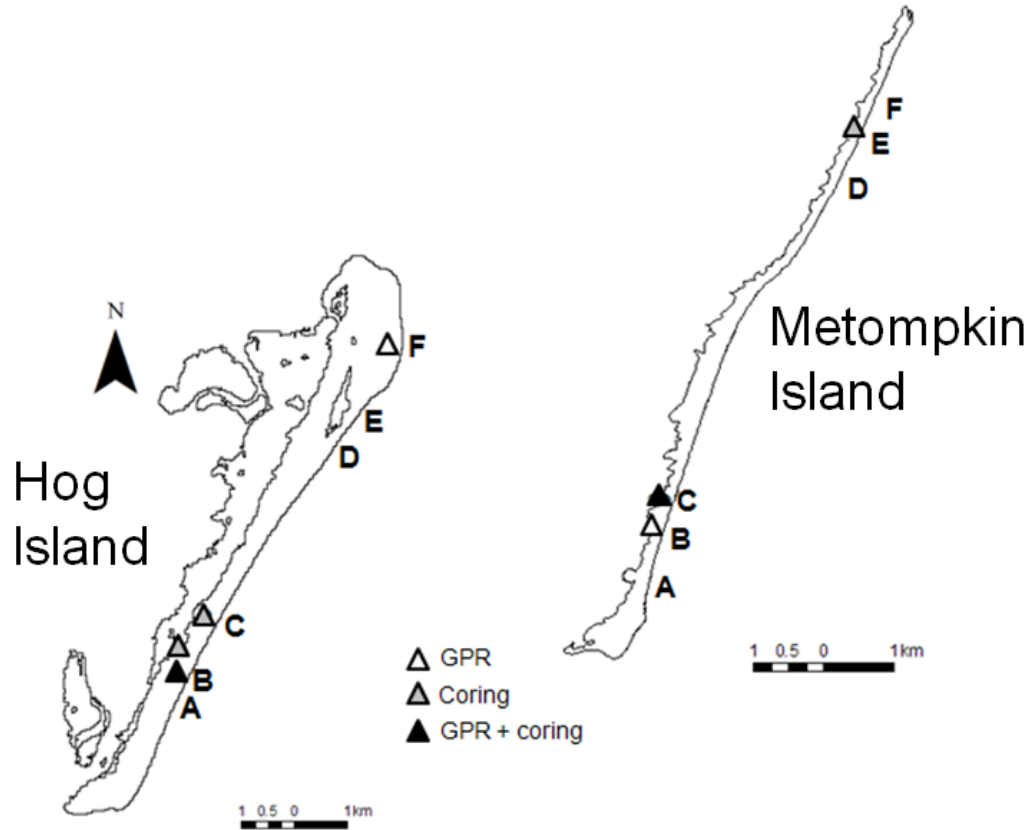


Figure 2.1. Representative transect survey sites (lettered A through F) on Hog and Metompkin Islands (not shown in actual spatial relationship to one another). Also shown are sites of ground-penetrating radar (GPR) surveys and vibracore collection.

Assessing overwash persistence: aerial photo and stratigraphic analyses

To examine overwash persistence on decadal timescales, we expanded a dataset of overwash shapefiles (polygons) digitized from orthorectified historical aerial photographs by Wilson et al. (2007). The authors delineated the boundaries of polygonal overwash zones using the expected position of the pre-overwash foredune (inferred from the surrounding intact foredune) and the apparent landward/lateral extent of fresh sand deposition (e.g., Kochel et al., 1985; M. D. Wilson, personal communication, 20 May 2010).

Wilson et al.'s (2007) dataset covered Hog and Metompkin Islands for the years 1962, 1977, 1985, 1994, and 2002, and Metompkin Island only for the years 1949 and 1955. We extended this dataset to include 2007 and 2009 for both islands using recently released aerial imagery (VGIN Virginia Base Mapping Program, © 2007 and 2009 Commonwealth of Virginia) and comparable digitization techniques (ESRI ArcGIS, Redlands, CA). In addition, we digitized island area—defined as the area between the wet/dry line (already digitized) and the island/backbarrier marsh boundary—for all photos of Hog and Metompkin Islands in the dataset.

For each photo year, we first calculated total overwash area on each island as a percentage of island area. As a metric of overwash persistence, we subsequently calculated the percent of island area also overwashed in the previous photo year (i.e., percent of island overwashed in 2 consecutive photo years, or, more briefly, the overlap percent). We compared both the percent of island overwashed and the overlap percent between Hog and Metompkin Islands using the Kruskal-Wallis test.

With the intent of assessing overwash persistence on longer timescales (decades to centuries), we conducted ground-penetrating radar (GPR) surveys and collected vibracores in select locations on each island (see Figure 2.1). The objective of these complementary approaches was to look for stratigraphic evidence of overwash persistence and/or recovery into dunes, as well as to use each method to inform and corroborate the results and interpretations of the other.

We collected GPR profiles using a PulseEKKO Pro 200 MHz system (step size = 20 cm; Sensors and Software, Mississauga, Ontario) integrated with the R7/8 Trimble GPS unit. Integrated data collection allowed us to apply cm-scale resolution topographic corrections to all profiles, except for two profiles on Hog Island (Site F) collected while the GPS was malfunctioning; for these two profiles, we applied user-input topographic corrections generated from field sketches and GPS data collected during vegetation surveys at the same site. On Hog Island, radar velocities determined using the common midpoint method (CMP; Appendix 2.3) varied with location, ranging from 0.09–0.13 m/ns; due to the enigmatic failure of a CMP survey on Metompkin Island, we assumed a radar velocity of 0.1 m/ns (a typical value for partially saturated sands: e.g., Bristow, 2009) for all surveys on this island. We applied exponential gain compensation (SEC 2; Appendix 2.3) to all GPR profiles.

GPR has been used successfully in barrier systems to identify both dune (e.g., Havholm et al., 2004) and overwash facies (e.g., Møller and Anthony, 2003) because the bedding patterns associated with each of these facies tend to produce distinctive radar signatures. Dune facies are associated with dipping reflections, which in some cases may be finely-spaced and chaotic (indicative of aeolian deposition of cross-strata that may be

thin, disturbed by rooting, and varying in orientation; e.g., Hayes, 1979; Byrne and McCann, 1990). Overwash facies, on the other hand, are associated with flat-lying, often widely-spaced reflections (indicative of hydraulic deposition of horizontal to massive bedding, often in thick units; e.g., Leatherman et al., 1977). Therefore, stacked, widely-spaced horizontal reflections under current overwash or transitional zones may indicate overwash persistence, while these same reflections under dunes (or interspersed with dipping or chaotic reflections) may indicate overwash recovery.

Exploratory GPR surveys conducted in 2009 revealed that in active overwash zones in the study area, the saline water table—which severely attenuates the GPR signal—is too close to the ground surface for effective data collection; furthermore, at low elevations, the radar signal showed a tendency to produce repeat reflections beginning at shallow depths (< 1 m). However, surveys of a known relict overwash channel among dunes on the southern end of Hog Island (Site B), where surface elevation above the saline water table was apparently higher overall, demonstrated that distinguishing between dune and overwash facies using the criteria described above is possible if depth of signal penetration is sufficient. We therefore limited our large-scale GPR surveys to dune complexes and transitional areas (southern and northern Hog, sites B and F; southern Metompkin, sites B and C; see Figure 2.1) where field reconnaissance and aerial photos suggested that overwash had previously occurred.

We collected cores ranging from 1 to 6 m in length (1.5 to 7+ m in total depth, including augering and compaction) using 3” aluminum irrigation piping and a portable, land-based vibracoring rig similar to the models described by Lanesky et al. (1979) and Finklestein and Prins (1981) (see also McBride and Robinson, 2003; Appendix 2.4).

Where necessary to avoid penetration problems associated with shell armoring or thick sand packages, we augered to a depth of between 0.5 and 1.25 m before coring. When augering, we collected grab samples of the augered sediment, noting depth and sediment characteristics.

Due to the infeasibility of coring through thick sand deposits (e.g., dunes), we collected all cores in overwash zones (active or relict), transitional areas, swales, or high marshes. Though coring locations were limited somewhat by logistical constraints, we were able to collect cores at sites that either corresponded with GPR transect locations (e.g., transitional and relict overwash zones) or covered areas of interest that could not be surveyed using GPR, such as active overwash zones and sites of historic large-scale overwash currently located in dense shrub thickets.

After collection, we opened the cores in the laboratory (Appendix 2.5), allowing them to dry for 0.5–2 days outside of cold storage before photographing and logging. Core descriptions (logs) were based on visual observations of sediment color (using a Munsell Soil Color Chart), bedding, composition, texture, and size.

In each core, we delineated sedimentary facies based on broad energetic and environmental differences (e.g., relatively high-energy sand packages vs. low-energy, organic-rich mud deposits) and subfacies based on more subtle energetic and depositional distinctions (e.g., medium clean planar sand vs. fine bioturbated sand). While we interpreted the entirety of each core based on these stratigraphic delineations, our primary interpretive objective was to identify overwash and aeolian deposits, as in the GPR surveys. We distinguished overwash deposits based on literature descriptions of typical characteristics observed in cores, including: moderately to very well sorted, fine to coarse

sand and shells with parallel, planar heavy mineral laminations; the presence of shell hash and/or shell lag deposits; and textural indications of decreasing energy up-unit, such as normal grading (coarse shell lag to finer sand) or inverse grading (fine heavy mineral lag to coarser sand) (e.g., Schwartz, 1975 and 1982; Leatherman and Williams, 1977 and 1983; Leatherman et al., 1977; Sedgwick and Davis, 2003; Wang and Horwitz, 2007; see Appendix 2.5). Because the characteristic cross-stratification associated with aeolian deposition is difficult to preserve in the vibracoring process, potential aeolian deposits could not be identified with the same degree of certainty. However, we made tentative identifications based on the co-occurrence of the following features: well to very well sorted fine to medium sand; discontinuous, wavy, or cross-cutting heavy mineral laminations; and visual assessments of quartz frosting (e.g., Byrne and McCann, 1990; Hayes, 1979; Margolis and Krinsley, 1971; R. McBride, personal communication, 12 February 2011; see Appendix 2.5).

3. RESULTS

Transect surveys

Cross-shore profiles at each transect site varied substantially in relief, vegetation cover and composition, beach width, shell armoring, and environment encountered at the transect's landward terminus (Figure 3.1). Vegetation cover was typically lower at disturbed transect sites (i.e., sites with lower topographic roughness). Coarse shell lag was evident only on Metompkin Island.

Vegetation and morphology

Percent frequency distributions of species across morphologic environments (Figure 3.2) generally conformed to expectations based on the characteristic traits of *A. breviligulata* and *S. patens*. On both islands, *A. breviligulata* was dominant (i.e., occurred more frequently) on dunes as well as in the comparatively low-lying transitional areas, confirming the association of this species with vertical accretion and recovery after disturbance. *A. breviligulata* occurred more frequently than *S. patens* in overwash zones on Hog Island, although it should be noted that large-scale overwash was limited to a single area (Site D, parts of Site E) at the rotational axis of the island, and observed vegetation cover in this area was exceptionally low overall. *S. patens* was dominant in interdunal swales on Hog Island, consistent with the affinity of this species for lower elevations and wetter soils. Relict overwash (landward half of Site B) was ecologically distinct from other morphologic environments in terms of overall species assemblage (S. T. Brantley, personal communication, 3 November 2010; Appendix 3.1), but did not

show any pattern with respect to *A. breviligulata* and *S. patens* (equal percent frequencies).

On Metompkin Island, again, vegetation cover was generally low in overwash zones as a whole, resulting in low percent frequencies (especially because the large overwash fan at Site A was almost entirely bare; see Figure 3.1). Nevertheless, *S. patens* was marginally dominant in overwash zones—a signal derived almost entirely from the denser stands of vegetation present in the overwash terraces on the northern half of the island (Sites D, E, and F). *A. breviligulata*, rather than *S. patens*, was dominant in the comparatively open swales (essentially backdune platforms grading into high marsh). No distinct relict overwash zones were present, likely because Metompkin Island has been transgressing too rapidly to preserve such features. Notably, *A. breviligulata* and *S. patens* appeared to be separated more sharply by morphology here than on Hog Island, where frequencies were more comparable across morphologic environments.

ISA results (Figure 3.3a) were broadly consistent with species frequency distributions. *A. breviligulata* was a strong and statistically significant indicator of dunes on both islands ($\alpha = 0.1$; $p < 0.04$). *A. breviligulata* was also a strong indicator of transitional areas on Hog Island. In contrast, neither species was a strong indicator of transitional areas on Metompkin Island—although *A. breviligulata* had a higher indicator value (IV)—likely because the overall species assemblage in this environment was more diverse than elsewhere (Appendix 3.1). *S. patens* was a significant indicator of swales on Hog Island ($p = 0.00$), although *A. breviligulata* also had a strong (but lower) IV; only *A. breviligulata* was a strong indicator in swales on Metompkin Island. On Hog Island, neither species was a strong or significant indicator of overwash (likely due to low

percent cover: only 11 of 74 overwash sampling points were vegetated) or of relict overwash. However, on Metompkin Island, while sparse cover in overwash zones (55 of 246 points vegetated) resulted in a relatively low IV, *S. patens* was, in fact, a significant indicator of overwash ($p = 0.08$). Again, the strong IV for *A. breviligulata* in dune environments (with a value of 0 for *S. patens*) and the low but significant IV for *S. patens* in overwash (with a value of 0 for *A. breviligulata*)—when contrasted with the more moderate, consistent values across environments on Hog Island—demonstrated a potentially greater distinction between communities on Metompkin Island.

These differences between the two islands became even clearer when bare sampling points were excluded in a subsequent analysis (Figure 3.3b). IVs for the species of interest on Hog Island were even more consistent across environments (generally between 5 and 20), especially for *A. breviligulata*; as a result, while this species still had a higher IV than *S. patens* in overwash, transitional, and dune environments, it was no longer strong or significant ($p > 0.1$). On Metompkin Island, however, *A. breviligulata* remained a strong and significant indicator of dunes. More notably, *S. patens* became a dramatically stronger and more significant indicator of overwash ($p = 0.00$), while no other species had an IV exceeding 5 in this environment (including *A. breviligulata*; other species not shown). Thus, where vegetation did occur in overwash on Metompkin Island, *S. patens* was the only strong indicator species.

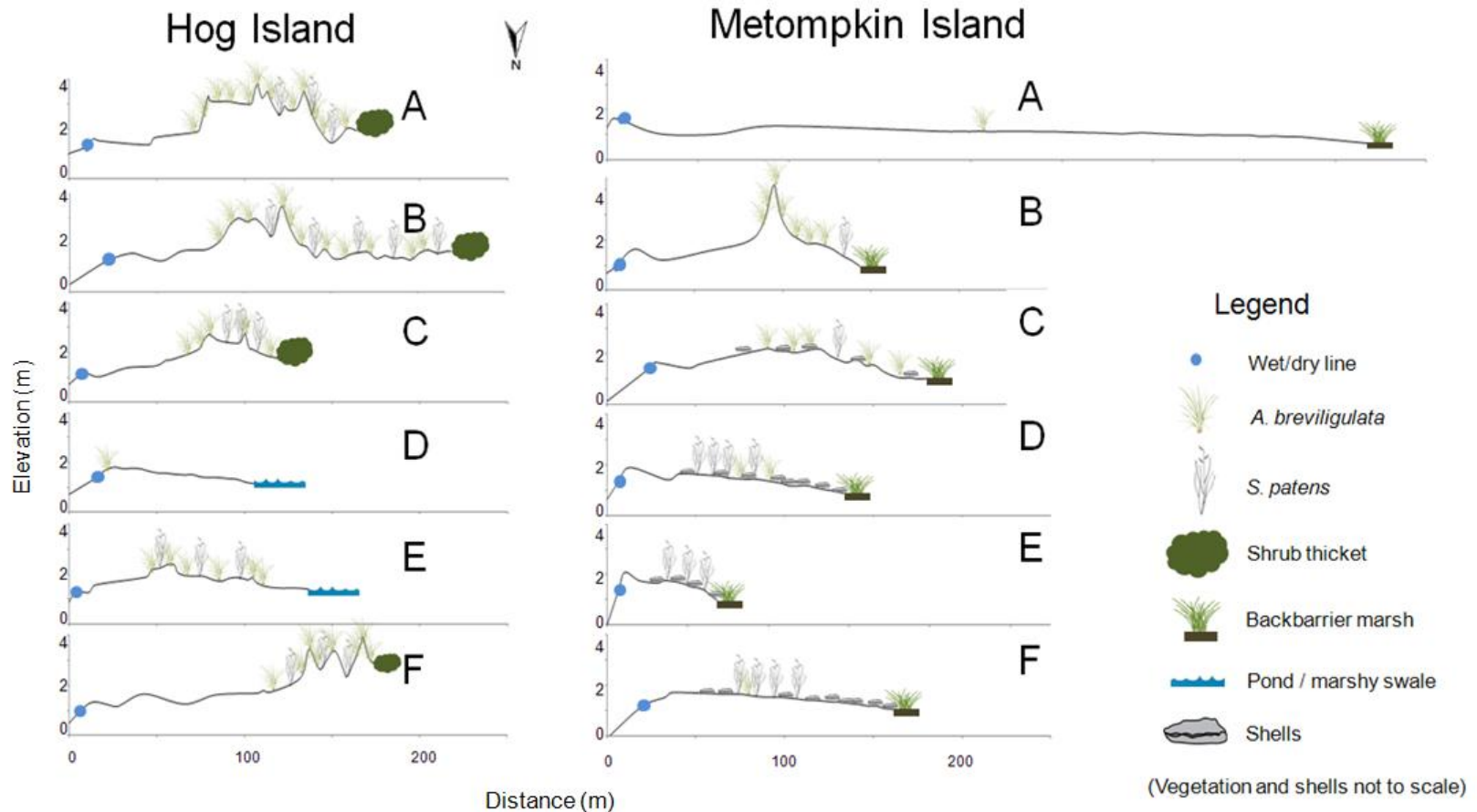


Figure 3.1 Cross-shore profiles for transect sites A–F on Hog and Metompkin Islands, from the water line (left) to the landward terminus (right—e.g., shrub thicket, pond/marshy swale, backbarrier marsh). Vegetation and shells are depicted representatively. For clarity, only the key dune-building and maintainer species—*A. breviligulata* and *S. patens*, respectively—are shown on the transects. While other species were also observed (e.g., *Panicum amarum* and *distichum*, *Solidago sempervirens*, *Cakile edentula*, etc.—see Appendix 3.1), *A. breviligulata* and *S. patens* were prevalent enough that excluding other species does not affect the representation of relative vegetation cover.

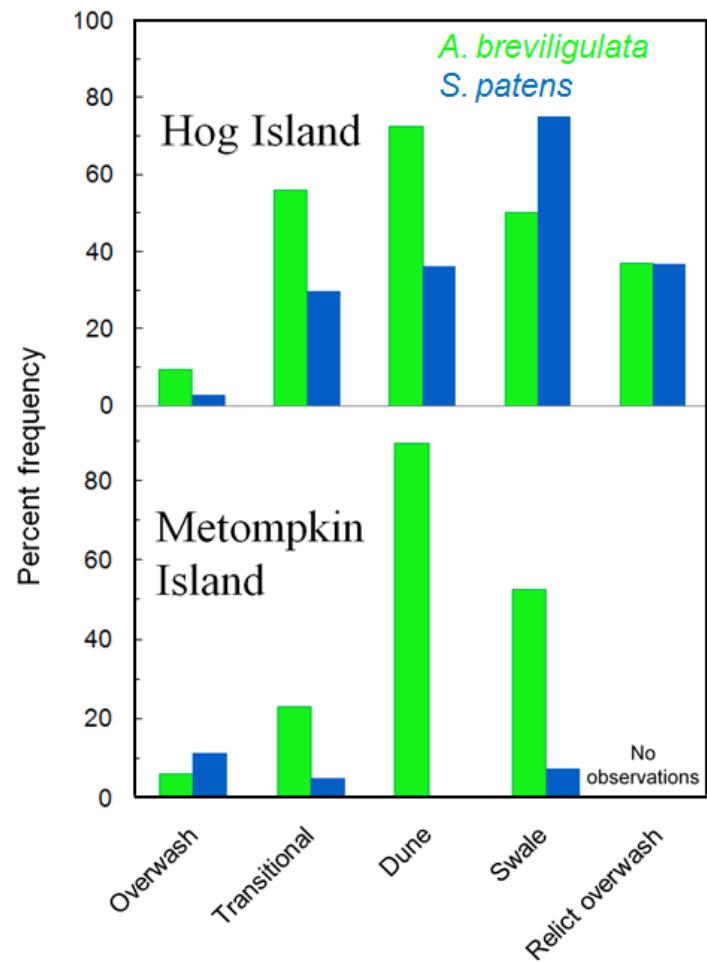


Figure 3.2. Frequency distributions of *A. breviligulata* and *S. patens* by morphologic environment on Hog and Metompkin Islands. Percent frequencies were derived from frequency data normalized using the number of observations in each morphologic environment. Modified from Wolner et al., 2011.

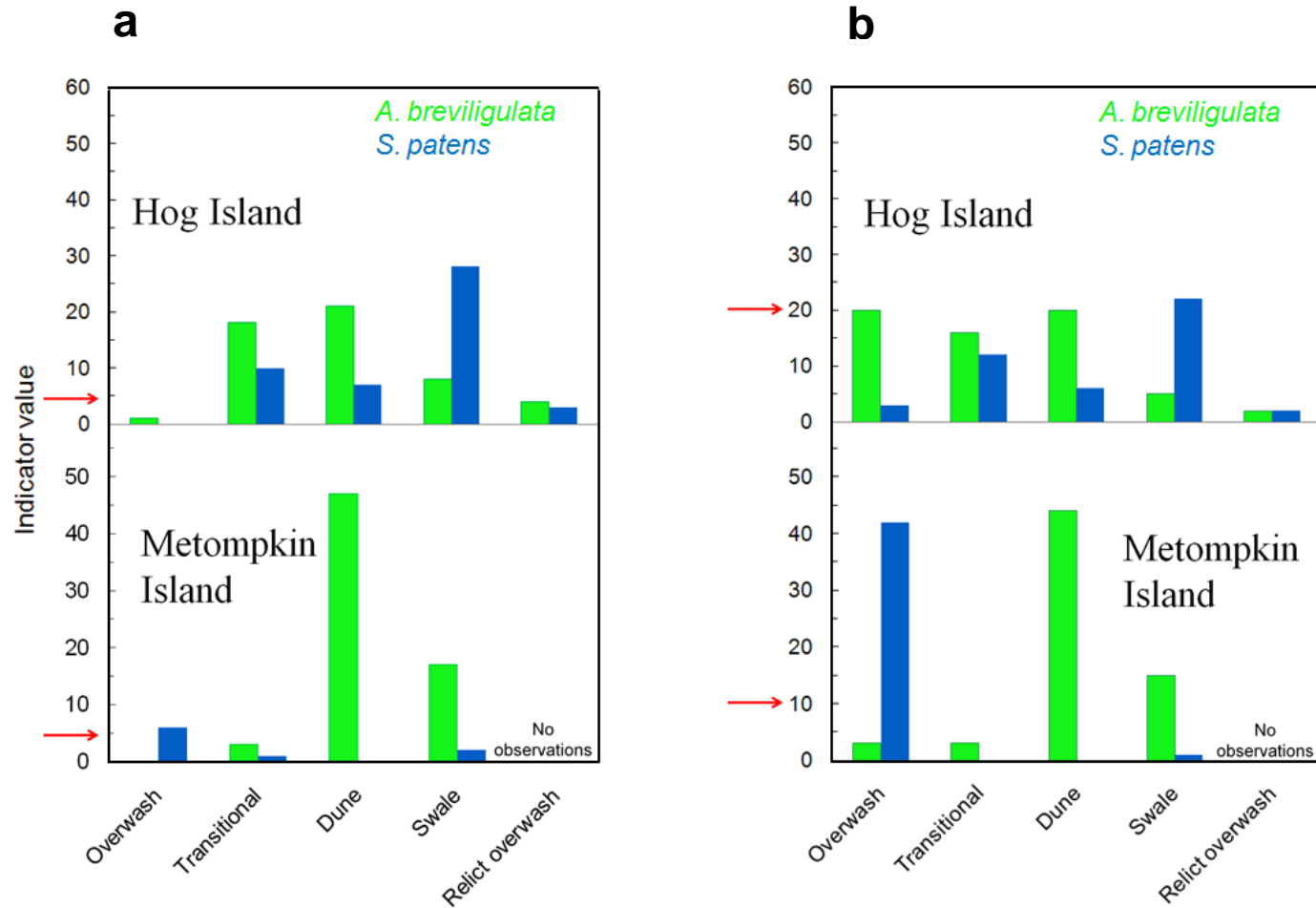


Figure 3.3. Indicator Species Analysis (ISA) results for Hog and Metompkin Islands. Higher indicator values signify stronger associations between species and morphologic environments. Arrows indicate the value above which the maximum indicator values of commonly occurring species like *A. breviligulata* and *S. patens* were statistically significant ($\alpha = 0.1$). a) Results including all sampling points (335 on Hog Island, 363 on Metompkin Island). b) Results including only vegetated sampling points (258 on Hog Island, 167 on Metompkin Island). Modified from Wolner et al., 2011.

Beach width

A strongly positive, significant correlation between beach width and mean transect elevation was apparent on Hog Island, but not on Metompkin Island (Figure 3.4). In a subsequent analysis (not shown; see Appendix 3.1), this continued to be the case even after correcting an anomalous point from Hog Island using a 2009 aerial photo (measured beach width = 1.2 m, corrected maximum beach width = 30 m), as well as after removing an outlying point from Metompkin Island (beach width = 176 m, a value supported by the 2009 aerial imagery). Overwash distribution on Hog Island thus appeared to be closely related to beach width—i.e., smaller beach widths were associated with higher degrees of disturbance (lower mean elevations). On Metompkin Island, however, beach width—as a proxy for sand supply from the beach to the dunes—did not appear to be linked to the distribution of disturbed areas.

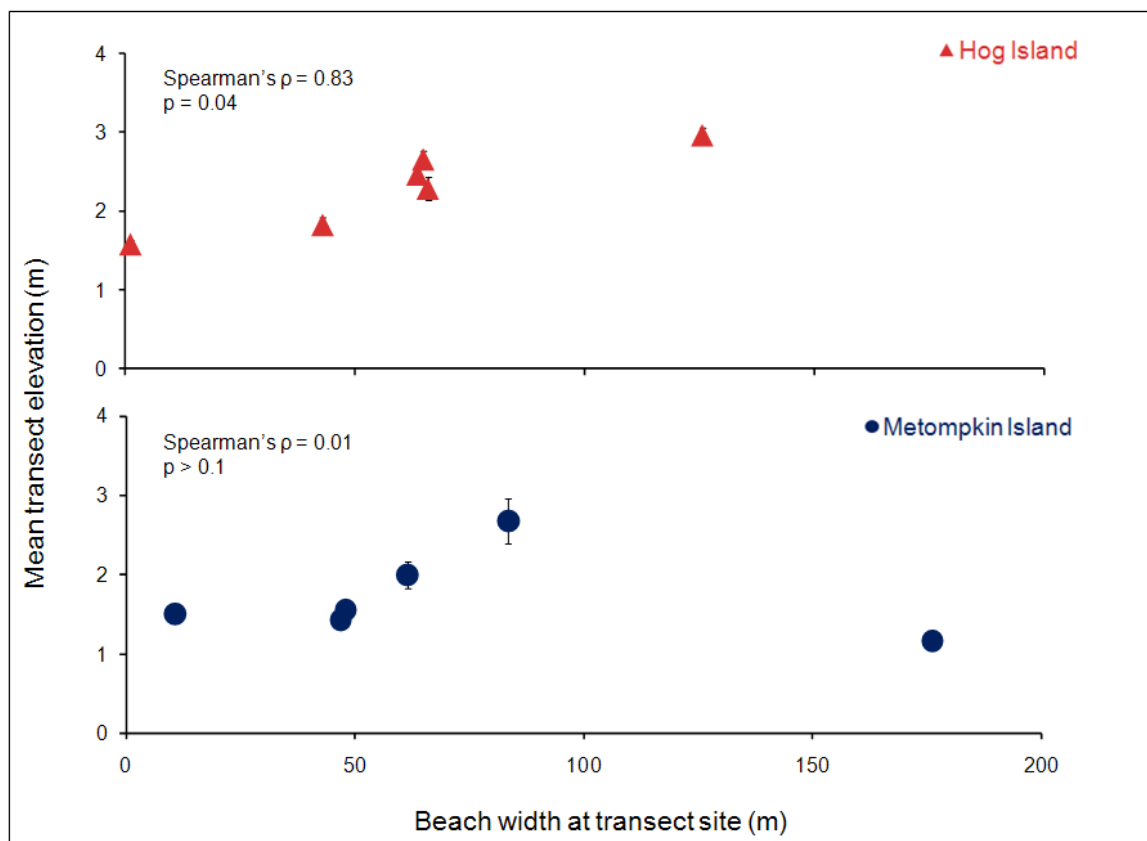


Figure 3.4. Mean transect elevation and beach width at each transect site, showing the correlation coefficient (ρ) and p value from Spearman correlation. Error bars represent 95% confidence intervals (not visible behind some markers). In a subsequent correlation analysis (Appendix 3.1), the anomalous point on Hog Island (beach width = 1.2 m) was corrected to 30 m using 2009 aerial imagery; however, there were no changes to the ρ or p values because Spearman correlation is a rank-order analysis. The correlation on Metompkin Island was still insignificant ($p > 0.1$) after removing the outlying point at beach width = 176 m (this value was corroborated by 2009 aerial imagery). Modified from Wolner et al., 2011.

Sediment properties

Sediment samples ranged in median grain size from fine to medium sand. Comparisons of transect site means showed that both medians and standard deviations of grain size distributions differed significantly between the two islands. Overall, sediment on Metompkin Island was coarser and more poorly sorted than on Hog Island (Figure 3.5).

Significant differences were also evident within islands in by-site comparisons (Table 3.1; Appendix 3.2). On Hog Island, sediment at Site D (the only overwash-dominated site) was clearly coarser than at all other sites, and also appeared to be less well sorted (Figure 3.6). Sediment at overwash-dominated sites on the northern half of Metompkin Island (Sites D, E, and F) was coarser and more poorly sorted than at sites on the southern end of the island, even though one of these southern sites (Site A) was also overwash-dominated (Figure 3.7). In fact, sediment at Site A appeared, if anything, to be finer and better sorted than at the dune-dominated and transitional sites (Sites B and C, respectively). Notably, Site A was the only overwash-dominated transect site on Metompkin without extensive shell armoring (see Figure 3.1).

Coarse (gravel-sized) shell lag was present on Metompkin Island only; within this island, shell gravel content varied significantly between sites (Figure 3.8). Again, the overwash-dominated northern sites (D, E, and F) clearly differed from the rest of the island (although not from one another). Shell gravel content was greatest at these sites (see Figure 3.1). At Site C (transitional), shell gravel content was significantly less than at the northern sites, but significantly greater than at Sites A and B, where shells were essentially nonexistent on the sampling transects.

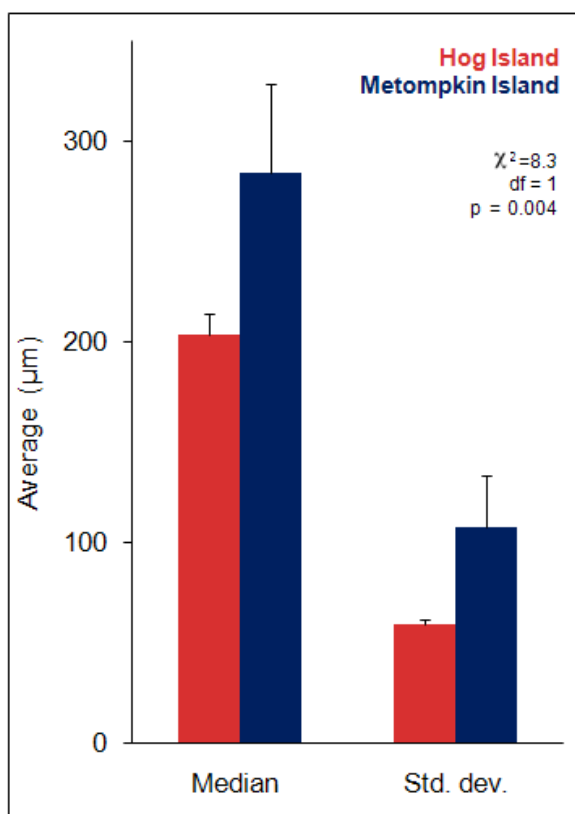


Figure 3.5. Averages of median grain sizes and standard deviations of grain size distributions on Hog and Metompkin Islands. Error bars represent 95% confidence intervals. Median grain sizes and standard deviations were averaged by site and compared (separately) between islands using Kruskal-Wallis tests. In both cases, all values for Metompkin Island exceeded all values for Hog Island. Because the Kruskal-Wallis test is a rank-order analysis, this resulted in identical χ^2 and p values (shown above) for both comparisons.

Table 3.1. Comparisons of median grain sizes and standard deviations across all sites within each island, using ANOVA (test statistic F) or the Kruskal-Wallis non-parametric analogue (test statistic χ^2). See Appendix 3.2 for by-site graphs with confidence intervals.

		Test statistic	df	p
Hog Island	Median	F = 21.8	5	<0.0001
	Std. deviation	$\chi^2 = 34.5$	5	<0.0001
Metompkin Island	Median	F = 125.2	5	<0.0001
	Std. deviation	F = 58.2	5	<0.0001

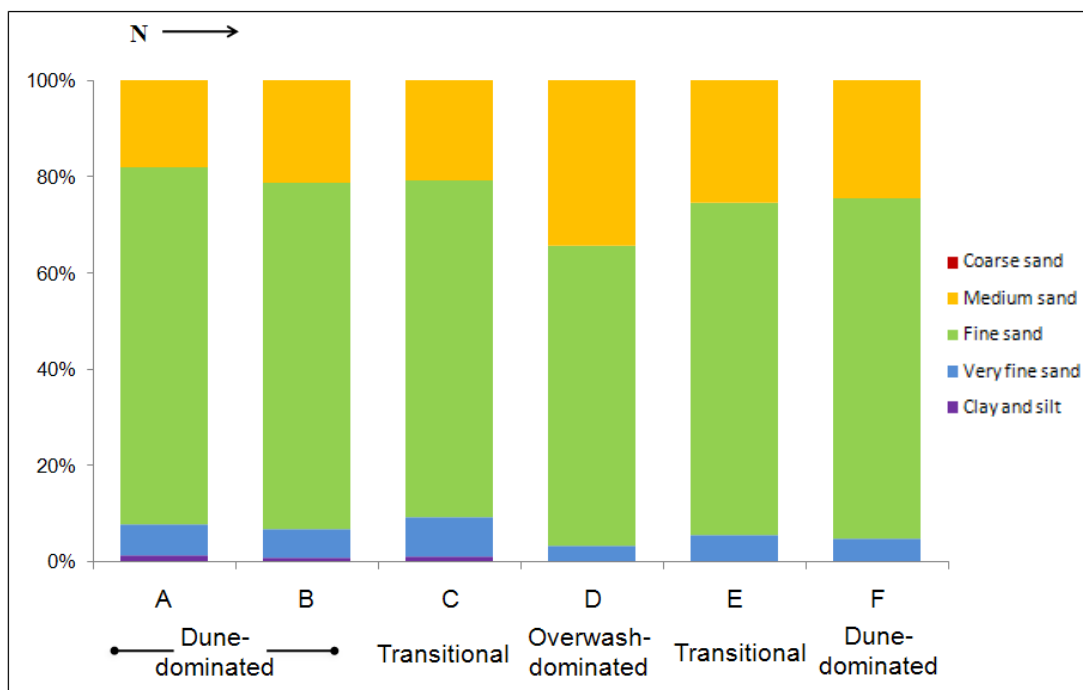


Figure 3.6. Grain size distribution by site on Hog Island.

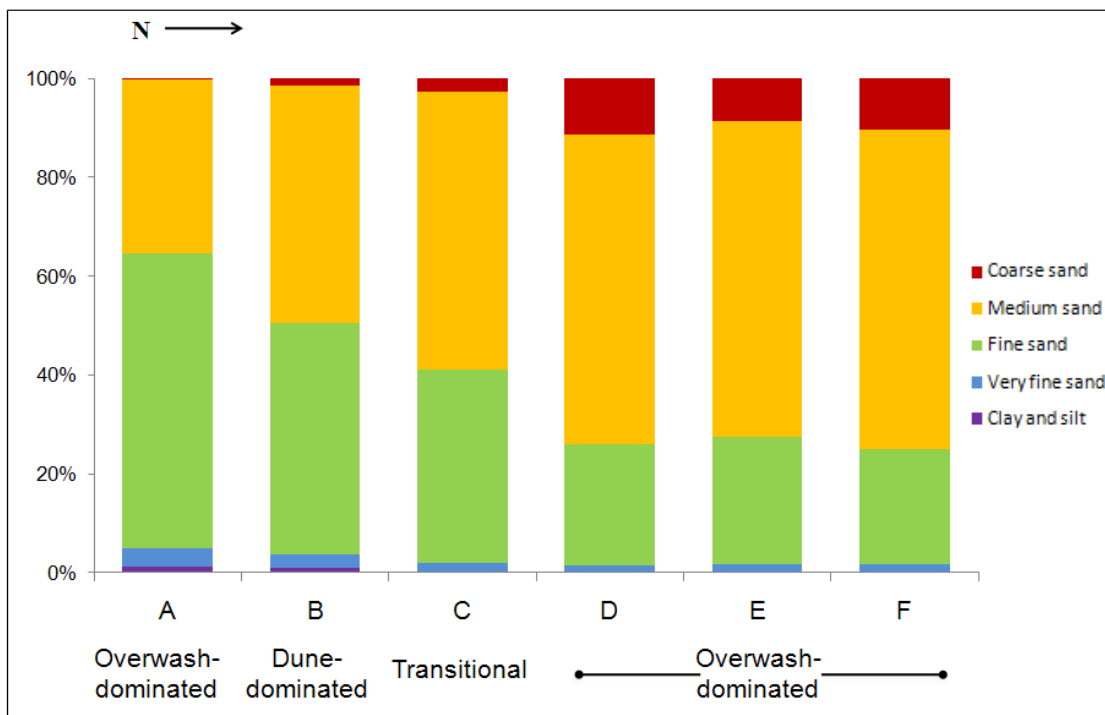


Figure 3.7. Grain size distribution by site on Metompkin Island.

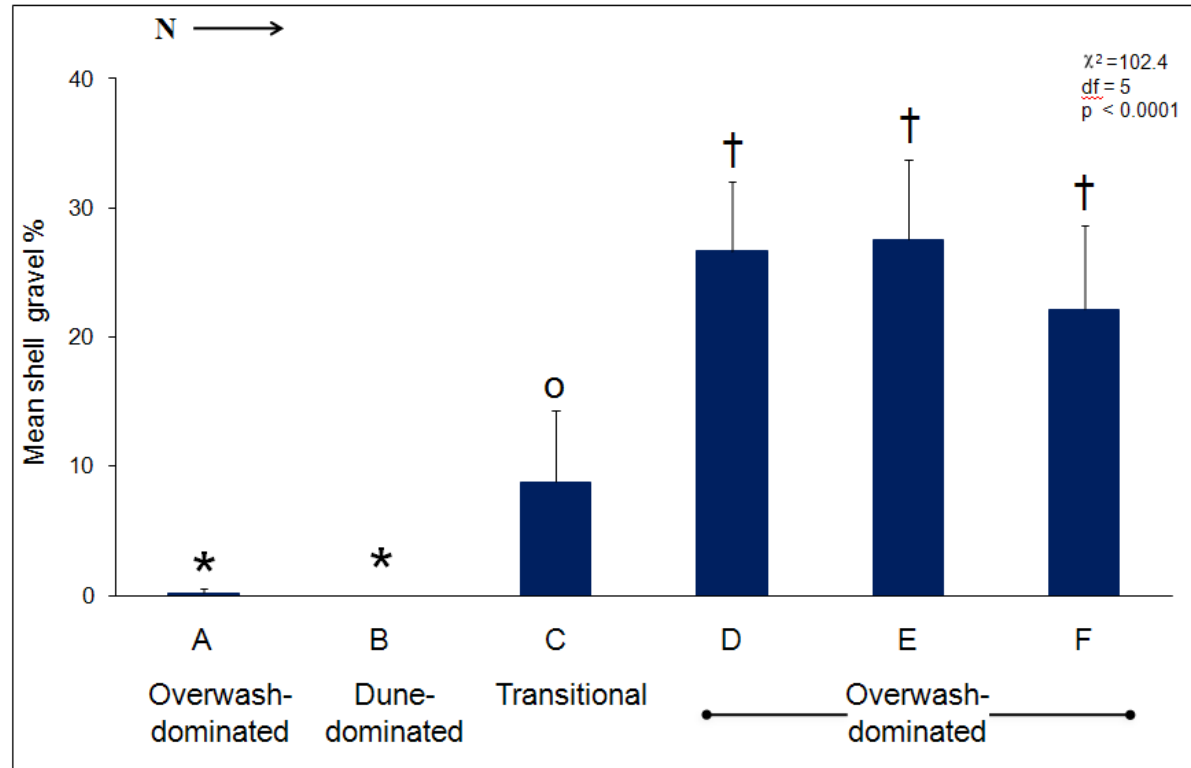


Figure 3.8. Mean shell gravel weight percent for transect sites on Metompkin Island (no shell gravel observed on Hog Island). Error bars represent 95% confidence intervals. Kruskal-Wallis tests were used for overall and pairwise comparisons of sites. Sites that share a symbol were not significantly different in 15 pairwise comparisons (Bonferonni $\alpha' = 0.003$).

Historical analyses

Aerial photos

The prevalence and distribution of overwash during the period of photo record varied markedly between the two islands (Figure 3.9). Overwash coverage as a percentage of island area was significantly greater on Metompkin Island than on Hog Island over time (Figure 3.10; Appendix 3.3). The percent of island overwashed peaked for both islands in 1962, the year in which the historic Ash Wednesday nor'easter impacted the VCR (e.g., Dolan and Davis, 1992). However, while subsequent values were typically > 20% on Metompkin Island, values on Hog Island stayed near zero. Both islands had apparent lows in 1977, but it should be noted that this was a low-quality photo year, making overwash zones particularly difficult to distinguish.

The overlap percent, or the percent of island overwashed in two consecutive photo years (a metric of overwash persistence), was also significantly greater on Metompkin Island (Figure 3.10; Appendix 3.3) throughout the period of photo record. Overlap percent values were very low on Hog Island; the highest values were associated with the photo years following the 1962 Ash Wednesday storm. On the southern end of Hog Island, large-scale overwash apparently associated with this storm persisted through 1985, but gradually recovered as the southern shoreline became accretional (Figure 3.9). Overlap percent values on Hog Island between 1994 and 2009 were associated solely with the overwash zone at the rotational axis of the island.

Metompkin Island appeared to have similarly low overlap percent values prior to 1994 (Figure 3.10). However, during this time period, shoreline change between photo years was very rapid (100s of m), resulting in little overlap of the island itself from photo

to photo. Once shoreline change between photo years slowed (10s of m), the overlap percent was clearly higher than on Hog Island, indicating that rapid island translation likely limited overlap values prior to 1994. Nevertheless, both the coverage and the spatial and temporal overlap of overwash zones were distinctly greater in scale and more general in distribution on Metompkin Island than on Hog Island.

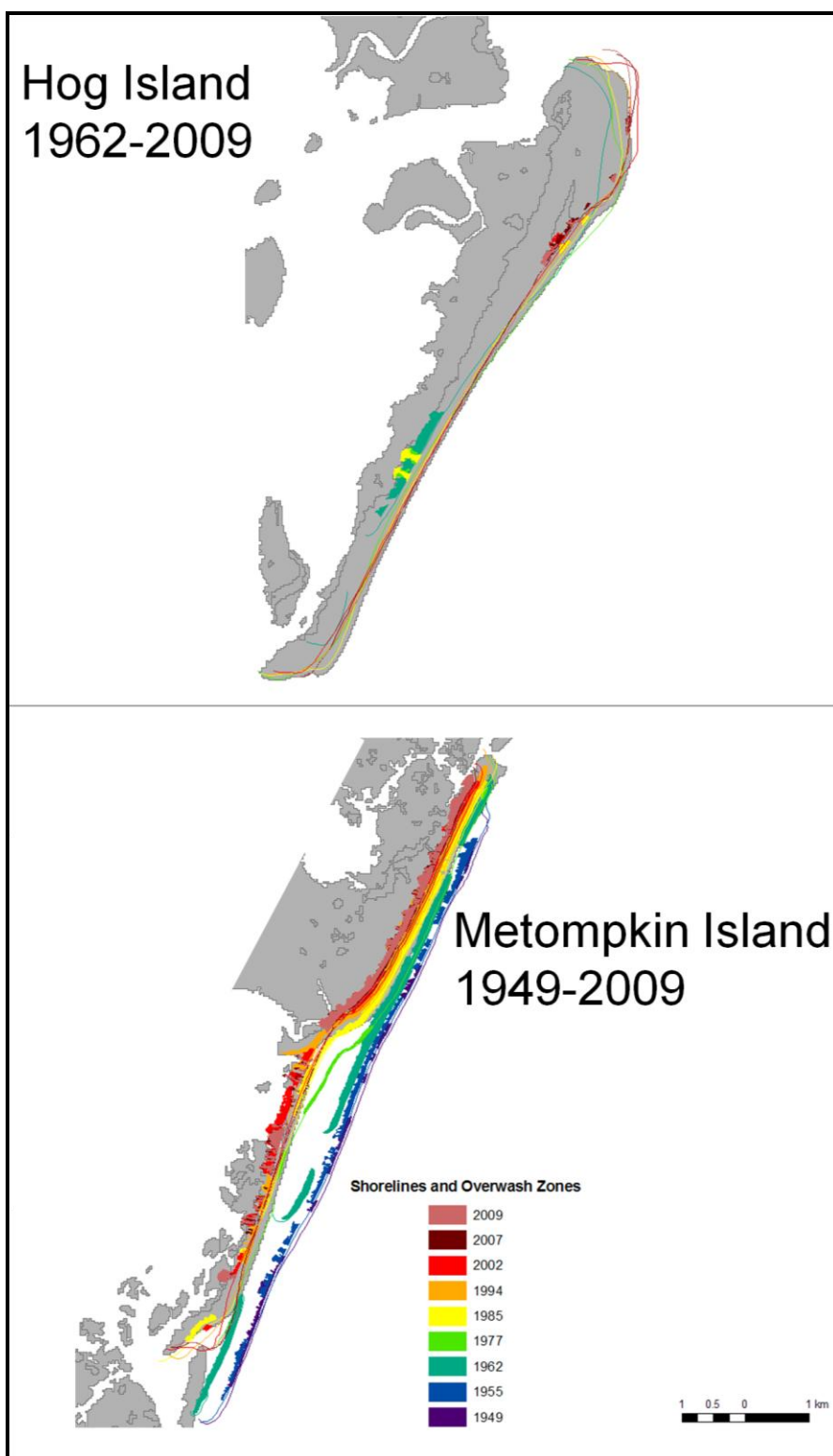
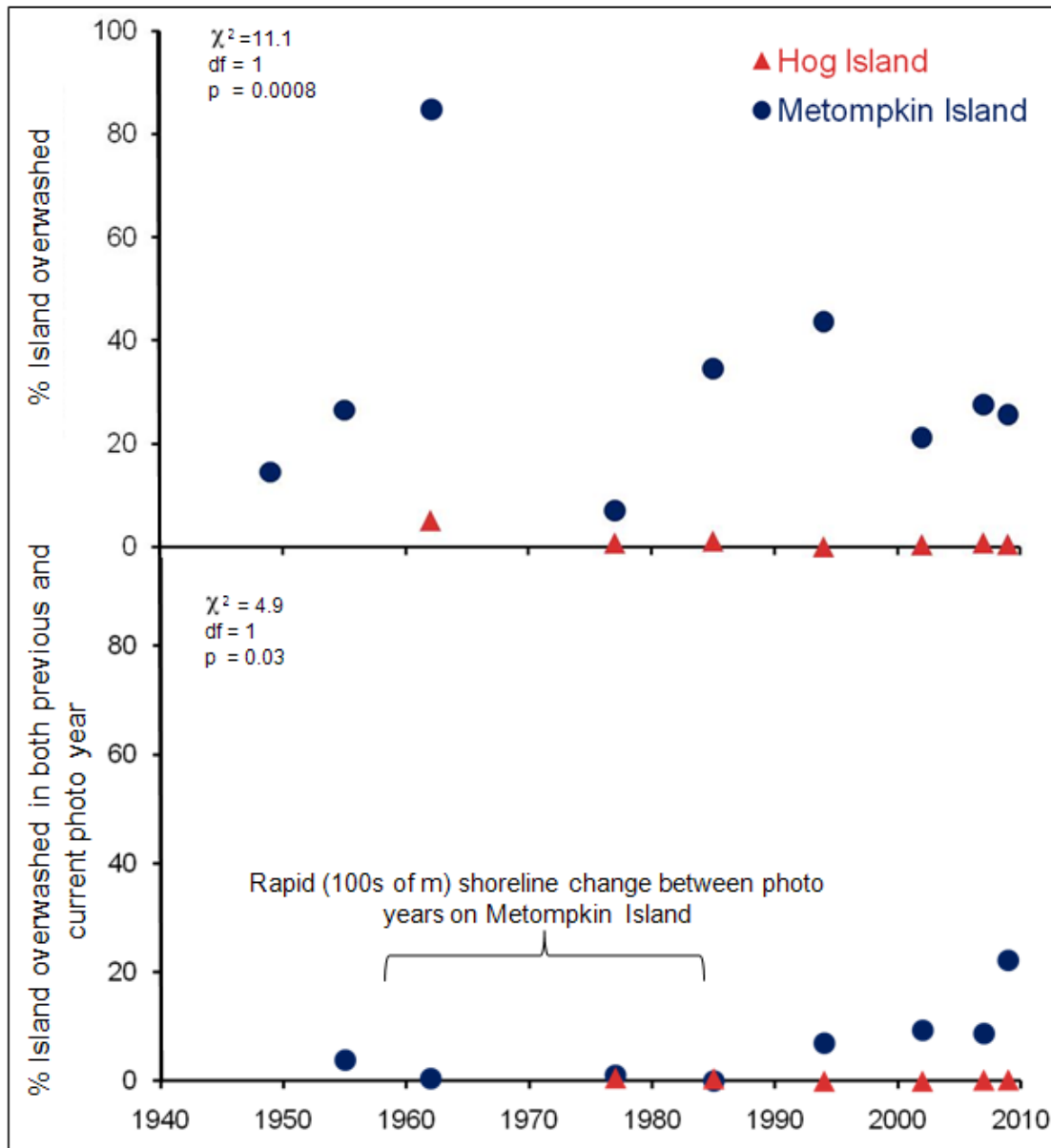


Figure 3.9. Shorelines and overwash zones digitized from aerial photos of Hog and Metompkin Islands (no data for Hog Island in 1949 and 1955). All shapefiles except for 2007 and 2009 from Wilson et al., 2007.



Figures 3.10. Top: percent of island area overwashed in each photo year (no data for Hog Island in 1949 and 1955). Bottom: percent of island also overwashed in the previous photo year (overlap percent). Rapid shoreline change on Metompkin Island likely limited overlap percent values prior to 1994 because little overlap of the island itself occurred between photo years. Statistical differences between islands were determined using Kruskal-Wallis tests.

Ground-penetrating radar

Distinctive overwash and aeolian facies were most apparent in alongshore GPR profiles. GPR surveys along the discontinuous dune crest on southern Metompkin Island, which is punctuated by small-scale active overwash channels and transitional areas, provided archetypal examples of the radar facies of interest (Figure 3.11).

Two alongshore profiles from Hog Island, associated with Sites B and F, were selected for formal interpretation based on quality and diversity of reflections. Flat-lying, evenly-spaced reflections (typical of overwash facies) beneath several meters of inclined, cross-cutting, finer-scale reflections (typical of dune facies) indicated the recovery of overwash into dunes on Hog Island both in the south (Figure 3.12a) and in the north (Figure 3.13a). The southern GPR transect also revealed the subsurface expression of the relict overwash channel at Site B, now part of a swale fronted by accretional secondary and foredune ridges.

In cross-shore profiles at Sites B and F, the most notable features were seaward-dipping reflections, possibly indicative of beach face deposits associated with accretional shoreline change (Figures 3.12b and 3.13b). At Site B on southern Hog Island, the seaward-dipping reflections in the center of the cross-shore transect corresponded at depth to the overwash channel observed in the alongshore transect, suggesting that the channel may have been located near the shoreline (in the active beach) and filled in tandem with shoreline accretion. A truncation surface was also apparent ~1 m below the surface.

On southern Metompkin Island, cross- and alongshore GPR profiles—associated with Sites C and B, respectively—showed a package of overwash layers overlain by

aeolian facies in transitional areas between dunes, evinced by flat-lying reflections that cross-cut near the surface (Figure 3.14; see Appendix 3.4 for the complete alongshore profile). Cross-cutting reflections in the low-lying transitional areas extended between ~0.5 and 1.5 m below the surface, suggesting aeolian deposition and reworking on the surface of older overwash deposits.

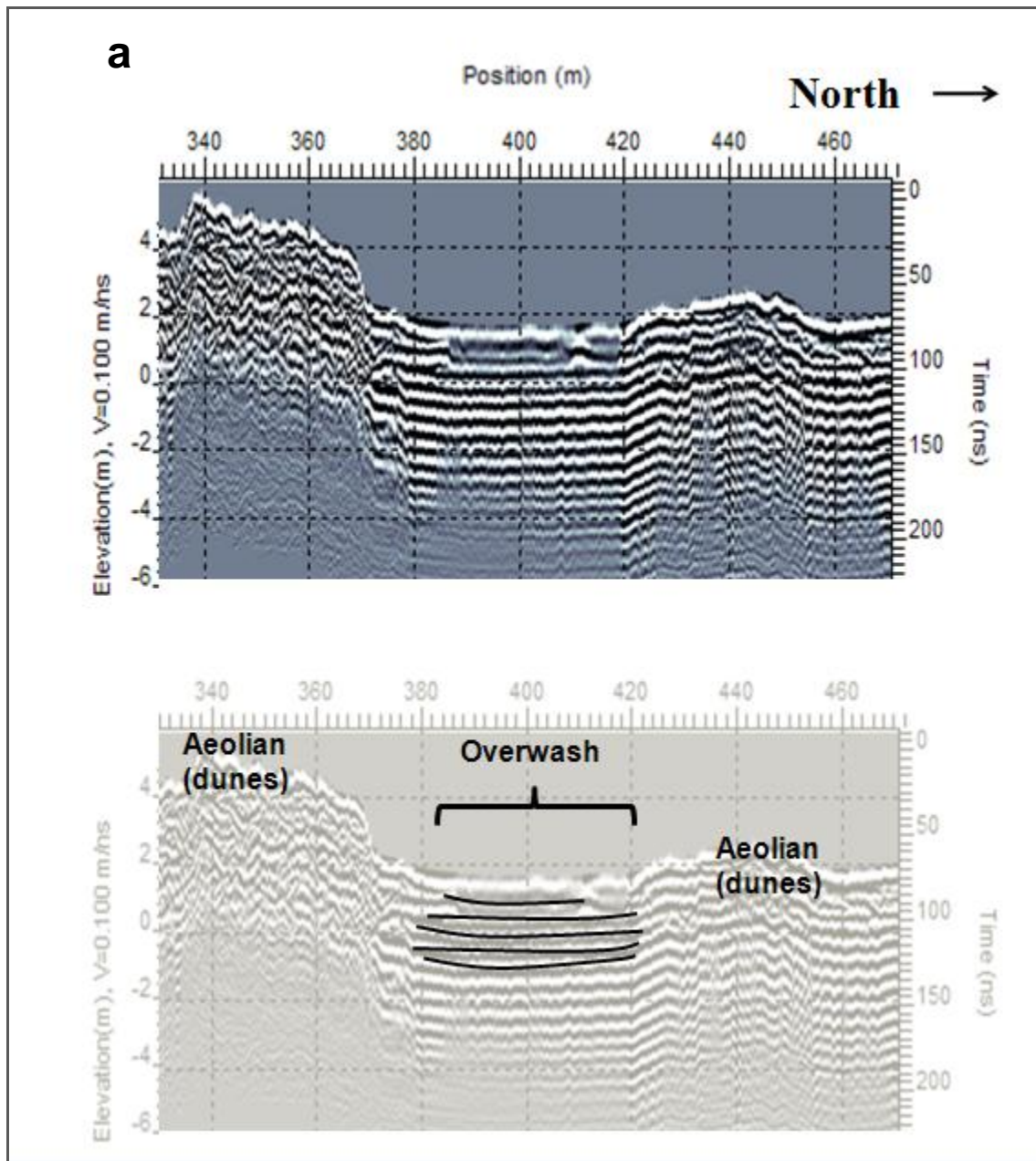


Figure 3.11. a) Example of an alongshore GPR profile through dunes and an overwash zone near Site B on Metompkin Island, illustrating the clear distinction between aeolian and overwash radar facies. Depth of signal penetration was unusually high in this overwash zone. Artificial repeat reflections under the overwash zone occur below the deepest highlighted flat-lying reflection (elevation ≈ -1 m).

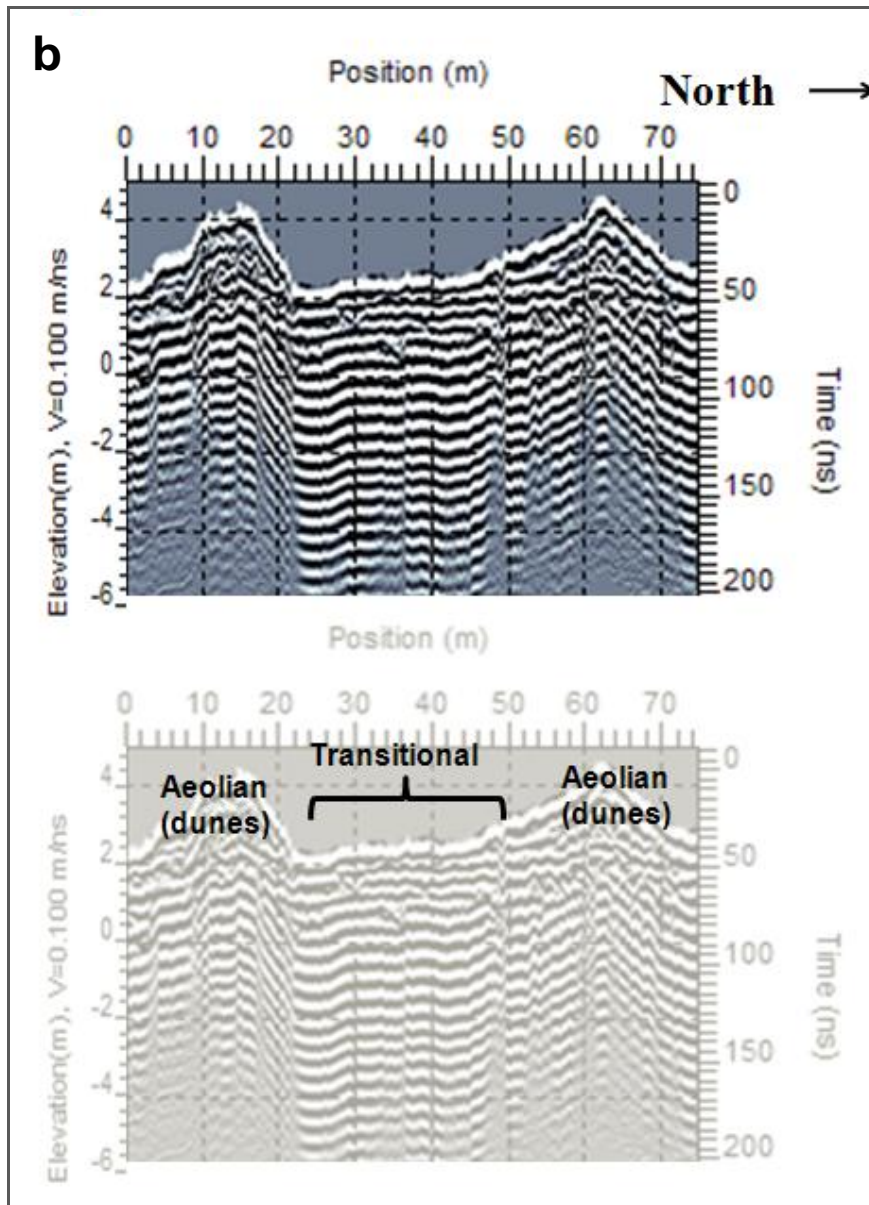


Figure 3.11(cont.). b) Example of an alongshore GPR profile through dunes and a transitional area (former overwash with aeolian surficial reworking) at Site C on Metompkin Island, showing the difference between aeolian and mixed aeolian/overwash radar facies. Artificial repeat reflections under the transitional area begin at elevation ≈ -1 m, and under the dunes at elevation ≈ 1 m.

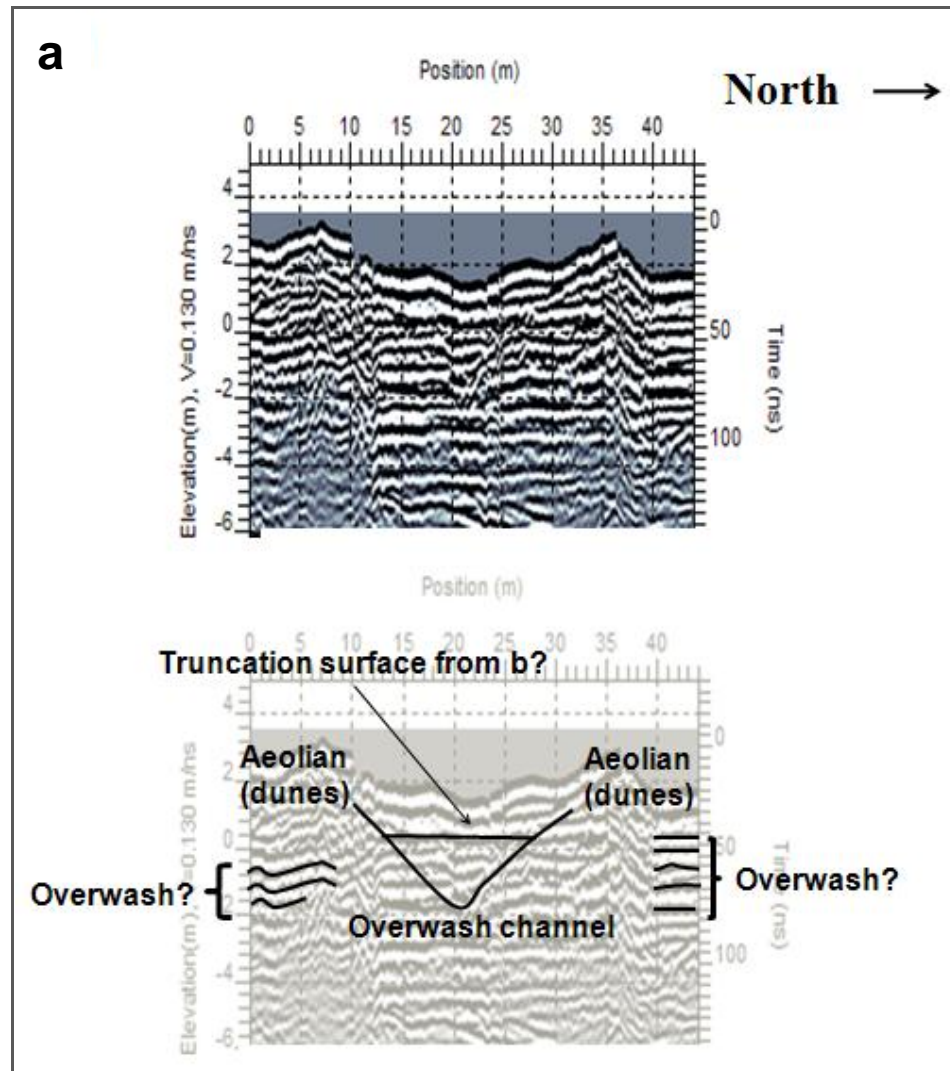


Figure 3.12. a) Interpretation of an alongshore GPR profile through the relict overwash channel at Site B on southern Hog Island. Cores HI B-2010-1 and 2 were obtained in a ~10 m alongshore section through the overwash channel.

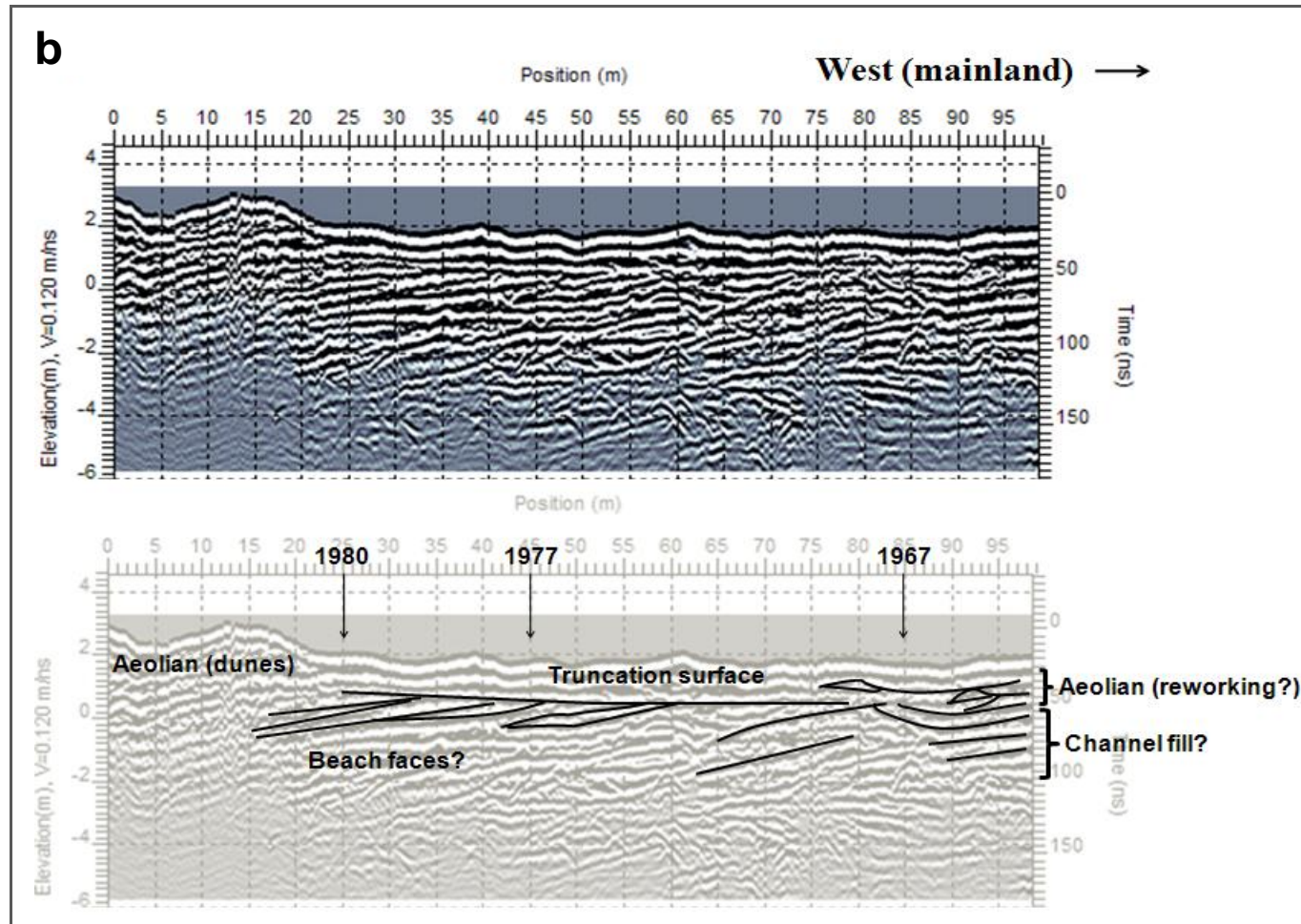


Figure 3.12 (cont.). b) Interpretation of a cross-shore GPR profile (starting at the foredune crest) at Site B on Hog Island, normal to the profile in (a) (intersection at ~20 m in (a), ~50 m in (b)). A relict overwash channel begins at ~25 m and extends through the western end of the transect. Dates with arrows indicate historic shoreline positions.

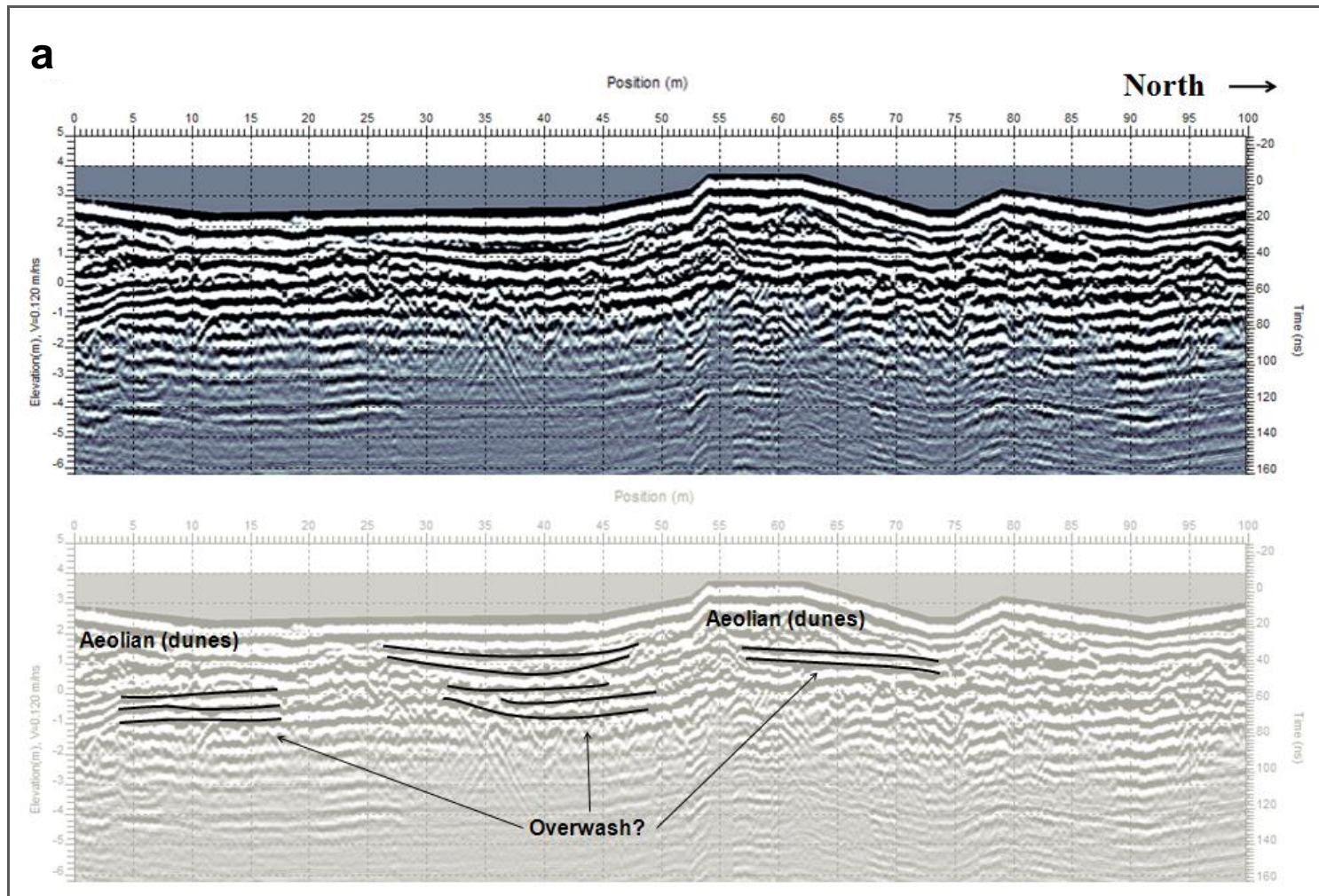


Figure 3.13. a) Interpretation of an alongshore GPR profile along the secondary dune at Site F on northern Hog Island. Due to malfunctioning GPS, we applied topographic corrections using an estimated profile based on field notes and elevation data collected during vegetation surveys.

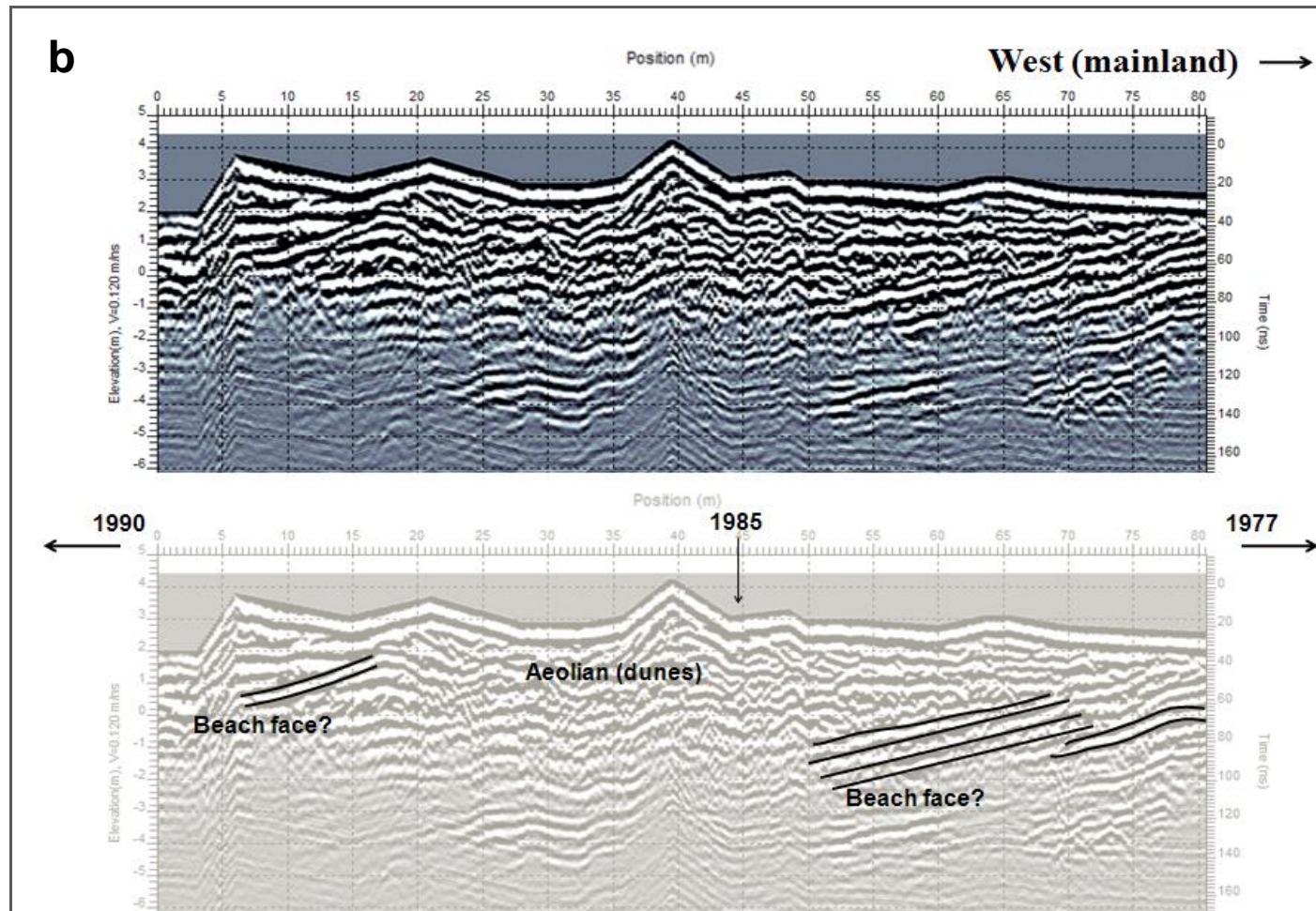


Figure 3.13 (cont.). b) Interpretation of a cross-shore GPR profile through dunes (starting at the foredune toe) at Site F on northern Hog Island, normal to the profile in (a) (intersection at ~50 m in (a), ~20 m in (b)). Dates with arrows indicate historic shoreline locations (1990 and 1977 are within ~50 m of either end of the transect). Due to malfunctioning GPS, we applied topographic corrections using an estimated profile based on field notes and elevation data collected during vegetation surveys.

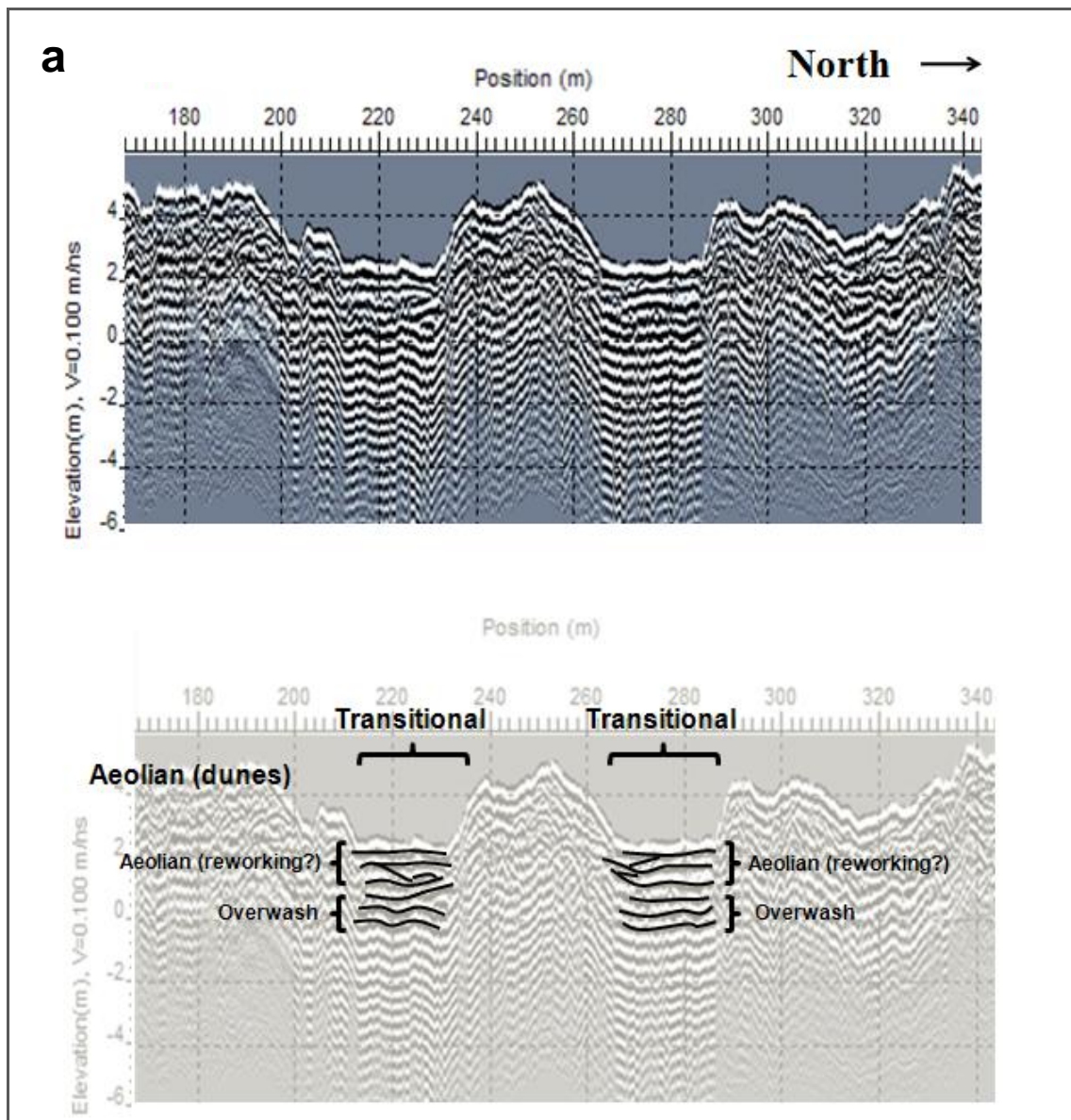


Figure 3.14. a) Interpretation of an alongshore GPR profile through dunes and transitional areas near Site B on southern Metompkin Island (from the same transect as Figure 3.11a). Numerous repeat reflections are evident, particularly underlying the overwash facies, beginning at elevation ≈ 0 m.

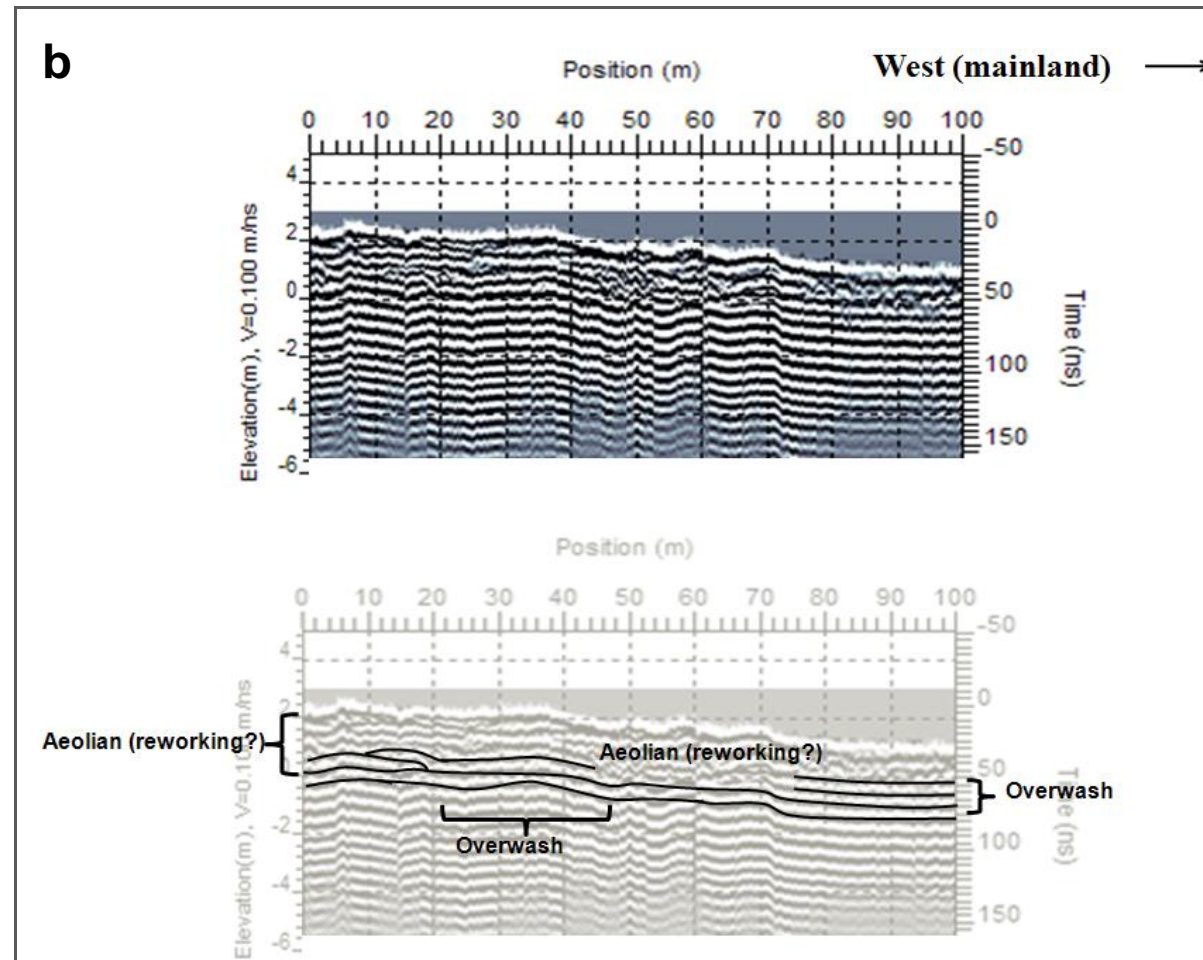


Figure 3.14 (cont.). b) Interpretation of a cross-shore profile through a transitional area at Site C on southern Metompkin Island, normal to the transect in Figure 3.11b (intersection at ~35 m in that figure, ~5 m in this figure). Numerous repeat reflections are evident beginning at elevation ≈ -1 m. Cores MI C-2010-3, 1, and 2 were collected at ~0 m, ~20 m, and ~90 m on this transect, respectively.

Cores

Cores were associated with Sites B and C on Hog Island, as well as an intermediate location (X) between the two sites, and Sites C and E on Metompkin Island (Figure 3.15), in both cross-shore and alongshore sections (see Appendix 4 for complete photos, descriptions, interpretations, and stratigraphic correlations of all cores).

On Hog Island, we obtained two short cores (< 1.5 m long, < 2.5 m deep), HI B-2010-1 and 2, in a 10 m alongshore section (Figures 3.15–16) through the relict overwash channel at Site B for the purpose of constraining GPR interpretations (and vice versa). These cores were characterized by moderately to very well sorted, fine to medium sand with heavy mineral laminations. Stratigraphic units with slightly coarser shell hash and/or planar heavy mineral laminations at depth transitioned up-core to units of better sorted, finer-grained, often frosted sediment displaying wavy, discontinuous, and/or cross-cutting laminations, as well as bioturbation near the surface (Figure 3.17). We interpreted this sequence as mixed-energy overwash deposits (or beach face deposits, which often appear similar to overwash in cores; Sedgwick and Davis, 2003) underlying possible aeolian deposition and reworking. The depth to the base of the possible aeolian units (0.5–1.5 m, depending on the core and the extent of compaction—see Figure 3.16 and Appendix 4) corresponded roughly to the depth of an apparent truncation surface in the associated cross-shore GPR profile (Figure 3.12), below which were overwash channel fill/beach face reflections consistent with the basal units in the cores.

We obtained three longer cores (1.5–6 m long, 2.5–7+ m deep) on Hog Island in an alongshore section starting from Site B and extending northward through interior

island locations known to have been affected by large-scale overwash during the 1962 Ash Wednesday nor'easter (when the shoreline was considerably landward of its current location): HI B-2010-3 (also part of a ~100 m dip section with B-2010-2), X-2010-1, and C-2010-1 (Figures 3.15–16). The characteristic pattern observed in these cores began with estuarine mud/intertidal deposits at the base (captured only in the two 4+ m cores, C- and X-2010-1; Figures 3.16 and 3.18–19). The estuarine/intertidal units were truncated by 1–2 pulses of planar-laminated, fine to medium sand that showed reworking (disturbed laminae) at the surface, interpreted as overwash (possibly part of a spit-building sequence). The surficial reworking at the surface of these units graded into organic-rich mud and muddy sand deposits containing roots and possible paleosols, which as a whole was interpreted as high marsh or low-lying stable interior facies. These deposits were truncated by 1–3 units of clean, planar, fine to medium sand; one core (C-2010-1) contained shells and exhibited textural evidence of depositional energy decreasing upward in each of these units (Figure 3.18), indicating pulses of overwash. The uppermost of these overwash deposits graded into possible aeolian and biologically reworked units underlying the modern surface, typified by rooted, mottled, fine to medium sand, sometimes exhibiting cross-cutting laminations (Figure 3.19). Overall, these longer Hog Island cores encompassed two sequences of stacked overwash deposits recovering into low-lying interior or high marsh environments (the current surficial environment at all three coring locations).

Cores on the rapidly transgressing Metompkin Island exhibited a somewhat different characteristic pattern. We obtained one core (MI E-2010-1) on northern Metompkin Island in an active overwash zone (Site E; Figures 3.15 and 3.20) after

augering ~1m through shell gravel and sand. Estuarine mud at the base of this core was overlain by a backbarrier marsh facies (sandy, bioturbated mud containing roots), which in turn was truncated by 3 clean, planar units of fine to medium sand with basal heavy mineral or shell lag deposits, signifying a decrease in depositional energy up-unit (i.e., 3 stacked pulses of overwash; Figure 3.21). The surface of the core site (recently overwashed) and the high shell content of the sediment removed by auger indicated that the augering process likely did not destroy any evidence of significant aeolian deposition near the surface.

On southern Metompkin Island, three cores (MI C-2010-1, 2, and 3) obtained in a ~100 m cross-shore section through a transitional area (Site C; Figures 3.15 and 3.20) corresponded fairly well to the associated GPR transect (Figure 3.14a): both appeared to show overwash (evident in the cores as shelly, fine to coarse sand in planar units) overlain by about 0.5–1 m (depending on cross-shore position and degree of compaction) of possible aeolian deposition and/or aeolian or biological reworking (evident in the cores as wavy, discontinuous, cross-cutting laminations and/or bioturbated sediments, commonly exhibiting quartz frosting). Estuarine and intertidal deposits were apparent at the base of all three cores. In the seaward-most core from this section (MI C-2010-3, Figure 3.22), overwash deposits showed a remarkable similarity to those in MI E-2010-1 (~6 km to the north). A possible ephemeral inlet deposit of mixed shell gravel and sand was present near the base of the landward-most core (MI C-2010-2, Figure 3.23).

Like the northernmost core (MI E-2010-1), these southern Metompkin Island cores were dominated overall by stacked overwash deposits. However, periods of

infrequent disturbance were suggested by thin, muddy or organic-rich layers (including possible paleosols), and 0.5+ m of possible aeolian/biological activity near the surface.

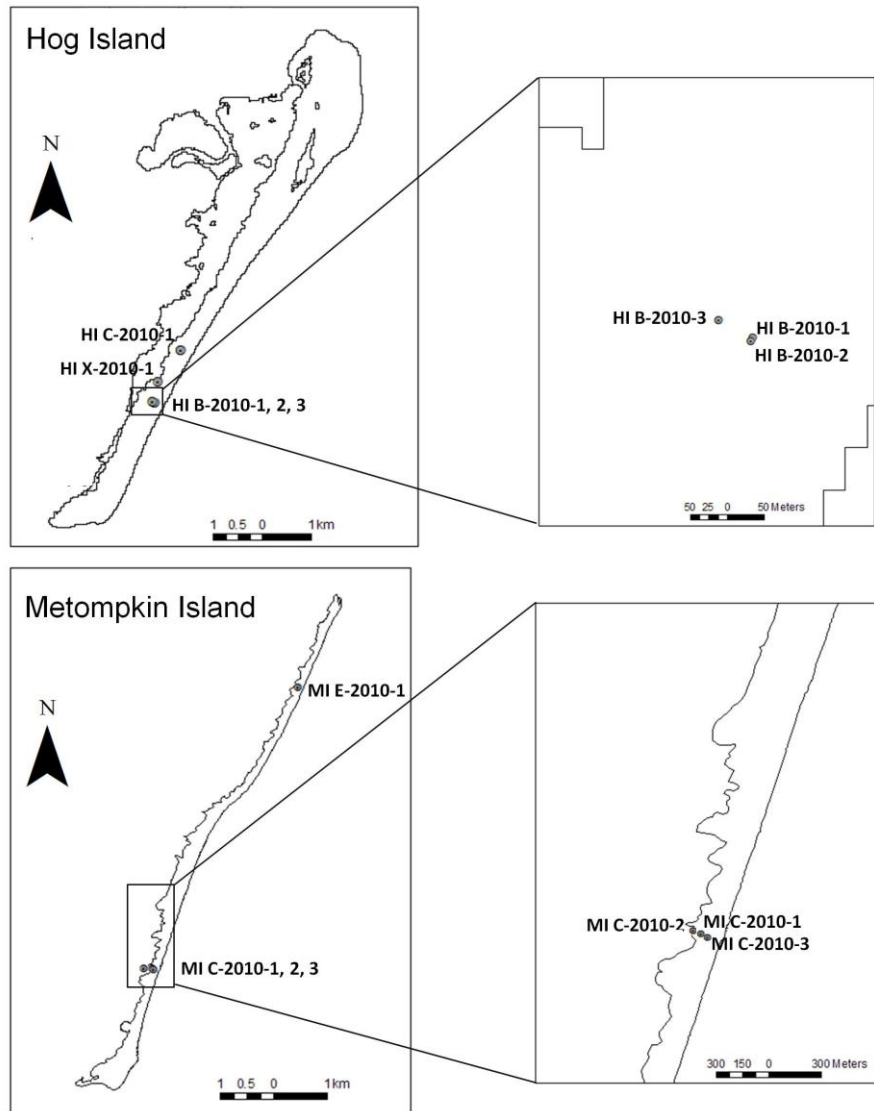


Figure 3.15. Maps of core locations on Hog and Metompkin Islands.

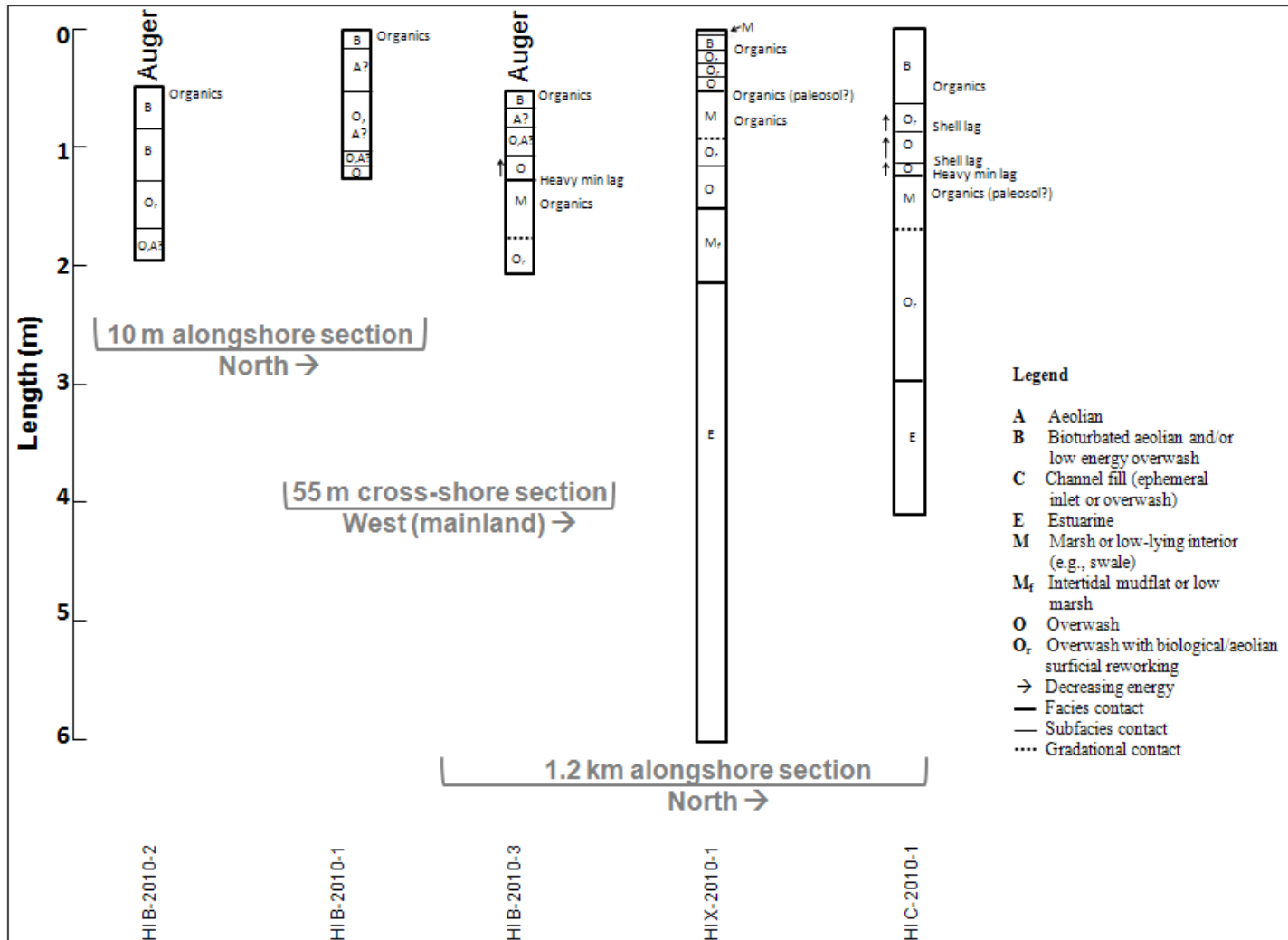
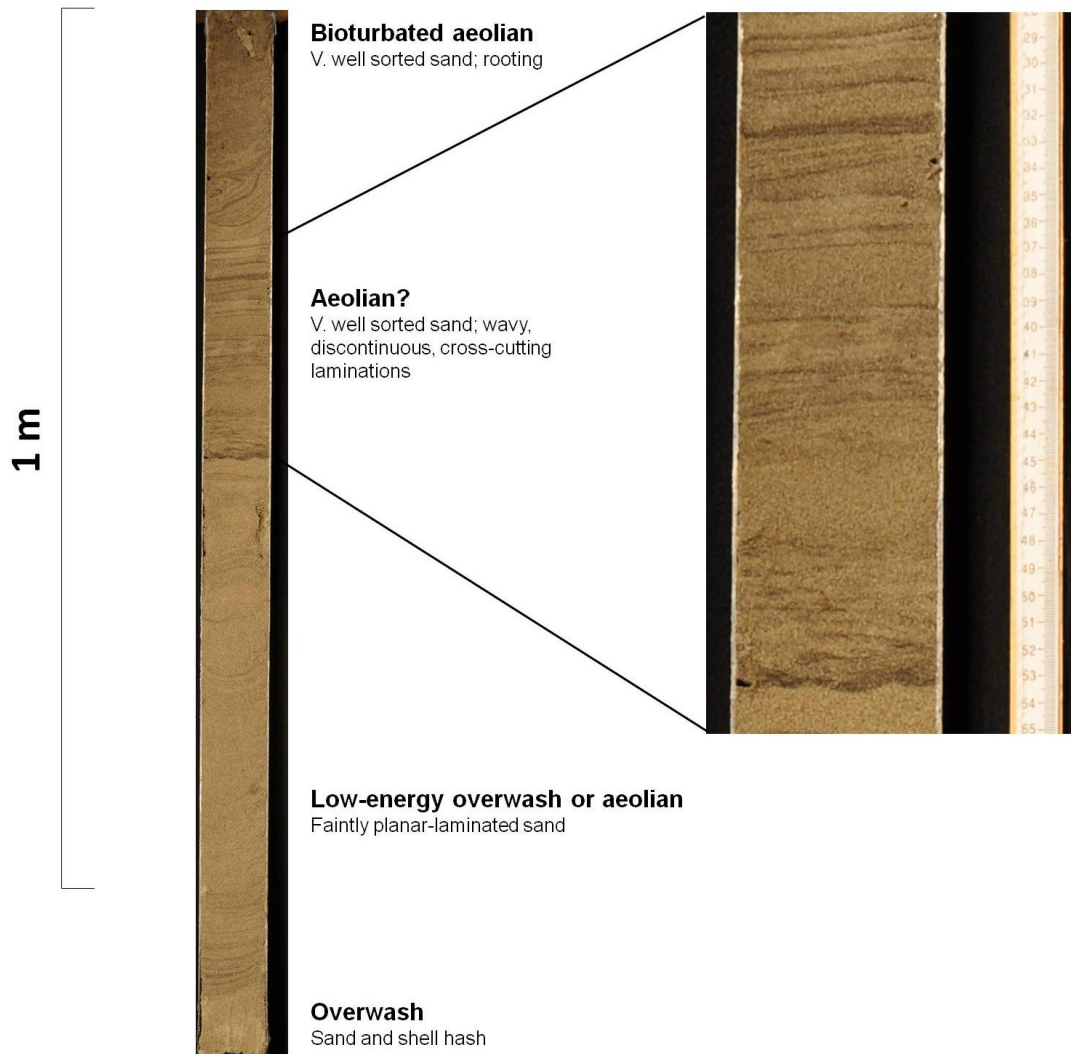


Figure 3.16. Interpretation of all Hog Island cores (see Appendix 4 for stratigraphic correlations). Lengths are not corrected for compaction.



Top - Bottom

Figure 3.17. Photo and interpretation of HI B-2010-1, a characteristic short core from Site B (relict overwash channel) on Hog Island. Wavy, discontinuous, and cross-cutting laminations suggesting aeolian deposition are enlarged in the right panel.

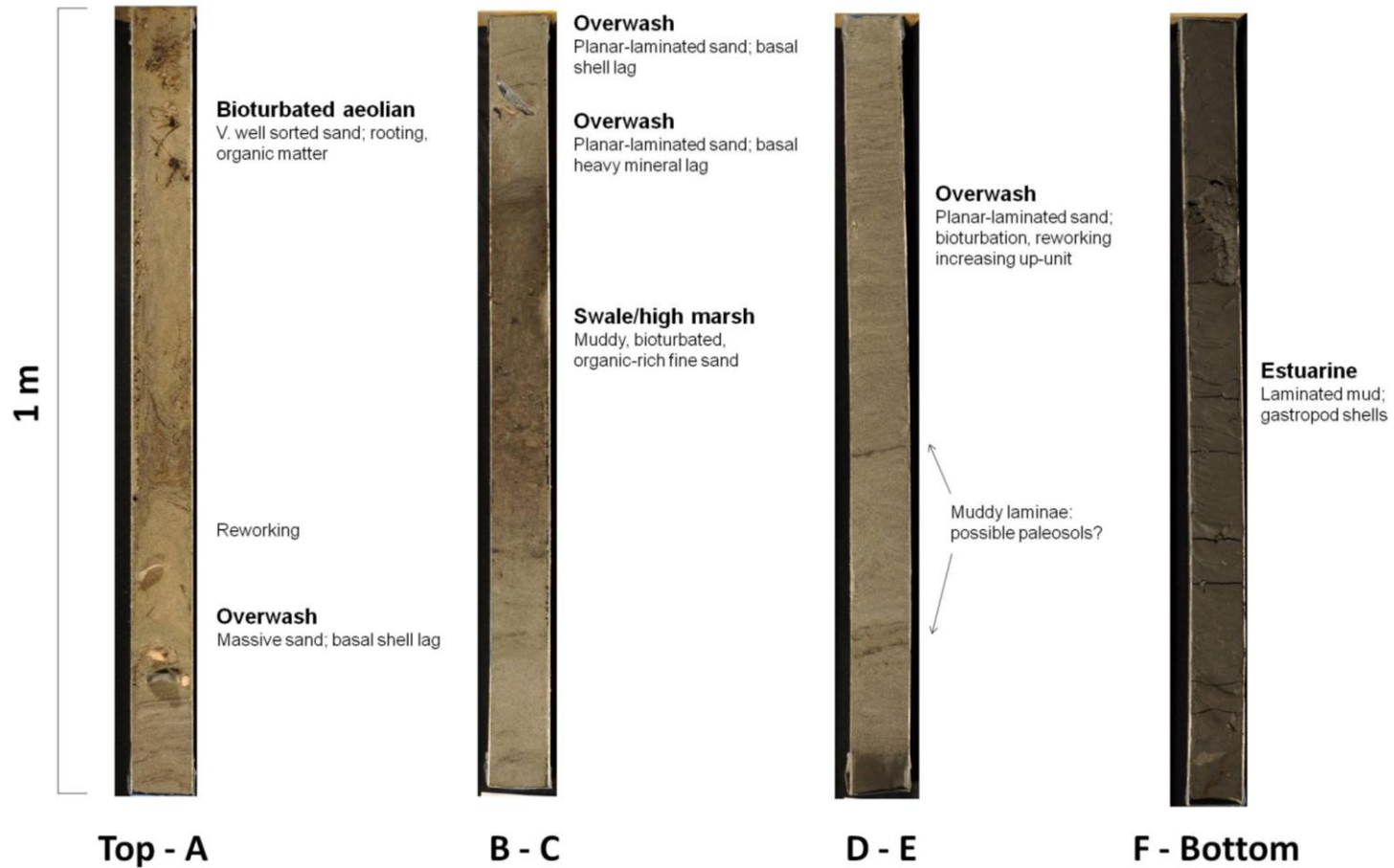


Figure 3.18. Photo and interpretation of HI C-2010-1, a characteristic long core from Hog Island, collected landward of Site C in the center of large-scale overwash associated with the 1962 Ash Wednesday nor'easter and subsequent storms (now part of the stable island interior).

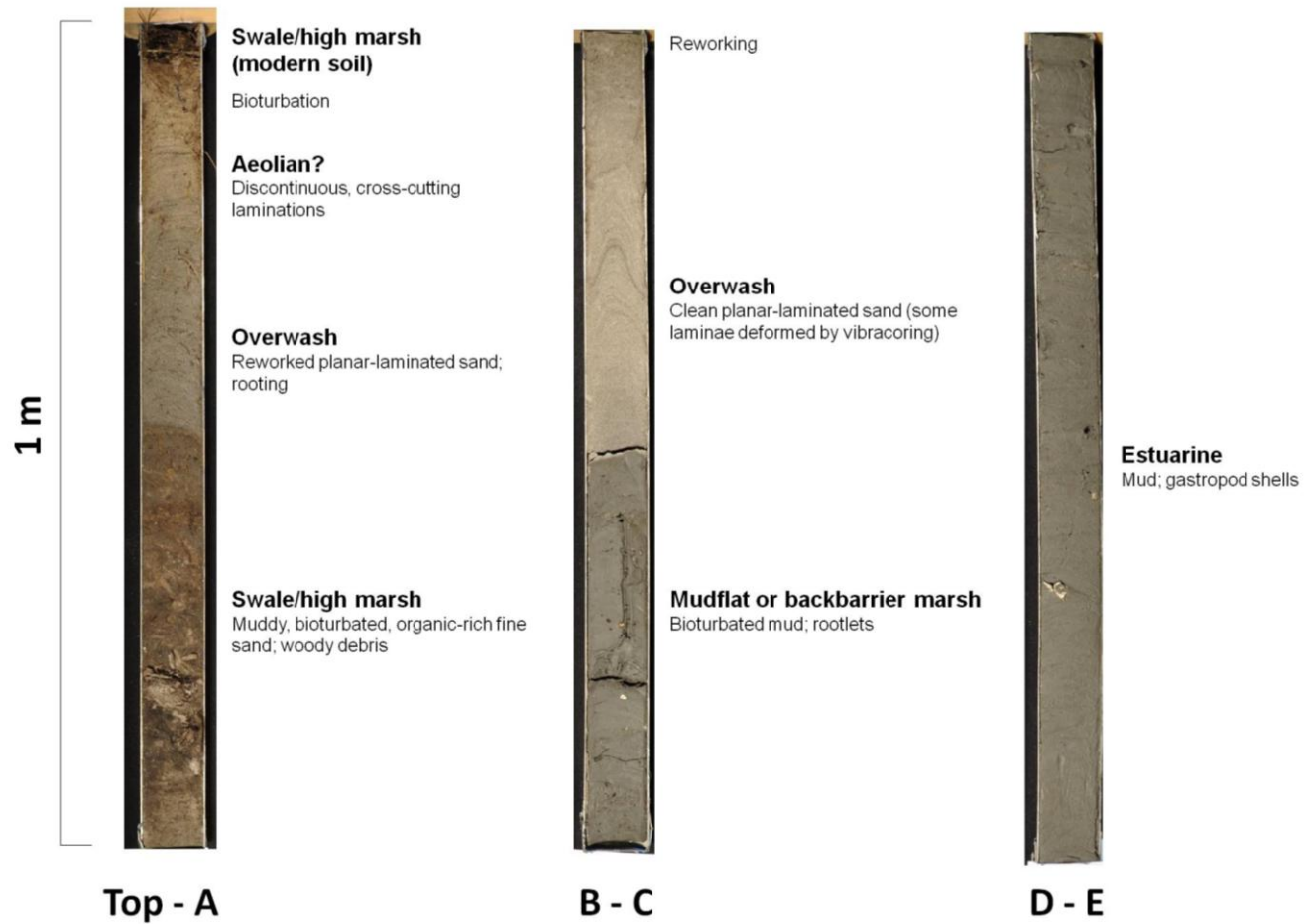


Figure 3.19. Photo and interpretation of HI X-2010-1, a characteristic long core from Hog Island, collected between Sites B and C at the distal extent of large-scale overwash associated with the 1962 Ash Wednesday nor'easter (now part of the stable island interior). The bottom 3 m (all estuarine mud) are not shown.

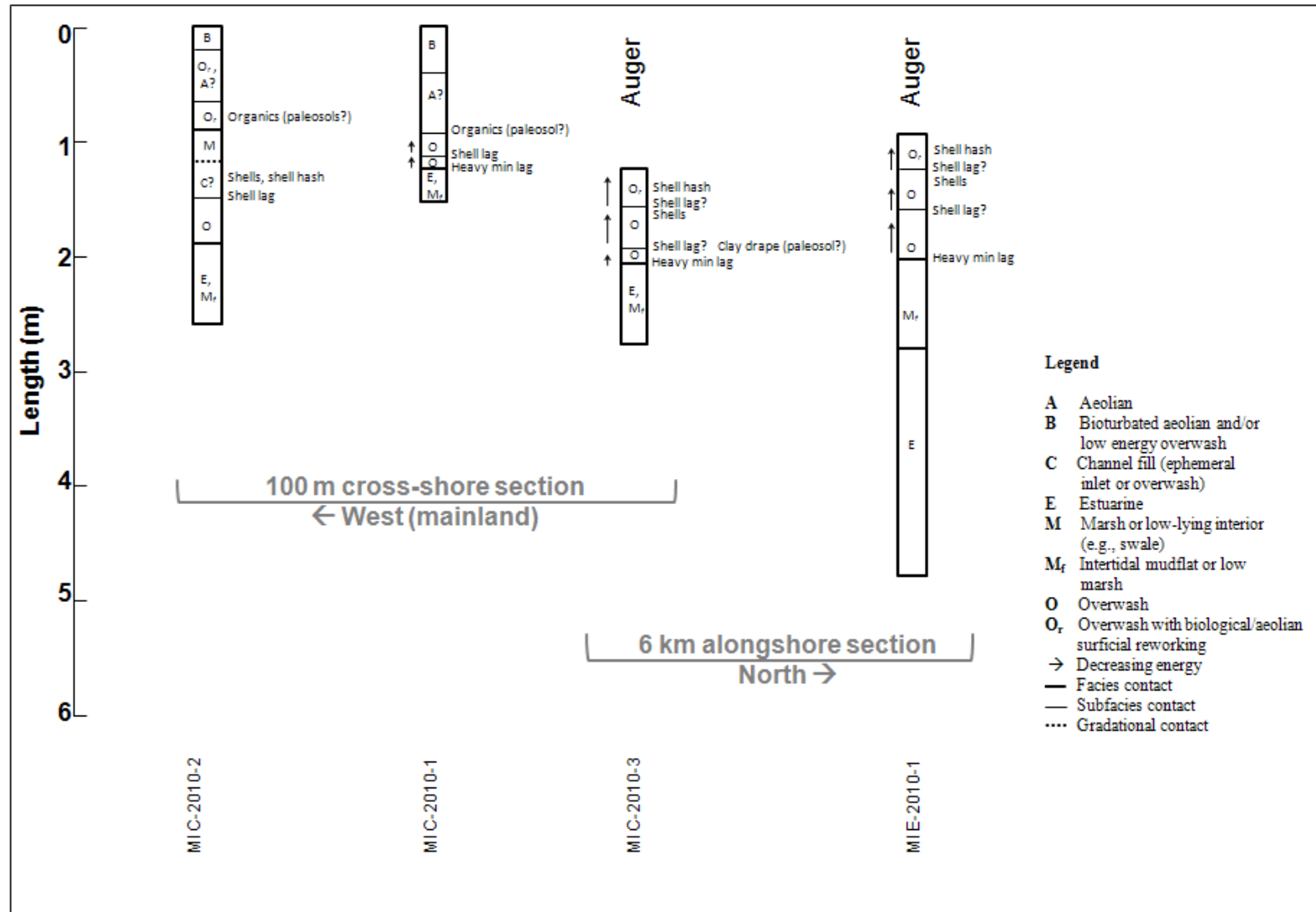


Figure 3.20. Interpretation of all Metompkin cores (see Appendix 4 for stratigraphic correlations). The length dimensions are not corrected for compaction.

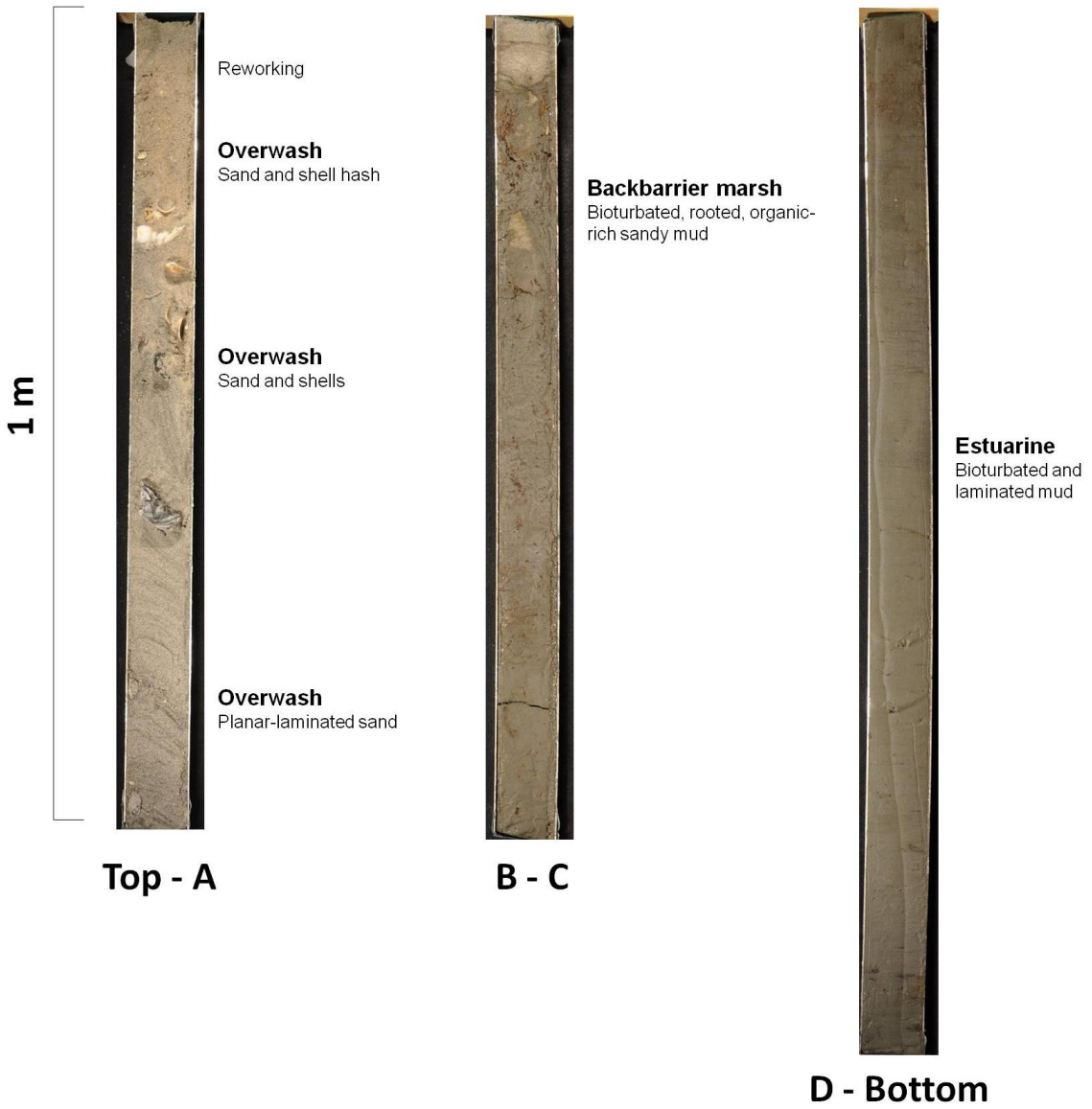


Figure 3.21. Photo and interpretation of MI E-2010-1 from Site E (active overwash) on Metompkin Island, collected near the vegetation line after augering 96 cm through layers of shell gravel and sand.

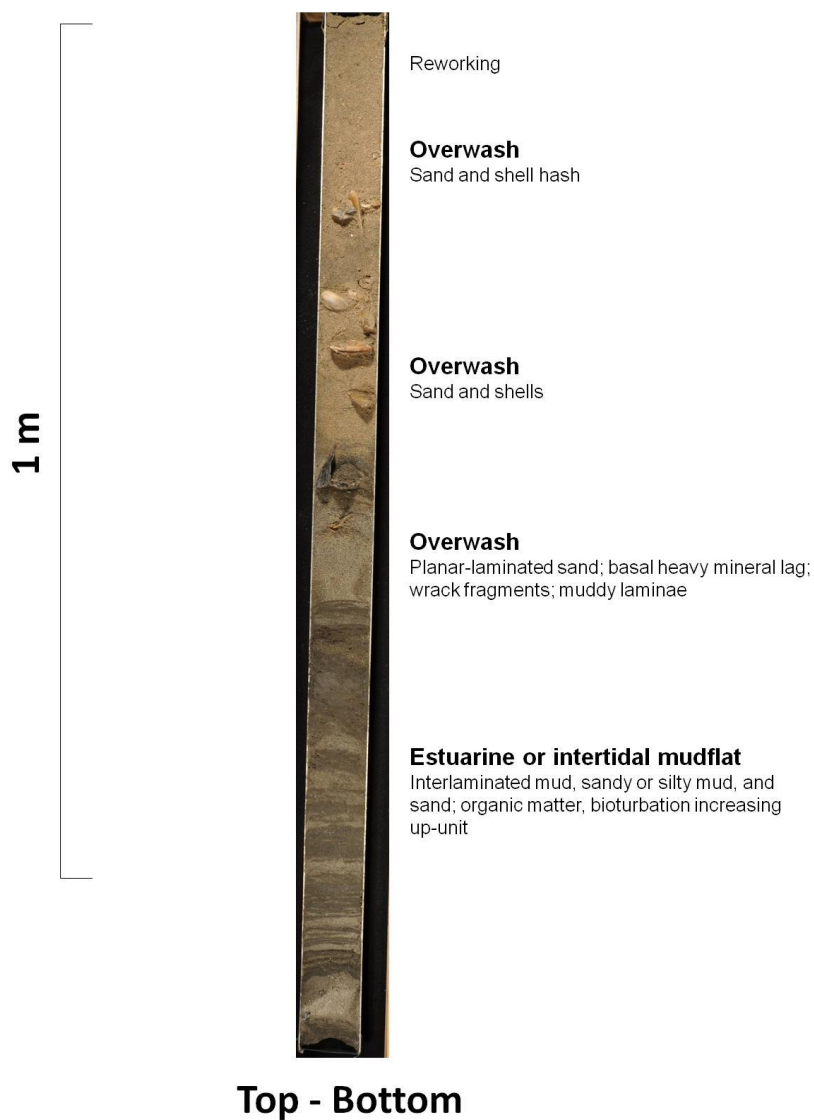


Figure 3.22. Photo and interpretation of MI C-2010-3 from Site C (transitional) on Metompkin Island, collected near the vegetation line (~20 m on the cross-shore GPR profile; Figure 3.14a) after augering 123 cm through sand and few shells. Note the strong similarities between the upper two overwash units in this core and MI E-2010-1 (previous figure), collected 6 km apart.

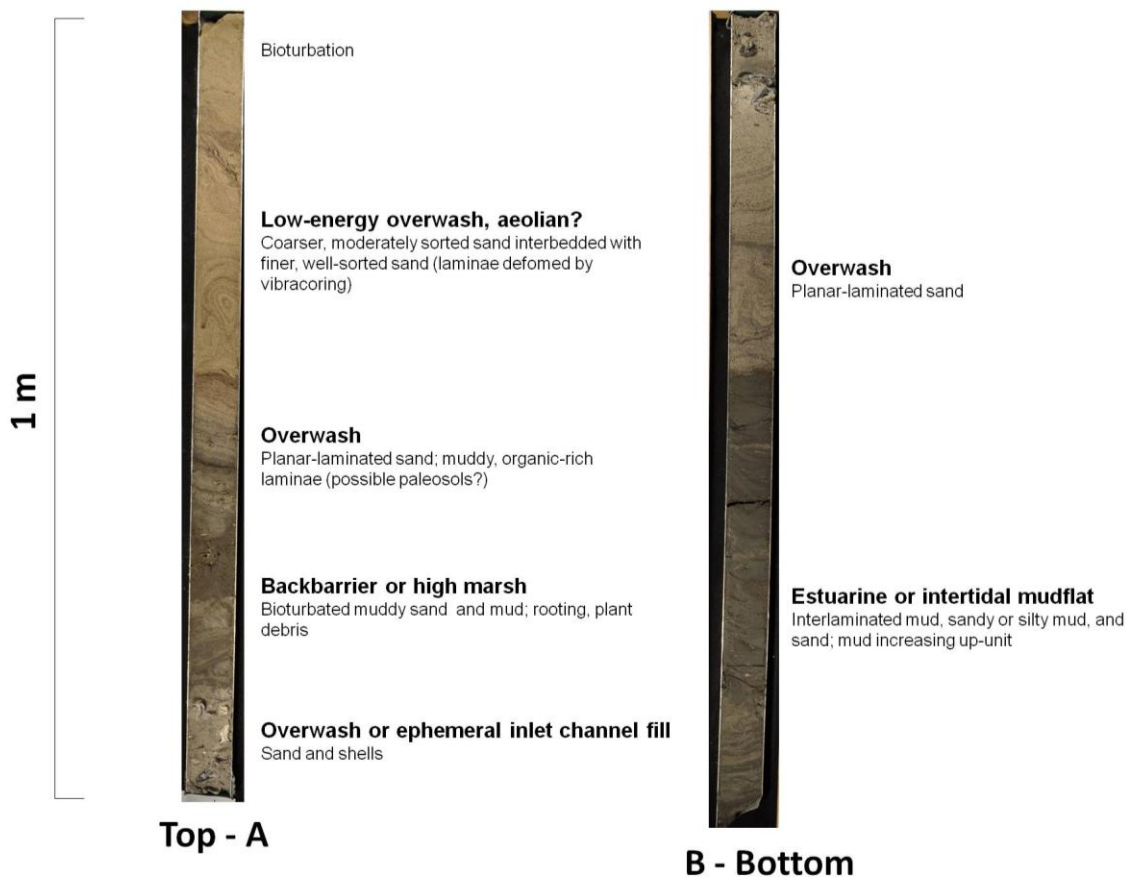


Figure 3.23. Photo and interpretation of MI C-2010-2 from Site C (transitional) on Metompkin Island, collected near the landward edge of the island (~90 m on the cross-shore GPR profile; Figure 3.14a).

4. DISCUSSION

Vegetation dynamics

The close association observed on both islands between dunes and *A. breviligulata* is consistent with the tendency of this species to thrive at higher elevations and to contribute to vertical accretion (dune-builder feedback). The similar (albeit weaker) relationship between *A. breviligulata* and transitional areas, particularly on Hog Island, supports the role of this grass in topographic recovery following disturbance. The co-occurrence of *S. patens* on dunes (on Hog Island) and in transitional areas is not entirely surprising: while both species have preferred habitats, they are also both fairly versatile and may grow under a range of conditions (see Appendix 1.1). The critical issue for our investigation is not where each species occurs, but the set of conditions (environments) under which each species *dominates*: in dune and transitional areas, *A. breviligulata* is dominant (i.e., likely to be more ecomorphodynamically important) relative to *S. patens* on both islands.

The key respect in which the two islands differ with regard to vegetation is the composition of species in overwash zones. Despite low overall vegetative cover, the significant association between overwash and the maintainer species *S. patens* on Metompkin Island—and the absence of this relationship on Hog Island—supports our hypothesis that the maintainer feedback is more likely to play a role where disturbance is more prevalent (i.e., on Metompkin Island). Again, while *A. breviligulata* did occur in overwash zones on Metompkin Island, the much stronger association with *S. patens* (the

dominant species)—which became especially clear when only vegetated sampling points were considered—is the essential differentiating factor in the context of this study.

On Hog Island, the marginal dominance of *A. breviligulata* in overwash zones (as well as dunes and transitional areas), although not a significant association in ISA, suggests that this island may follow the post-overwash trajectory typical of disturbance-resisting systems in which the dune-builder feedback is the primary ecomorphodynamic process—i.e., gradual recolonization by vegetation, with the ultimate success of *A. breviligulata* contributing to vertical accretion and the eventual redevelopment of dunes (Godfrey et al., 1979; Figure 1.3). Furthermore, while relict overwash channels (now cut off from the active beach by continuous, accretional dunes) on southern Hog Island are ecologically distinct from the surrounding dunes and swales, their preservation likely is not a product of the maintainer feedback (since no relationship with *S. patens* was apparent), but rather of local shoreline accretion subsequent to channel incision (Harris, 1992).

The difference in species dominance between swales on Hog Island and Metompkin Island (*S. patens* vs. *A. breviligulata*, respectively) may be explained by differences in island morphology, and consequently in freshwater availability. Hog Island is a wide (~1 km), high-relief barrier with multiple shore-parallel dune ridges, and thus is likely to retain a relatively large freshwater lens that discharges in the interdunal swales. In contrast, Metompkin Island is thin (< 0.5 km) and low-relief, typically having only a single dune ridge; consequently, the swales sampled on Metompkin Island are flat, open platforms running from the dune ridge to the marsh. Freshwater on this island is probably limited and not likely to pool in these swales, resulting in drier soils than in the swales

between the foredune and tertiary dune ridges on Hog Island. The success of *S. patens* in swales on Hog Island but not on Metompkin Island, therefore, likely arises from its tendency to grow more densely in wet soils. Given the dominance of this species in Hog Island swales, if the frontal dunes were lost to erosion (thereby linking swales to the active beach), the maintainer feedback potentially could become a more important dynamic here than it currently appears to be: increased overwash exposure in low, flat areas already densely populated by an overwash-adapted maintainer species would likely inhibit topographic recovery. This scenario would likely arise first at the rotational axis of the island, where overwash is already beginning to encroach on a wide, marshy swale.

The sharper ecological distinction (with respect to *A. breviligulata* and *S. patens*) between morphologic environments on Metompkin Island relative to Hog Island, which was particularly evident when only vegetated sampling points were considered, may be the result of differences in disturbance regime. On Hog Island, the relative rarity of disturbance (both spatially and temporally) may allow grass communities to intermingle over time; when overwash does occur, seed dispersal in wrack and lateral encroachment by surrounding vegetation determines the composition of the recovering community (e.g., Fahrig et al., 1993; Godfrey et al., 1979), as expected for a disturbance-resistant island where the dune-builder feedback is dominant. On Metompkin Island, however, disturbance is comparatively heterogeneous. Frequent, widespread disturbance in low-relief overwash zones may lead to the dominance of only the most overwash-adapted species (i.e., *S. patens*), while the infrequently disturbed, patchy dunes—which are characterized by relatively high elevations (Figure 3.1)—tend to be occupied largely by species that prefer higher topographic roughness and drier soils (i.e., *A. breviligulata*).

Thus, Metompkin Island may be an example of a barrier in which both feedbacks play an important role: discontinuous but relatively tall dunes in the south resist overwash *locally* (remaining dunes), while low elevations and the dominance of *S. patens* reinforce continued disturbance in widespread overwash zones (particularly in the north), leading to distinct communities. In other words, while disturbance is more frequent overall on Metompkin Island, spatial heterogeneity within this disturbance regime introduces greater compositional variability between morphologic environments.

Stallins and Parker (2003), in a comparison of two barriers in separate island chains, found that compositional variability was higher in the *less* frequently disturbed system, a result which initially appears to contradict our findings. However, unlike our study, their work compared a completely overwashed barrier (as the frequently disturbed end-member) with a barrier consisting of alternating dunes and overwash zones (as the infrequently disturbed end-member). The authors argued that spatially homogeneous disturbance in the former case (i.e., overwash zones only) led to relatively uniform communities, while spatially heterogeneous disturbance in the latter case (i.e., overwash alternating with dunes) produced a patchwork of distinct communities. Thus, our findings are in fact similar: because disturbance on Hog Island as a whole is *homogeneously* infrequent, vegetative composition in different morphologic environments may become more similar over time, while comparatively frequent (overall) but *heterogeneous* disturbance on Metompkin Island introduces greater compositional variability between dunes, transitional areas, and overwash zones.

Physical dynamics

Properties of surficial sediment < 2 mm do not appear to influence topographic roughness on either island. While statistically significant differences were evident between islands and sites, and while overwash-dominated sites tended to be texturally distinct from other sites, appropriately-sized sediment for aeolian transport (fine to medium sand) was abundant at all sites. Beach width may affect dune development by controlling the supply of this sediment (as suggested by the relationship between beach width and mean elevation on Hog Island), but the sediment itself is not likely to be a limiting factor.

However, on Metompkin Island, the variability in shell gravel content (> 2 mm) between sites suggests that armoring may influence morphological differences on this island. The correlation between low topographic roughness and high shell gravel content indicates that armoring may have a suppressive effect on topographic recovery, particularly in the northern overwash terraces (Sites D, E, and F) where thick, extensive shell deposits were observed in the field. Shell armoring may be a factor in transitional areas as well: Site C was low-lying in spite of apparently sufficient sand supply (moderate beach width, abundant fine to medium sand), the presence of *A. breviligulata* (dominant with respect to *S. patens*), and evidence of possible aeolian deposition near the surface—perhaps because surficial shell gravel was more prevalent here than at other sites along the southern half of the island.

Elevation itself may also be an important variable in limiting topographic development on Metompkin Island. Priestas and Fagherazzi (2010) found that exceptionally low elevations produced by scouring can inhibit recovery after overwash.

Although certain species of vegetation are tolerant of some flooding (e.g., *S. patens*; Silander and Antonovics, 1979), recolonization may be limited if inundation occurs too frequently (e.g., if elevations are lower than in typical overwash zones). Furthermore, if sand is often or always wet, transport by wind (and thus dune recovery) is likely to be restricted. Aerial photos and field reconnaissance show that the large, especially low-relief overwash fan at Site A on southern Metompkin Island—a site located at the widest part of the beach and surrounded by dunes—has been extant since at least 2007, without any noticeable changes to its dimensions. Vegetation and shell cover were almost entirely absent at this site during field expeditions in 2009 and 2010, making it distinctive from the overwash-dominated sites on northern Metompkin Island (although it was representative of smaller-scale overwash zones observed elsewhere along the island’s southern half). The elevation of Site A relative to the wet/dry line and the beach was lower overall than at other sites (Figure 3.1), and during field visits, the surficial sand was generally wet. This suggests that relative elevations here may be low enough to allow regular flooding to occur at high tide levels, either as a result of the freshwater lens rising with the saline water table (e.g., Hayden et al., 1995), or due to spillover from a frequently inundated runnel observed on the adjacent beach. Thus, the overwash fan at Site A may have persisted not because of the presence of maintainer species or shell armoring (as in the north, where overwash terraces have persisted at least as long; Figure 3.9), but rather because of recurrent flooding due to critically low elevations.

On Hog Island, the occurrence and persistence of overwash appears to be related principally to rotational shoreline dynamics. Large-scale overwash currently occurs only at the rotational axis of the island (lowest observed elevations, Sites D and E; Figures 1.5

and 2.1), where the beach has been narrowing over the last several decades (Fenster and Hayden, 2007) and is presently thinner than at any other point on the island; this relationship between beach width and overwash distribution on Hog Island reflects the generally recognized role of windblown sand supply and shoreline position in the (re-) development of dunes and the determination of disturbance frequency (e.g., Bauer and Davidson-Arnott, 2002; Fahrig et al., 1993). The rotational axis of the island has also been the sole site of persistent overwash over the last several decades as the shoreline has eroded locally (Figure 3.9). On the other hand, the *recovery* of an area of persistent overwash on southern Hog Island (apparently initiated during the Ash Wednesday storm, as indicated by aerial photo analyses) occurred in association with a local shift from shoreline erosion to accretion ca. 40 years BP. Moreover, overwash has recovered into dunes on both northern and southern Hog Island (evident in GPR surveys) in areas associated with recent local shoreline accretion (Fenster and Hayden, 2007). Thus, narrow and eroding shorelines may be linked to overwash persistence, while accreting shorelines appear to be related to overwash recovery.

The characteristic repeating sequence in the longer cores from southern Hog Island (backbarrier or stable interior facies truncated by overwash, overwash grading into aeolian or stable interior facies) generally resembles the stratigraphic pattern of overwash and aeolian units overlying organic-rich, muddy backbarrier strata observed by Godfrey et al. (1979) in a disturbance-resistant barrier system (Nauset Spit, MA). The stratigraphic sequence identified in our cores further underscores the role of rotational shoreline change in overwash dynamics on Hog Island, suggesting that overwash may persist in the short term when the local shoreline is eroding (as the southern shoreline was

during the clockwise rotational episode that began in the late 1800s; Harris, 1992) and/or in response to extreme events like the Ash Wednesday storm, but that it gradually recovers into dunes or stable interior when the shoreline reverses and becomes accretional (as the southern shoreline did in the late 20th century).

In contrast to Hog Island, overwash occurrence and persistence do not appear to be related to local beach width or patterns of shoreline change on Metompkin Island; rather, overwash is spatially widespread and has been prevalent across time scales of at least decades. The greater coverage and spatial and temporal overlap of overwash on Metompkin Island (as determined by aerial photo analyses) indicate that overwash has been more persistent here than on Hog Island. The absence of a relationship between beach width and mean transect elevation suggests that factors affecting sand transport/supply *other* than beach width—such as the dominance of maintainer species (northern Metompkin Island), critically low elevations (southern Metompkin Island), and/or the presence of shell armor (both northern and southern Metompkin Island)—may be contributing to the occurrence and maintenance of low topographic roughness.

While we were not able to isolate any specific instances of overwash recovering into dunes on Metompkin Island, some aeolian deposition and reworking in the low-lying transitional areas between dunes appeared to be evident in GPR and cores from Site C. Considered along with the organic-rich, muddy laminae (possibly paleosols) observed in the cores, this stratigraphic evidence suggests that periods of infrequent disturbance may have occurred in these low-lying areas on southern Metompkin Island. Intervals of infrequent disturbance may explain why the surficial sedimentological characteristics of overwash-dominated (Site A) and transitional (Site C) areas on southern Metompkin

Island were more similar to those of the dune-dominated Site B than the coarser, more poorly sorted distributions associated with the overwash terraces on the northern half of the island.

In contrast, comparatively frequent disturbance on northern Metompkin Island has contributed to a uniform morphology of active overwash terraces. This current morphology may also be representative of conditions over the past several decades, as indicated by the stacked deposits of clean planar sand and shells in the northernmost core, with no apparent evidence of paleosol development, lower energy conditions, or any facies other than overwash overlying the backbarrier marsh.

Overall, the stratigraphic pattern observed in cores on Metompkin Island largely resembles the sequence identified by Godfrey et al. (1979) in a disturbance-reinforcing barrier system (Core Banks, NC): repeated high-energy overwash deposits, sometimes with organic-rich (paleosol?) layers associated with low or high marsh. This stratigraphic resemblance to a disturbance-reinforcing system—which contrasts sharply with the sequence observed on Hog Island—further suggests that overwash is more persistent on Metompkin Island, thereby supporting our hypothesis that the maintainer feedback is more likely to be playing a role (reinforcing disturbance) here.

Synthesis and implications

Though Hog and Metompkin Islands have evolved in response to a range of physical drivers (see Appendix 1.2) which have established different overall disturbance regimes on the two islands (infrequent vs. frequent, respectively), ecomorphodynamic feedbacks (along with physical processes) have contributed to the continuation of these

disturbance conditions. Here we consider synthetically the contributions of both physical and ecological factors within the framework of ecomorphodynamic models of disturbance resistance and reinforcement (Figure 4.1).

Hog Island generally appears to conform to the disturbance-resistant model of barrier island vulnerability. High-relief, continuous dunes built by *A. breviligulata* resist overwash; in the apparently rare event that overwash does occur (e.g., during extreme storms or in association with exceptionally narrow beaches), dune recovery happens gradually via recolonization by *A. breviligulata*, as evinced by the dominance of this species in overwash and transitional areas—except where physical conditions such as beach width are prohibitive. Overwash may persist where the beach is narrow and eroding, but where the beach is accreting, overwash recovers into dunes (as indicated by GPR surveys) or stable interior (as indicated by cores), depending on distance from the prograding shoreline.

Overall, the distribution and persistence of overwash on Hog Island does not appear to be a function of the maintainer feedback, but rather of rotational shoreline dynamics and sand supply mediated by changes in beach width. As hypothesized, the dune-builder feedback appears to be the dominant ecomorphodynamic process on this island.

Metompkin Island, on the other hand, may be classified overall as a disturbance-reinforcing system (although patchy dunes in the southern half of the island resist disturbance locally). Overwash occurs frequently on this low-relief barrier, driving the island's rapid landward migration (Byrnes and Gingerich, 1987). Spatial and temporal persistence of overwash is considerably greater than on Hog Island (although rapid

transgression between the 1950s and the 1990s obscures this signal to some extent). On the northern half of Metompkin Island—where overwash is more widespread and apparently more frequent than on southern Metompkin Island—the presence of shell armoring and the dominance of the maintainer species *S. patens* combine to reinforce continued disturbance, resulting in the development of persistent overwash terraces. On the southern half, where periods of infrequent disturbance in low-lying areas appear to have taken place, *A. breviligulata* successfully colonizes sites of previous disturbance and some aeolian deposition may occur (as suggested by vegetation frequencies, GPR surveys, and cores from transitional areas), but shell armoring may ultimately suppress the reestablishment of fully formed dunes; in addition, if overwash incises the island surface to critically low elevations, recovery of vegetation and topography may not be possible. Shell armoring and critically low elevations therefore may result in the persistence of low, flat topography among the discontinuous dunes in the south.

The distribution and persistence of overwash on Metompkin Island thus appears to be influenced by a combination of interacting physical and ecological factors: transgressive shoreline behavior, sedimentological and morphological characteristics, and ecomorphodynamic feedbacks. On this island, both the dune-builder feedback (south) and the maintainer feedback (north) appear to contribute to the development and maintenance of morphology, resulting in sharp compositional distinctions between morphologic environments.

Consistent with our hypothesis, the maintainer feedback appears to be more important on Metompkin Island as whole than on Hog Island, although we emphasize that it is not the primary driver of or sole influence on overwash frequency; rather,

physical factors such as shell armoring, critically low elevations, and initial conditions conducive to frequent disturbance also play crucial roles in limiting sand supply for dune building and reinforcing persistent disturbance (see Figures 1.2 and 4.1). Maintainer species may have a greater impact in the presence of shell armoring (e.g., in the overwash terraces on northern Metompkin Island), since these two factors are likely to reinforce the effects of one another (as long as armoring is not extensive enough to entirely suppress the recolonization of vegetation). Moreover, armoring may limit available space for recolonization, making the dominance of *S. patens* in those areas in which vegetation *can* grow even more impactful.

In aggregate, therefore, the Virginia Coast Reserve (VCR) is an ecomorphodynamically “mixed” barrier system in which both disturbance-resistant and disturbance-reinforcing conditions exist, and in which both *A. breviligulata* and *S. patens* appear to be morphodynamically important species. In the VCR—as well as in other systems where continuous dune-building grasses and overwash-adapted maintainer species coexist—infrequently disturbed, high-relief islands are likely to resist disturbance via the dune-builder feedback (with maintainer species playing a subordinate role), and physical processes (e.g., shoreline dynamics) are likely to determine where overwash will be persistent. Conversely, on frequently disturbed, low-relief islands, the maintainer feedback is likely to be more influential (assuming disturbance frequency is not so high that all vegetation is suppressed), with both physical and ecological processes controlling the occurrence of persistent overwash.

Though quantifying the effects of the maintainer feedback is beyond the scope of this study, our findings have significant implications for barrier island evolution under

changing climate conditions. As sea level rises and storms become more intense, disturbance frequency on barrier islands is likely to increase. Consequently, overwash persistence may also increase in barrier systems like the VCR, especially if the maintainer feedback becomes progressively more important in reinforcing vulnerability. In combination with physical dynamics, this feedback—while not responsible for initiating frequent disturbance—nevertheless has the potential to intensify barrier island response to climate change by accelerating large-scale shifts from dune-dominated to overwash-dominated morphologies (i.e., from the top scenario to the bottom scenario in Fig. 1.3) as the time needed for dunes to reestablish lengthens beyond the time scale of successive overwash events. Furthermore, the rate of transgression or the risk of inundation may increase on islands which are already low in relief. Continued investigation of the effects of ecomorphodynamic feedbacks on barrier island evolution—both in the VCR and in other barrier systems with similar morphological and ecological relationships—will be necessary to develop a more quantitative understanding of the rates and scales at which each feedback is likely to operate, especially as climate conditions change.

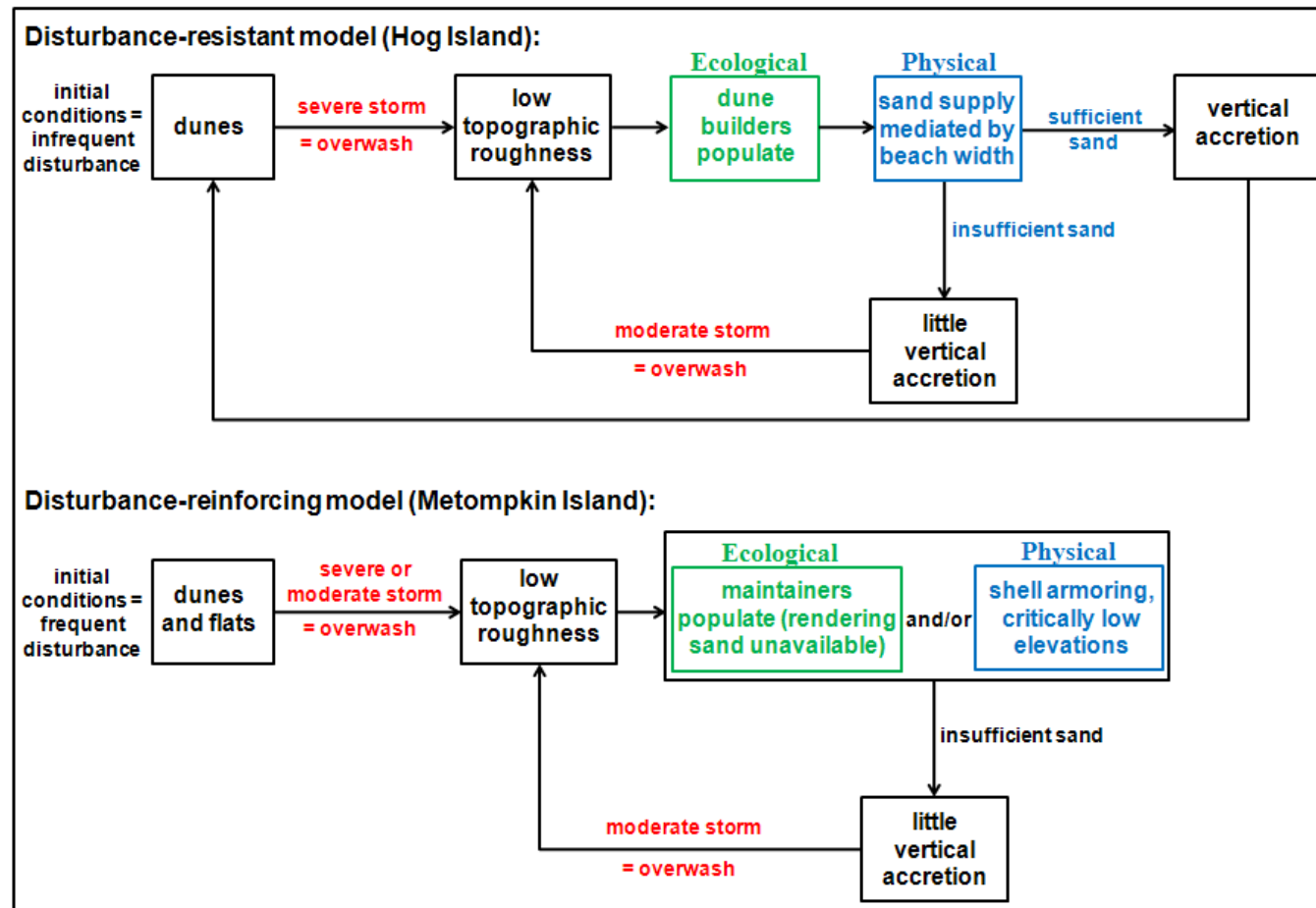


Figure 4.1. Expanded ecomorphodynamic conceptual models of barrier island susceptibility and response to overwash, based on results from the VCR. Initial conditions (disturbance regimes) are set by physical factors such as relative sea level rise rate, antecedent geology and topography, sediment supply, wave climate, shoreline orientation, etc. (Appendix 1.2 provides background on how these factors pertain to the contrasting evolutions of Hog and Metompkin Islands). In the bottom panel, insufficient sand supply is caused by a combination of ecological and physical processes.

5. CONCLUSIONS

The Virginia Coast Reserve (VCR) is a morphologically variable mid-Atlantic barrier system in which both the dune-building grass *A. breviligulata* and the overwash-adapted *S. patens* are principal species. Our aim was to investigate the potential role of an ecomorphodynamic process that we have called the “maintainer” feedback—whereby frequent disturbance is reinforced by the preferential survival of species that maintain low topographic roughness (*S. patens*)—in the context of two morphologically distinct islands within this system: Hog Island (dune-dominated, rotating) and Metompkin Island (overwash-dominated, transgressing).

A strong association between *A. breviligulata* and dunes was evident throughout the study area; to a lesser extent, this relationship was also apparent in transitional areas, consistent with the role of this species in topographic recovery. Large-scale overwash on Hog Island was limited to a single site (at the rotational axis of the island) and was apparently unrelated to *S. patens*. However, *S. patens* was clearly associated with overwash on Metompkin Island (especially when only vegetated areas were considered), supporting our hypothesis that the maintainer feedback is more likely to be at work on the more frequently disturbed island. The species of interest were separated more sharply by morphologic environment on Metompkin Island than on Hog Island, possibly due to spatially heterogeneous disturbance. Mean elevation (an inverse proxy for degree of disturbance) was linked to beach width (an important control on sand supply for dune building) on Hog Island; this relationship was not evident on Metompkin Island, suggesting that factors other than beach width may influence the occurrence of low topographic roughness on this island. Overwash-dominated transect sites on Metompkin

Island (all of which had persisted on at least annual to decadal time scales) were characterized by abundant shell armoring and dominant populations of *S. patens* (northern half), or by exceptionally low elevations relative to the beach and the water table (southern half). Shell armoring was evident, to a lesser extent, in low-lying transitional areas on southern Metompkin Island as well.

Overwash has been much more widespread on Metompkin Island than Hog Island not only recently, but also on (at least) decadal timescales. Overwash also appears to have been more persistent spatially and temporally on Metompkin Island (particularly in the north), consistent with expectations for an island on which the maintainer feedback is at work. Recent overwash persistence on Hog Island has been limited to the rotational axis of the island, where the beach is exceptionally narrow and eroding; former overwash has apparently recovered in association with localized shoreline accretion.

Overall, Hog Island more closely resembles the disturbance-resistant ecomorphodynamic model of barrier island vulnerability: in the rare event that the largely continuous dunes are overtopped or penetrated by overwash, *A. breviligulata* helps to drive the recovery process (except where beach width is prohibitive), and persistent overwash is related to rotational shoreline dynamics rather than the maintainer feedback. Metompkin Island, on the other hand, is generally a disturbance-reinforcing island: while discontinuous dunes in the south may resist overwash locally, low topographic roughness persists at critically low elevations, in the presence of shell armoring, and/or where maintainer species are dominant. All of these factors are likely to increase the probability of continued overwash by inhibiting (or lengthening the time scale of) dune recovery.

In barrier systems like the VCR, physical processes are likely to control overwash persistence on infrequently disturbed, high-relief islands, whereas both physical and ecological processes may contribute to overwash persistence on frequently disturbed, low-relief islands. Overwash on barrier islands will likely become more common with the effects of climate change (sea level rise, increased storminess). As a result, the maintainer feedback—in combination with physical factors that also limit dune recovery—may become increasingly important in reinforcing frequent disturbance, leading to increased overwash persistence.

While physical and geological factors (e.g., sand supply, shoreline dynamics, antecedent topography) are the central controls on barrier island evolution and response to climate change, the impacts of ecomorphodynamic feedbacks should not be overlooked. The maintainer feedback, while not necessarily the primary driver of overwash persistence, nevertheless may have the potential (in concert with physical processes) to catalyze and accelerate large-scale changes in morphology and vulnerability as climate changes and disturbance becomes more common.

REFERENCES

- Bakker, J. D. 2008. Increasing the utility of indicator species analysis. *Journal of Applied Ecology* 45: 1829-1835.
- Bauer, B. O., and R. G. D. Davidson-Arnott. 2003. A general framework for modeling sediment supply to coastal dunes including wind angle, beach geometry, and fetch effects. *Geomorphology* 49 (1-2): 89-108.
- Bender, M. A., T. R. Knutson, R. E. Tuleya, J. J. Sirutis, G. A. Vecchi, S. T. Garner, and I. M. Held. 2010. Modeled impact of anthropogenic warming on the frequency of intense Atlantic hurricanes. *Science* 327: 454-458.
- Bertness, M. D. 1999. *The ecology of Atlantic shorelines*. Sunderland, MA: Sinauer Associates, Inc. 417 pp.
- . 1991. Zonation of *Spartina patens* and *Spartina alterniflora* in a New England salt marsh. *Ecology* 72: 138-48.
- Bristow, C. 2009. Ground penetrating radar in aeolian dune sands. In *Ground penetrating radar: Theory and practice*, ed. H. M. Jol. Oxford, UK: Elsevier. Pp. 273-298.
- Byrne, M. L., and S. B. McCann. 1990. Stratification and sedimentation in complex vegetated coastal dunes, Sable Island, Nova Scotia. *Sedimentary Geology* 66 (3-4): 165-179.
- Byrnes, M. R. 1988. Holocene geology and migration of a low-profile barrier island system, Metompkin Island, Virginia. Doctoral dissertation, Old Dominion University, Norfolk, Virginia, USA.
- Byrnes, M. R., and K. J. Gingerich. 1987. Cross-island profile response to Hurricane Gloria. Proceedings Coastal Sediments '87. New Orleans, LA, USA.
- Christian, D. G., A. B. Riche, and N. E. Yates. 2002. The yield and composition of switchgrass and coastal panic grass grown as a biofuel in Southern England. *Bioresource Technology* 83: 115-124.
- Church, J. A., and N. J. White. 2006. A 20th century acceleration in global sea-level rise. *Geophysical Research Letters* 33: L01602.
- Curtis, P. S., L. M. Balduman, B. G. Drake, and D. F. Whigham. 1990. Elevated atmospheric CO₂ effects on belowground processes in C3 and C4 estuarine marsh communities. *Ecology* 71: 2001-2006.

- Dolan, R., and R. E. Davis. 1992. An intensity scale for Atlantic Coast northeast storms. *Journal of Coastal Research* 8 (4): 840-853.
- Dolan, R., B. Hayden, and C. Jones. 1979. Barrier island configuration. *Science* 204: 401-403.
- Dufrene, M. and Legendre, P. 1997. Species assemblages and indicator species: the need for a flexible asymmetrical approach. *Ecological Monographs* 67 (3): 345-366.
- Duncan, W. H., and M. B. Duncan. 1987. *The Smithsonian guide to seaside plants of the Gulf and Atlantic Coasts from Louisiana to Massachusetts*. Washington, DC: Smithsonian Institution Press. 400 pp.
- Ehrenfeld, J. G. 1990. Dynamics and processes of barrier island vegetation. *Reviews in Aquatic Sciences* 2: 437-480.
- Fahrig, L., D. P. Coffin, and W. K. Lauenroth. 1994. The advantages of long-distance clonal spreading in highly disturbed habitats. *Evolutionary Ecology* 8 (2): 172-187.
- Fahrig, L., B. P. Hayden, and R. Dolan. 1993. Distribution of barrier island plants in relation to overwash disturbance: a test of life history theory. *Journal of Coastal Research* 9: 403-412.
- Fenster, M. S., and B. P. Hayden. 2007. Ecotone displacement trends on a highly dynamic barrier island: Hog Island, Virginia. *Estuaries and Coasts* 30 (6): 978-989.
- Finklestein, K., and D. Prins. 1981. *An inexpensive, portable vibracoring system for shallow-water and land application*. Fort Belvoir, VA: U.S. Army Corps of Engineers Coastal Engineering Research Center, Coastal Engineering Technical Aid No. 81-8.
- Godfrey, P. J. and M. M. Godfrey. 1976. Barrier island ecology of Cape Lookout National Seashore and vicinity, North Carolina. NPS Scientific Monograph Series No. 9. 160 pp.
- Godfrey, P. J., S. P. Leatherman, and R. Zaremba. 1979. A geobotanical approach to classification of barrier beach systems. In *Barrier islands: From the Gulf of St. Lawrence to the Gulf of Mexico.*, ed. S. P. Leatherman. New York, NY: Academic Press. Pp. 99-126.
- Harris, M. S. 1992. The geomorphology of Hog Island, Virginia. Master's thesis, University of Virginia, Charlottesville, VA, USA.

- Havholm, K. G., D. V. Ames, G. R. Whittecar, B. A. Wenell, S. R. Riggs, H. M. Jol, G. W. Berger, and M. A. Holmes. 2004. Stratigraphy of back-barrier coastal dunes, northern North Carolina and southern Virginia. *Journal of Coastal Research* 20 (4): 980-999.
- Hayden, B. P., R. Dolan, and P. Ross. 1980. Barrier island migration: thresholds in geomorphology. Proceedings of Thresholds in Geomorphology, Binghamton, NY, USA.
- Hayden, B. P., M. C. F. V. Santos, G. Shao, and R. C. Kochel. 1995. Geomorphological controls on coastal vegetation at the Virginia Coast Reserve. Proceedings of the 26th Binghamton Symposium in Geomorphology: Biogeomorphology, terrestrial and freshwater systems, Binghamton, NY, USA.
- Hayes, M. O. 1979. Barrier island morphology as a function of tidal and wave regime. In *Barrier islands: From the Gulf of St. Lawrence to the Gulf of Mexico.*, ed. S. P. Leatherman. New York, NY: Academic Press. Pp. 1-28.
- Intergovernmental Panel on Climate Change (IPCC). 2007. *Climate Change 2007: The Physical Science Basis*. Cambridge, UK and New York, NY: Cambridge University Press. 1008 pp.
- Knutson, T. R., J. L. McBride, J. Chan, K. Emanuel, G. Holland, C. Landsea, I. Held, J. P. Kossin, A. K. Srivastava, and M. Sugi. 2010. Tropical cyclones and climate change. *Nature Geoscience* 3: 157-163.
- Kochel, R. C., and R. Dolan. 1986. The role of overwash on a mid-Atlantic coast barrier island. *Journal of Geology* 94 (6): 902-906.
- Kochel, R. C., J. H. Kahn, R. Dolan, B.P. Hayden, and P. F. May. 1985. U.S. mid-Atlantic barrier island geomorphology. *Journal of Coastal Research* 1 (1): 1-9.
- Komar, P. D., and J. C. Allan. 2007. Higher waves along U.S. east coast linked to hurricanes. *Eos* 88 (30): 301-308.
- Lanesky, D. E., B. W. Logan, R. G. Brown, and A. C. Hine. 1979. A new approach to portable vibracoring underwater and on land. *Journal of Sedimentary Petrology* 49 (2): 654-657.
- Leatherman, S. P., and A. T. Williams. 1983. Vertical sedimentation units in a barrier island washover fan. *Earth Surface Processes & Landforms* 8: 141-150.
- . 1977. Lateral textural grading in overwash sediments. *Earth Surface Processes & Landforms* 2: 333-341.

- Leatherman, S. P., A. T. Williams, and J. S. Fisher. 1977. Overwash sedimentation associated with a large-scale northeaster. *Marine Geology* 24 (2): 109-121.
- Leatherman, S. P., and R. E. Zaremba. 1987. Overwash and aeolian processes on a U.S. northeast coast barrier. *Sedimentary Geology* 52: 183-206.
- Leatherman, S. P., T. E. Rice, and V. Goldsmith. 1982. Virginia barrier island configuration; a reappraisal. *Science* 215: 285-287.
- Levine, J. M., J. S. Brewer, and M. D. Bertness. 1998. Nutrients, competition, and plant zonation in a New England salt marsh. *Journal of Ecology* 86: 285-292.
- Margolis, S. V., and D. H. Krinsley. 1971. Submicroscopic grain frosting on eolian and subaqueous quartz sand grains. *GSA Bulletin* 82: 3395-3406.
- McBride, R. A., and M. M. Robinson. 2003. Geomorphic evolution and geology of Old Currituck Inlet and its flood tidal delta, Virginia/North Carolina, USA. Proceedings Coastal Sediments '03 (CD-Rom), eds. R. A. Davis, A. H. Sallenger, Jr., and P. Howd. Am. Soc. Civ. Eng. 14 pp.
- McCune, B., and J. B. Grace. 2002. *Analysis of ecological communities*. Glendale, OR, USA: MJM Software Design. 304 pp.
- Møller, I., and D. Anthony. 2003. A GPR study of sedimentary structures within a transgressive coastal barrier along the Danish North Sea coast; ground penetrating radar in sediments. *Geological Society Special Publications* 211: 55-65.
- Priestas, A. M., and S. Fagherazzi. 2010. Morphological barrier island changes and recovery of dunes after Hurricane Denis, St. George Island, Florida. *Geomorphology* 114 (4): 614-626.
- Qi, M. Q., and R. E. Redmann. 1993. Seed germination and seedling survival of C3 and C4 grasses under water stress. *Journal of Arid Environments* 24: 277-285.
- Sallenger, A. H., Jr. 2000. Storm impact scale for barrier islands. *Journal of Coastal Research* 16 (3): 890-895.
- Schwartz, R. K. 1982. Bedform and stratification characteristics of some modern small-scale washover bodies. *Sedimentology* 29: 835-849.
- . 1975. *Nature and genesis of some storm washover deposits*. Fort Belvoir, VA: US Army Corps of Engineers Coastal Engineering Research Center, Coastal Engineering Research Center Technical Memorandum 61.

- Sedgwick, P. E., and R. A. Davis Jr. 2003. Stratigraphy of washover deposits in Florida: Implications for recognition in the stratigraphic record. *Marine Geology* 200: 31-48.
- Silander, J. A., and J. Antonovics. 1979. The genetic basis of the ecological amplitude of *Spartina patens*: I. Morphometric and physiological traits. *Evolution* 33: 1114-1127.
- Stallins, J. A. 2005. Stability domains in barrier island dune systems. *Ecological Complexity* 2: 410-430.
- Stallins, J. A., and A. J. Parker. 2003. The influence of complex systems interactions on barrier island dune vegetation pattern and process. *Annals of the Association of American Geographers* 93 (1): 13-29.
- U.S. Department of Agriculture National Resources Conservation Service (USGS NCRS). 2010. The PLANTS database. In: National Plant Data Center [database online]. Baton Rouge, LA [cited 2/1/10]. Available: <http://plants.usda.gov>.
- Vick, J. K., and D. R. Young. 2011. Spatial variation in environment and physiological strategies for forb distribution on coastal dunes. *Journal of Coastal Research In-Press*.
- Wang, P., and M. H. Horwitz. 2007. Erosional and depositional characteristics of regional overwash deposits caused by multiple hurricanes. *Sedimentology* 54: 545-564.
- Wilson, M. D., B. D. Watts, and J. E. Leclerc. 2007. *Assessing habitat stability for disturbance-prone species by evaluating landscape dynamics along the Virginia Barrier Islands*. Williamsburg, VA: College of William and Mary, Center for Conservation Biology Technical Report Series CCBTR-07-06.
- Wolner, C. W. V., L. J. Moore, D. R. Young, S. T. Brantley, S. N. Bissett, M. D. Wilson, and B. D. Watts. 2011. Dune builders vs. overwash maintainers: Ecomorphodynamic feedbacks on the Virginia Coast Reserve barrier islands. *Proceedings Coastal Sediments 2011*, eds. P. Wang, J. D. Rosati, and T. M. Roberts. Miami, FL, USA. World Scientific. Pp. 258-271.
- Young, D. R., S. T. Brantley, J. C. Zinnert, and J. K. Vick. 2011. Landscape position and habitat polygons in a dynamic coastal environment. *Ecosphere* 2 (6): Article 71.
- Ziska, L. H., and J. A. Bruce. 1997. Influence of increasing carbon dioxide concentration on the photosynthetic and growth stimulation of selected C4 crops and weeds. *Photosynthesis Research* 54: 199-208.

APPENDIX 1: STUDY AREA BACKGROUND

1.1 Attributes of common strand species in the Virginia Coast Reserve

Names and attributes of common strand plants in the VCR. Numbers in parentheses refer to reference list, below. Attributes without reference numbers indicate information that is either generally accepted or apparent from field observations but not yet documented in the literature. Life span abbreviations indicate annual (A), biannual (B), and perennial (P). Table assembled collaboratively with S. N. Bissett, S. T. Brantley, and J. Deemey.

Species	Tolerance of disturbance (sand burial, salt-water flooding)	Propagation strategy	Elevation range	Life span (A/B/P)	Photo-synthetic pathway	Competitor?	Dune-builder or maintainer?
<i>Ammophila breviligulata</i>	Yes: needs addition of windblown sand (9); intolerant of frequent flooding (9), but tolerant of soils with or without high salinity (13)	Guerilla, seed + rhizomes in wrack (9)	Broad elevation range near shore, higher elevations preferred inland (15)	P (13)	C3	No (2)	Dune-builder (9)
<i>Spartina patens</i>	Very: burial stimulates growth, survives < 30cm of overwashed sand (6, 9); highly salt tolerant (12)	Phalanx	Broad range of elevations (12); may do better in low, flat strand areas than less salt tolerant grasses; stressed at high elevations (8)	P (13)	C4 (4)	Yes (1, 9)	Maintainer (9)
<i>Solidago sempervirens</i>	Yes: survives < 56cm burial (6, 7, 9)	Seed, phalanx (13)	Mostly low/flat but can inhabit a broad range	P (13)	C3	No, prefers sparsely vegetated areas	Maintainer or no effect? (9)
<i>Cakile edentula</i>	Yes : < 4mm wk-1 stimulates growth (6, 7, 9)	Seed in wrack, phalanx (6)	Mostly low/flat but can inhabit a broad range	A / P (13)	C3?	No (2)	—
<i>Panicum amarum</i>	Medium salt tolerance (13)	Seed (13)	—	P (13)	C4 (3)	No (2)	Minor dune-builder
<i>Rumex acetosella</i>	Low salt tolerance (14)	—	—	P (13)	—	—	—
<i>Conyza Canadensis</i>	No salt tolerance (13)	Seed (13)	—	A/B (13)	—	—	—
<i>Panicum dichotomiflorum</i>	Medium salt tolerance (13)	Seed (13)	—	A (13)	C4 (16)	—	—
<i>Morella cerifera</i>	—	Seed or container (13)	—	P (13)	C3	Yes (2)	—
<i>Andropogon scoparius</i>	—	Seed (13)	—	P (13)	C4 (11)	—	—
<i>Gnaphalium purpureum</i>	—	—	—	A / B (5)	—	—	—

References: 1) Bertness, 1991. 2) Bertness, 1999. 3) Christian et al., 2002. 4) Curtis et al., 1990. 5) Duncan and Duncan, 1987. 6) Ehrenfeld, 1990. 7) Fahrig et al., 1993. 8) Godfrey and Godfrey, 1976. 9) Godfrey et al., 1979. 10) Levine et al., 1998. 11) Qi and Redmann 1993. 12) Silander and Antonovics, 1979. 13) USDA, NCRS, 2010. 14) Vick and Young, 2011. 15) Young et al., in review. 16) Ziska and Bruce, 1997.

1.2 Morphological evolution of Hog and Metompkin Islands

Hog Island

Sources: Harris, 1992; Leatherman et al., 1982; historical aerial photos; field mapping.

- **Holocene formation:**
 - Hog Island and neighboring barriers formed on regressive Pleistocene beach ridges (paleotopographic highs), with inlets corresponding to thalwegs of Pleistocene drainages.
 - These Pleistocene beach ridges are inferred to be responsible for stalling Hog Island's landward migration.

- **1600s–late 1800s**
 - The island oscillated cyclically (clockwise and counter-clockwise rotation).
 - Leatherman et al. (1982) ascribed this rotational shoreline change to inlet dynamics, particularly with respect to ebb-tidal delta morphology. The large ebb-tidal deltas and the changing ebb channel orientations in the inlets bounding Hog Island affect wave refraction and sediment by-passing, driving local reversals of littoral drift.
 - Harris (1992) related the oscillatory pattern to a regional-scale storm cycle in which a regime of infrequent, continental storms (counter-clockwise rotation) alternates with a regime of frequent, maritime storms (clockwise rotation).
 - The peak-to-peak (maximum clockwise rotation to maximum clockwise rotation) cycle had a periodicity of ~120 years (i.e., 60 years between peak of infrequent continental storm regime/counter-clockwise rotation and peak of frequent maritime storm regime/clockwise rotation).
 - Maximum clockwise rotation occurred around 1600, 1720, and 1840.

- **Late 1800s:**
 - Starting at this time and peaking around 1960, general storm patterns shifted gradually from infrequent and continental to frequent and maritime, causing the dominant wave climate to switch from mainly southeast and accretionary to a more northerly and erosional regime.

- These changes were associated with a switch from counter-clockwise to clockwise rotation for the island. The timing of this switch was concordant with the 120-year cyclic periodicity described above.
- **Late 1800s–early 1900s:**
 - The land south of Broadwater Tower (southern 1/3 of island), which previously had been covered by a maritime forest and inhabited by humans, was almost entirely eroded away in a series of storms.
 - A new spit began to form, prograding southward from Broadwater Tower.
 - The island continued to rotate clockwise.
- **Early 1900s–mid 1900s:**
 - The spit extending south from Broadwater Tower continued prograding southward, while undergoing frequent overwash and moving landward.
 - The north end of the island generally accreted and became substantially wider than the south end, leading to the development of the characteristic drumstick shape associated with the island.
 - The island continued to rotate clockwise.
- **1940s–1960s:**
 - In the late 1940s, the north end of the island (fattest part of the drumstick shape) was largely an open, active overwash flat with an embryonic dune field.
 - The south end of the island continued to behave as described above. Overwash channels were incised across the width of the island, and overwash terraces accumulated on the backbarrier.
 - In the 1950s, overwash began to penetrate the (formerly) continuous dunes immediately north of Broadwater Tower.
 - This increase in overwash activity in the south/south-central areas of the island may have been related to the north-trending shoreline which, combined with ebb-delta positions and the overall shape of the island at this time, caused wave action to be primarily focused in these areas.
 - In 1962, the historic Ash Wednesday storm impacted the island. The south end of the island was breached by an inlet (ephemeral). Overwash occurred in the south and south-central areas.
 - The island continued to rotate clockwise, contrary to the previously established 120-year periodicity (60-year per rotational direction).

- **1960s–early 1990s**

- The north end of the island generally accreted and the drumstick-shape became more distinct. The embryonic dunes on the north end (described above) coalesced into dune ridges, cutting off the overwash flats from wave exposure. These flats were stabilized by vegetation. However, by the late 1980s, island oscillation had exposed the south end of the flats (now part of a swale with a large intermittent pond) to wave action at the rotational axis of the island (the point at which the drumstick shape narrows). Overwash was reactivated at this site, with overwash fans spreading into the pond.
- Overwash continued to be active from about 1 km north of the Broadwater Tower to the southern end of the island; south of Broadwater Tower, overwash occurred primarily in the incised channels. Embryonic and discontinuous dunes developed between these overwash channels.
- The island continued to rotate clockwise until the 1980s, when it began accreting across nearly its entire extent (not rotating in either direction). Most overwash apparently recovered by the early 1990s.

- **Early 1990s–present**

- The north end of the island generally accreted until 2001; between 2001 and 2009, this same area generally eroded. With accretion in the south during the same period of time, the island appears to be rotating counter-clockwise.
- Nor’Ida, a severe storm, impacted the island in 2009, causing little change in the south but erosion and overwash in the north, with scarping and localized, small-scale overwash of the seaward-most dune.
- The pond at the rotational axis of the island—where the beach pinches out to its narrowest point—continues to experience large-scale overwash, with transitional areas flanking the overwash fans.
- Continuous dunes persist in the central portion of the island.
- For roughly 1.5 km north of Broadwater Tower, the dune line is low and apparently young with periodic evidence of partial or recovering overwash (i.e., a transitional area).
- South of the road, a wide (accretional) beach and largely continuous foredunes (1–2 m) and secondary dunes (2–4 m) front the relict overwash channels. Relict overwash channels are generally reworked, vegetated, and difficult to trace continuously. The overwash terraces have converted to swale and high marsh.

Metompkin Island

Sources: Byrnes and Gingerich, 1987; Byrnes, 1988; Leatherman et al., 1982; historical aerial photos; field mapping.

- **Holocene formation–late 1800s:**
 - Metompkin Island formed ~1 km seaward of its present location, as a comparatively wide and extensive barrier relative to its current state.
 - As sea level rose, the shoreline eroded and the island thinned progressively.

- **Late 1800s–mid 1900s:**
 - Gradual shoreline erosion proceeded.
 - The development and migration of other spits and islands elsewhere on the coast impeded littoral drift, initiating sediment starvation in the Chincoteague Bight.
 - The island thinned at 7 m/yr until inlets began breaching in the southern half (lagoon-backed).

- **1955–1980:**
 - Landward migration (rollover) via overwash and inlet transport began. Metompkin Island and the adjacent barriers were characterized by parallel shoreline retreat (rather than rotation, like Hog Island and other barriers to the south). Migration rates for Metompkin Island were as high as 13+ m/yr.
 - The southern half (lagoon-backed, breached by inlets) was highly mobile relative to the northern half (marsh-backed, not breached by inlets), migrating up to 2.5 times faster. This difference in migration rates resulted in a shoreline offset of ~400 m.

- **1980–1985:**
 - Inlets in the southern half closed; overwash became the primary mechanism of migration.
 - The northern half began migrating faster (by up to 4 times) than the southern half, reducing the magnitude of the shoreline offset. Byrnes (1988) speculated that this change occurred in response to the coastline attempting to straighten (presumably via alongshore sediment redistribution).

- In 1985, Hurricane Gloria impacted the island, reopening an inlet at the location of the shoreline offset. The southern half of the island maintained its elevation, but elevations in the northern half decreased (although island width stayed the same).
- By this time (if not earlier), Metompkin Island and the adjacent barriers in the northern VCR were low-relief, dominated by overwash, and located landward of Hog Island and other high-relief barriers to the south. Leatherman et al. (1982) postulated that this profound difference in behavior and morphology among barriers within the same island chain was driven by sediment starvation of the northern group by Fishing Point (off Assateague Island), differential subsidence increasing northward (resulting in relative sea-level rise being highest in the north), and shoreline orientation in the northern group allowing uniform wave attack.
- **1985–present:**
 - The island has continued to migrate landward rapidly, particularly in the northern half.
 - In 2009, the severe storm Nor’Ida impacted the island, causing little change in the south (no sign of new overwash or beach erosion) but contributing to shoreline migration and fresh overwash of the already low-relief, overwash-dominated northern half.
 - The southern half of the island is currently characterized by discontinuous dunes punctuated by thin, linear overwash fans and channels in various stages of recovery (i.e., both active and transitional). The northern half of the island, however, is characterized entirely by overwash terraces. The ephemeral inlet at the location of the shoreline offset has closed.

APPENDIX 2: FIELD AND LABORATORY METHODS

2.1 GPS surveys

Collection specifications:

- Surveying units: R7 and R8 GNSS Systems with external HB450 radio (Trimble Navigation Limited, Sunnyvale, CA)
- Survey style: RTK (stationary base receiver at a known location broadcasting corrections to a mobile rover receiver)
- Datum and geoid model: NAVD88, Geoid09
- Horizontal accuracy (after post-processing): 1 cm
- Vertical accuracy (after post-processing): 2–3 cm



Base station configuration (left: external radio; right: R8 base receiver). Photo: M. Weakley, 2010.

Post-processing:

- Base station coordinates: Online Positioning User Service (OPUS), National Geodetic Survey (NGS): <http://www.ngs.noaa.gov/OPUS/>.
- Survey coordinates: Trimble Geomatics Office (Version 1.62).

2.2 Sediment sample preparation and analysis

Preparation procedure:

1. For each grab sample, we agitated the sample bag by hand before transferring roughly 30–150 g of representative sample into a foil container (archiving the remaining sample).
2. We dried samples at 60°C for 24–48 hrs.
3. We passed samples through a 2 mm sieve to separate coarse shells* and weighed both the >2 mm and <2 mm fractions. Contents of the >2 mm fraction, if other than shells and shell fragments, were noted.**
4. We combusted the <2 mm sample fractions in a muffle furnace at a minimum of 550°C (higher for samples with woody debris) for at least 5 hours (longer for samples with woody debris) to remove organics. We weighed the ashed <2 mm sample fractions.

* We performed sieving before combustion due to explosive behavior of coarse shells in the muffle furnace. We therefore calculated total dry weight as (dry >2 mm) + (ashed <2 mm) + (organics), relying on the assumption that organic matter present among coarse shells was negligible (weight percent change after combustion for a test sample of coarse shells was ~1%).

** In the rare event that coarse organic debris (root fragments, wrack, etc.) was separated during the sieving process, it was manually returned to the <2 mm fraction before weighing and combustion. Sediment >2 mm consisted entirely of shells except for 2 samples from Metompkin Island, each of which contained a single quartz pebble (<0.01% of total dry weight), which was discarded.

Particle size analysis:

- From each sample, we obtained 3 representative subsamples (3–6 grams each) for analysis with the LS 13 320 laser diffraction particle size analyzer (Beckman Coulter, Brea, CA).
- Subsamples were either manually loaded into the LS 13 320 sample cell, or placed in a test tube and loaded automatically using the Auto Prep Station. A comparison of 3 samples processed using both manual and automated loading showed no significant differences between the two methods in the estimation of

the means, medians, standard deviations, or 90th percentiles of the grain size distributions.

- Using the LS 13 320 software, we averaged subsample distributions by sample for within-island statistical comparisons; we averaged sample distributions by transect site for between-island statistical comparisons and for graphical representations of each transect site.

2.3 Ground-penetrating radar (GPR) surveys

Collection specifications:

- Collection system: PulseEKKO Pro (Sensors and Software, Mississauga, Ontario)
 - Configuration: stepwise
 - Frequency: 200 MHz
 - Step size: 20 cm
 - Time window: 200 ns (reflection survey), 300 ns (CMP)
 - Antennae separation: 60 cm (reflection survey), 50 cm (CMP)
 - Trace stacks: 64
-
- SmartCart 250 MHz and rolling 1000 MHz configurations (both with DynaQ stacking) were also attempted, but were not appropriate for resolving the features of interest in this environment.



Stepwise GPR configuration, with antennae (transmitter and receiver) resting on the ground surface. Photo: D. Oster, 2010.

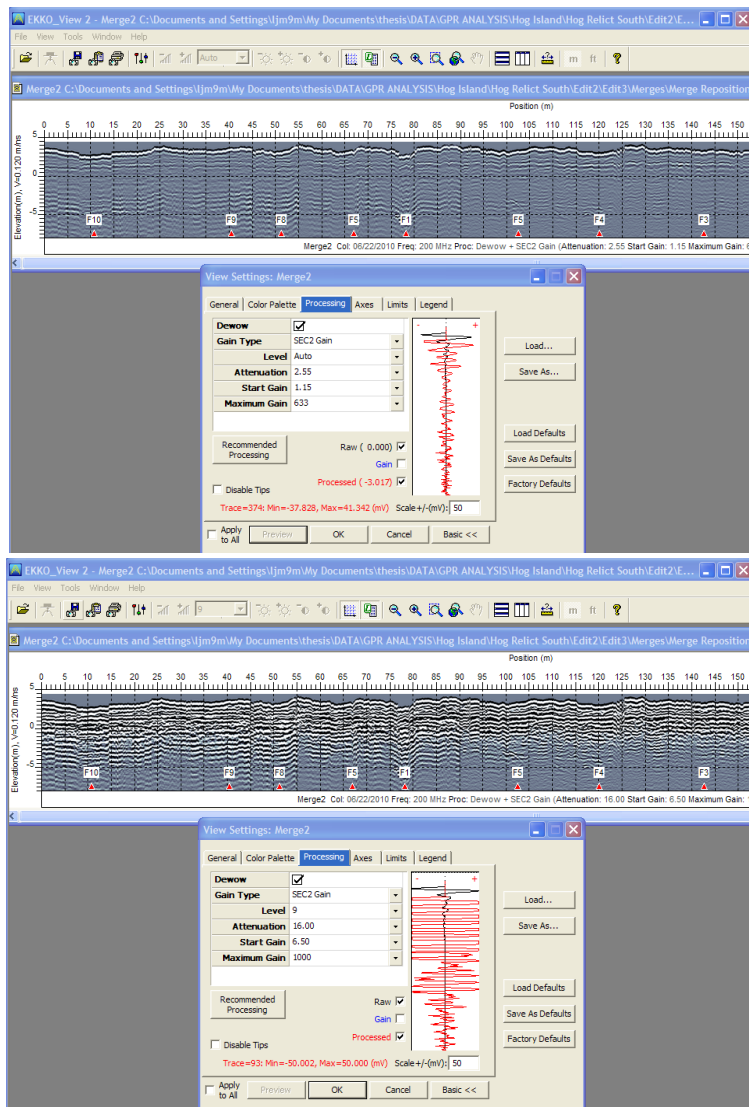


Stepwise GPR collection with integrated backpack GPS. Photo: D. Oster, 2010.

Post-processing:

- CMP (common midpoint) method of determining velocity:
 - In the field, GPR antennae (transmitter and receiver) are progressively separated by a known increment over a flat-lying reflector.
 - In the laboratory, the EKKO_View Deluxe software (Version 1 Release 4) uses changes in the time required for the signal to pass between antennae in combination with the known changes in distance to determine a range of possible radar velocities.
 - Plotting the results of a CMP in EKKO_View 2 shows a peak in signal strength at the intersection of the flat-lying reflector's y-axis position and the correct radar velocity (m/ns) on the x-axis. The velocity can then be applied to GPR profiles in order to convert the default y-axis (time, ns) into depth or elevation (m).
- Topographic corrections (cm-scale): elevation values from integrated GPS (except for Lines 00 and 01 from northern Hog Island, which were manual inputs of estimated elevations).
- Dewow (high-pass filter) applied automatically.

- Gain: SEC 2. SEC 2 (exponential gain compensation) works by applying a linear gain to radar signal strength in concert with an exponential gain over time—i.e., the greatest gain is applied to the deepest reflections—in order to compensate for the signal attenuation that occurs at depth, without compromising the relative strength of the radar reflections across the GPR profile.



A GPR profile in EKKO_View 2 before (above) and after (below) applying SEC2 gain.

2.4 Vibracoring apparatus

The portable, land-based vibracoring rig used in this study was designed similarly to the rigs described by Lanesky et al. (1979) and Finklestein and Prins (1981) (see also McBride and Robinson, 2003). The rig is powered by a gasoline engine connected by several meters of flexible shaft to a concrete vibrator, which is welded to a pipe vice. During the coring procedure, the pipe vice is clamped around the top of the core pipe. The core pipe is then positioned vertically in the center of a ~5 m aluminum tripod. Different gears on the engine correspond to different vibration speeds, which help to drive the core pipe smoothly into the sediment. The aim is to facilitate complete penetration of the core pipe as rapidly as possible: the longer the pipe remains vibrating in the sediment, the more likely that strata will be deformed by friction along the pipe wall or vibration-induced porewater movement.

Cores are typically driven into the ground until refusal. When cores cannot penetrate any farther, they are removed using a series of hand winches after creating a seal at the top of the core pipe.



The vibracoring rig on Hog Island, showing tripod, core pipe, and concrete vibrator attached to top of core pipe (engine not shown). Photo: R. McBride, 2010.

2.5 Core processing and interpretation

In the laboratory, we cut cores longer than 2 m into 1 m segments. We opened these segments using a circular saw to cut the pipe wall longitudinally on either side of the core; we then passed a stainless steel 18-gauge wire through the saw incisions in order to separate the sediment within the core. After splitting, we scraped and brushed the sediment surfaces. Cores were recapped, sealed in plastic, and kept in cold storage when not in use.



A freshly opened core in the laboratory.

During description, we left cores out of cold storage to dry for 0.5–2 days before photographing to ensure that the maximum variability in strata would be clearly visible. We logged each core in detail based on visual assessments of color (Munsell soil color chart), bedding, mineralogy, texture, and size.

Characteristics used to distinguish overwash and aeolian deposits in cores during the interpretation process. Numbers in parentheses refer to reference list, below.

OVERWASH	AEOLIAN
<ul style="list-style-type: none"> • Horizontal to v. low angle sub-horizontal (1–4 °) strata, parallel planar laminations/beds, may be >1 m thick (2, 4, 5, 6, 7, 8, 10, 11, 12) • Rhythmic/alternating layering of sand, heavy minerals and shells (5, 6, 11, 12) • Clean, moderately sorted to v. well sorted sand throughout (8, 12) • May overlay any of the following: lagoonal sediments, marsh peat, grassland soils, shell lag layers, coarse quartz or heavy mineral lag layers, truncated dune deposits (2, 12, 13) • Normal or inverse or no grading (depending on whether scour/reworking/bioturbation takes place, and the homogeneity of sediments) (7, 8, 10, 12, 13) • Variable concentrations of heavy minerals in stacked beds; thick heavy mineral zones may indicate erosional concentration produced by repeated overwash surges (8) • May resemble shoreface deposits (12) • Shells include shoreface/open water species (12) • May include roots and wrack (4) • Wet, reducing environments: possibly greyer colors (14) • Sediment sources: shoreface, beach, foredune (11) 	<ul style="list-style-type: none"> • Faint to strong cross-bedding indicates dune-building; may be high- or low-angle and varying in direction (1, 2, 3) • Flat or wavy bedding/lamination produced by grainfall also possible, particularly in the alongshore direction on vegetated dunes (1) • Heavy mineral laminations may truncate or cross one another, or be discontinuous (14) • May overlay overwash deposits, beach sediments, marsh peat (2, 3) • Well to v. well sorted sand throughout (3, 14) • May include roots, stems, plant stains (1) • Finer than overwash, beach, or inlet sediments (3), unless sediment is very homogeneous (4, 6, 13) • Surface of quartz grains may be frosted—more consistently than in other, non-aeolian strata (9) • Dry, oxidizing environment: possibly lighter colors (14) • Sediment sources: beach, adjacent overwash (11)

References: 1) Byrne and McCann, 1990. 2) Godfrey et al., 1979. 3) Hayes, 1979. 4) Hennessy and Zarillo, 1987. 5) Kochel and Dolan, 1986. 6) Leatherman and Williams, 1977. 7) Leatherman and Williams, 1983. 8) Leatherman et al., 1977. 9) Margolis and Krinsley, 1971. 10) Schwartz, 1975. 11) Schwartz, 1982. 12) Sedgwick and Davis, 2003. 13) Wang and Horwitz, 2007. 14) R. McBride, personal communication, 12 February 2011.

APPENDIX 3: SUPPLEMENTARY DATA SUMMARIES

3.1 Spearman correlations

Spearman monotonic correlation coefficients (ρ) and p values for beach width and mean transect elevation on each island.

		Beach width x mean elevation
Hog Island	Spearman's ρ	0.83
	p	0.04
Metompkin Island	Spearman's ρ	0.09
	p	0.87

Spearman correlation coefficients (ρ) and p values for beach width and mean transect elevation after correcting an anomalous point on Hog Island using a 2009 aerial photo (measured beach width = 1.2 m, corrected maximum beach width = 30 m), and after removing an outlying point on Metompkin Island (beach width = 176 m, a value supported by the 2009 aerial photo).

		Beach width x mean elevation
Hog	Spearman's ρ	0.83
	p	0.04
Metompkin	Spearman's ρ	0.70
	p	0.19

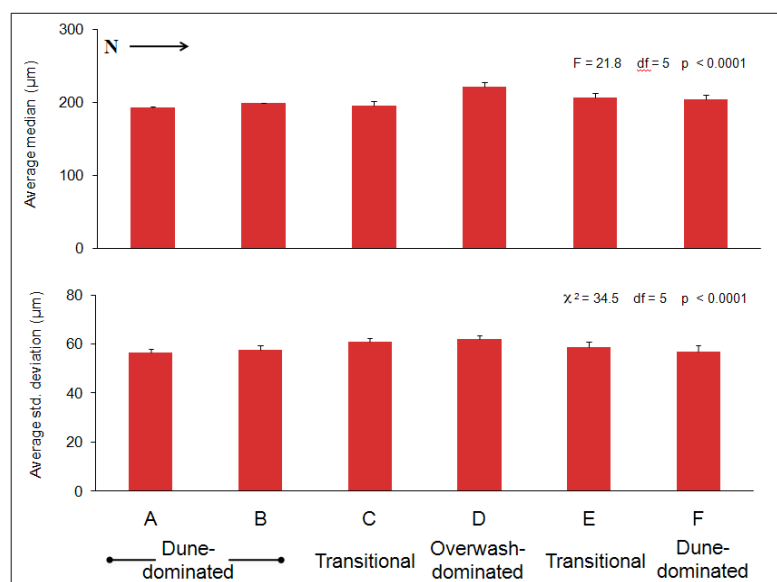
3.2 Sediment properties

Averages of select sediment properties by site on Hog Island.

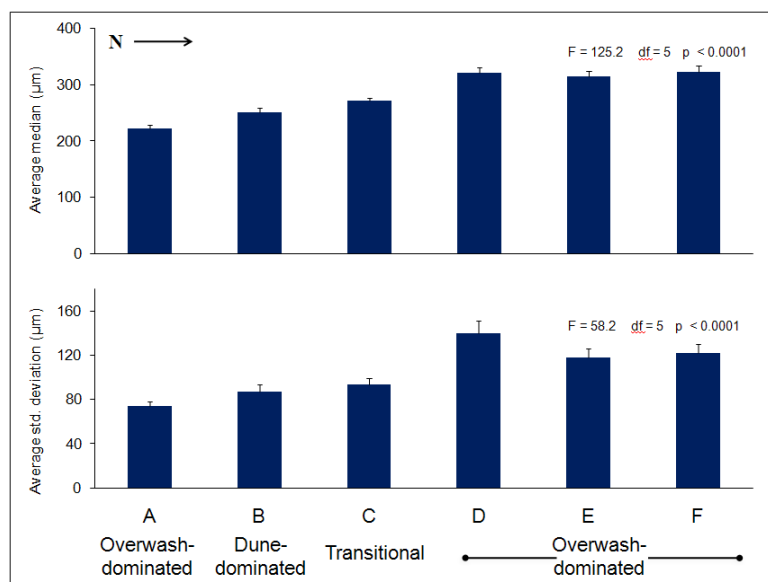
Site	Shell (>2mm) weight %	Organic weight %	Mean (μm)	D10 (μm)	D50 (μm)	D90 (μm)	Std. deviation (μm)	Skewness (μm)
A (n=31)	0.0	0.7	198	132	194	274	56.3	0.15
B (n=35)	0.0	0.5	204	136	199	283	57.5	0.30
C (n=26)	0.0	0.7	201	129	196	283	61.0	0.27
D (n=29)	0.0	0.2	227	151	222	313	62.1	0.36
E (n=24)	0.0	0.2	212	141	207	293	58.9	0.35
F (n=26)	0.0	0.3	209	140	204	288	56.7	0.38

Averages of select sediment properties by site on Metompkin Island.

Site	Shell (>2mm) weight %	Organic weight %	Mean (μm)	D10 (μm)	D50 (μm)	D90 (μm)	Std. deviation (μm)	Skewness (μm)
A (n=41)	0.2	0.4	231	146	222	333	74.9	0.48
B (n=27)	0.0	0.5	260	157	251	382	88.4	0.42
C (n=31)	8.8	0.2	283	174	271	413	94.7	0.58
D (n=29)	26.1	0.1	344	197	321	513	141.0	1.49
E (n=29)	27.5	0.1	329	195	314	487	119.4	0.84
F (n=31)	22.2	0.1	339	199	323	502	123.8	0.79



Median grain sizes and standard deviations (averaged by site) on Hog Island. Error bars represent 95% confidence intervals. Medians were compared across all sites using ANOVA; standard deviations were compared using a Kruskal-Wallis test.



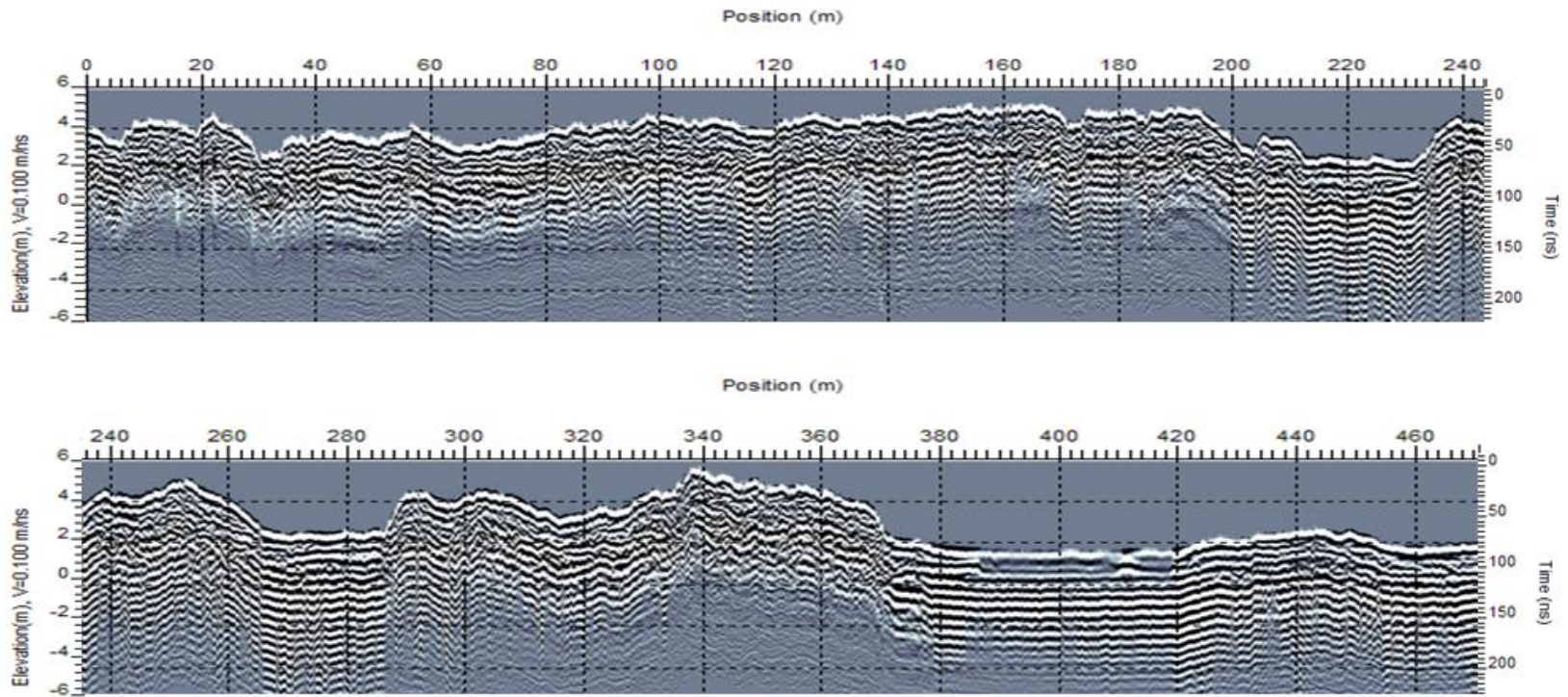
Median grain sizes and standard deviations (averaged by site) on Metompkin Island. Error bars represent 95% confidence intervals. Both medians and standard deviations were compared across all sites using ANOVA.

3.3 Aerial photo features

Morphological features digitized from historical aerial photos (expanded from Wilson et al.'s (2007) database). Overlap area signifies the total island area overwashed in both the previous and current photo year.

Photo year	Island area (km ²)		Overwash area (km ²)		Overlap area (km ²)	
	Hog Island	Metompkin Island	Hog Island	Metompkin Island	Hog Island	Metompkin Island
1949	No data	2.00	No data	0.29	—	—
1955	No data	1.74	No data	0.46	—	0.07
1962	5.39	1.17	0.28	0.99	—	0.00
1977	8.13	1.26	0.06	0.09	0.05	0.01
1985	7.73	1.97	0.09	0.68	0.04	0.00
1994	7.54	2.27	0.00	0.99	0.00	0.16
2002	7.79	2.48	0.03	0.53	0.00	0.23
2007	7.72	2.38	0.06	0.66	0.02	0.21
2009	7.81	2.42	0.04	0.62	0.02	0.54

3.4 Unedited GPR profile, S. Metompkin Island



Alongshore GPR profile through dunes, transitional areas (210–235 m; 265–285 m), and the throat of an overwash fan (380–420 m) on southern Metompkin Island.

APPENDIX 4: CORE DESCRIPTIONS AND INTERPRETATION

Red arrows in core photos indicate facies boundaries. Descriptions and interpretations developed collaboratively with R. McBride.

Hog Island

HI B-2010-1

Coordinates (UTM 18N NAD83): N 4138549, E 437504

Total length (cm): 121.5

Compaction (cm): 46

Auger (cm): 0

Total Depth (cm): 167.5

- **Facies 1, BTM–TOP:** Fine to medium, massive to planar laminated to discontinuous/cross-cut laminated, moderately to v. well sorted sand.
 - Subfacies 1, BTM–114 cm: Massive, moderately well sorted, fine to coarse sand with sand-sized shell bits.
 - Subfacies 2, 114–102 cm: V. well sorted fine sand with planar heavy mineral laminations.
 - Subfacies 3, 102–53 cm: Well sorted, fine to medium sand with faint, sporadic, planar heavy mineral laminations.
 - Subfacies 4, 53–18 cm: V. well sorted fine sand with heavy mineral laminations of variable thicknesses, sometimes discontinuous, sometimes cross-cutting (especially at base of unit and at 33 cm; “Bengal tiger” pattern). Comparatively high percentages of quartz frosting.
 - Subfacies 5, 18 cm–TOP: Massive, bioturbated, v. well sorted fine sand, with root fragments and a single shell fragment near the surface.

Interpretation:

Sbf 1: Overwash or beach face. Physical processes dominate.

Sbf 2: Lower energy overwash or aeolian? Physical processes dominate.

Sbf 3: Lower energy overwash or aeolian? Physical processes dominate.

Sbf 4: Aeolian? Physical processes dominate.

Sbf 5: Bioturbated aeolian. Biological processes dominate.



TOP

HOG ISLAND
B-2010-1

HI B-2010-2

 Coordinates (UTM 18N NAD83): N 4138544, E 437501

Total length (cm): 146.5
Compaction (cm): 40
Auger (cm): 52
Total Depth (cm): 238.5

- **Facies 1, BTM–TOP:** Moderately to v. well sorted, fine to medium, massive to planar laminated to discontinuous laminated sand.
 - Subfacies 1, BTM–121 cm: Well sorted, fine to medium sand with faint, planar heavy mineral laminations.
 - Subfacies 2, 121–75 cm: Planar stratified, fine to medium sand with laminations heavy minerals and shelly, slightly coarser sand. Possibly two sequences of fining upward. Planar heavy mineral laminations are most distinct in uppermost bed of unit.
 - Subfacies 3, 75–34 cm: Generally massive, well sorted, fine to medium sand with faint, discontinuous heavy mineral laminations. Bioturbated.
 - Subfacies 4, 34–TOP: Massive, v. well sorted, fine sand. Bioturbated. Darker than underlying unit. Plant stains and mottling apparent in the upper half of unit.

Interpretation:

Sbf 1: Aeolian or lower energy overwash? Physical processes dominate.

Sbf 2: Overwash with variable energy and possible periods of aeolian reworking/bioturbation. Physical processes dominate.

Sbf 3: Aeolian, or lower energy overwash with aeolian reworking/bioturbation? Biological processes dominate.

Sbf 4: Bioturbated aeolian. Biological processes dominate.



HI B-2010-3

Coordinates (UTM 18N NAD83): N 4138571, E 437457

Total length (cm): 155
Compaction (cm): 41
Auger (cm): 50
Total Depth (cm): 246

- **Facies 1, BTM–126 cm:** Grey, generally massive, well sorted fine sand with faint planar mineral laminations and two thin organic-rich laminae (rafted organic matter?). Bioturbated, particularly near top of unit.
 - Gradational, bioturbated contact with Facies 2.
- **Facies 2, 126–70 cm:** Bioturbated silty v. fine sand and mud, with fine plant matter (not clearly in or ex situ).
 - Sharp, clay-rich disconformity with Facies 3.
- **Facies 3, 70 cm–TOP:** Well to v. well sorted fine to medium sand, massive to planar laminated to discontinuous/cross-cut laminated.
 - Subfacies 1, 70–66 cm : Clean, grey, v. well sorted medium sand.
 - Subfacies 2, 66–40 cm: V. well sorted fine sand with faint, discontinuous heavy mineral laminations.
 - Subfacies 3, 40–15 cm: Well sorted, fine to medium sand with planar to wavy, cross-cutting heavy mineral laminations. Comparatively high percentages of quartz frosting.
 - Subfacies 4, 15 cm–TOP: Massive, bioturbated, well sorted fine to medium sand with organic matter near top of unit. Comparatively high percentages of quartz frosting.

Interpretation:

Facies 1: Overwash with reworked surface. Physical processes dominate.

Facies 2: Low energy period (high/low marsh, swale, or intertidal environment)

Facies 3:

Sbf 1. Overwash. Physical processes dominate.

Sbf 2. Aeolian or lower energy overwash? Physical processes dominate.

Sbf 3. Aeolian, with possible reworked overwash at the border with Sbf 2?
Physical processes dominate.

Sbf 4. Bioturbated aeolian. Biological processes dominate.



HI C-2010-1

Coordinates (UTM 18N NAD83): N 4139665, E 438045

Total length (cm): 407.5
Compaction (cm): 133
Auger (cm): 0
Total Depth (cm): 540.5

- **Facies 1, BTM to 296 cm:** V. dark grey, laminated to subtly bioturbated mud with few gastropod shells.
 - Sharp disconformity with Facies 2.
- **Facies 2, 296–137 cm:** Planar stratified to massive, v. well sorted, fine to medium sand.
 - Subfacies 1, 296–172 cm: V. well sorted, fine to medium sand with heavy mineral laminations, either planar with subtle bioturbation causing irregularity/discontinuity, or possible cross-cutting/wavy.
 - Subfacies 2, 172–137 cm: Bioturbated, fine sand with increasing mud, rooting, bioturbation and organic material up unit.
 - Gradational, bioturbated contact with Facies 3.
- **Facies 3, 137–126 cm:** V. dark grey to grey, bioturbated (large, possible crab burrows), in situ rooted, muddy fine sand to sandy mud. Mud and organics increase up unit, with an especially mud-rich layer occurring at the top of the unit.
 - Top of unit is possible paleosol.
 - Sharp disconformity with Facies 3 (truncation surface topped with dense heavy mineral layer).
- **Facies 4, 126 cm–TOP:** Fine to medium, well sorted to v. well sorted, planar stratified (lower) to bioturbated (upper) sand.
 - Subfacies 1, 126–114 cm: Fine to medium sand with dense heavy mineral layer at the base (truncation surface) and heavy min concentration (energy level) decreasing up unit.
 - Subfacies 2, 114–87 cm: Fine to medium sand with large shell fragment layer (possible lag deposit?) at the base of the unit, planar heavy mineral laminated, with heavy mineral concentration increasing up unit (new pulse of energy also decreasing upward)
 - Subfacies 3, 87–64 cm: V. well sorted fine sand with large shell fragment layer at the base (possible lag deposit?), topped by massive sand with some rooting, fining upward (energy level decreasing upward).
 - Subfacies 4, 64 cm–TOP: Bioturbated, mottled, massive, v. well sorted, fine to medium sand with rooting and organic (unlayered) material increasing up unit.

Interpretation:

Facies 1. Estuarine/mudflat.

Facies 2. Overwash or beach, with possible aeolian reworking/bioturbation, particularly towards the top of the unit. Physical processes dominate.

Facies 3. Lower energy period (high/low marsh or intertidal mud flat). Biological processes dominate.

Facies 4:

Sbf 1–3: Three pulses of overwash, with aeolian reworking and/or bioturbation at the top of the third. Physical processes dominate.

Sbf 4: Bioturbated aeolian. Biological processes dominate.

***Sequence of facies strongly resembles sequence of facies in HI X-2010-1, but with thicker sand units (expected based on this core's more central position in the Ash Wednesday storm overwash).



HI X-2010-1

Coordinates (UTM 18N NAD83): N 4138998, E 437586

Total length (cm): 601
Compaction (cm): 61
Auger (cm): 0
Total Depth (cm): 662

- **Facies 1, BTM–220 cm:** V. fine sandy mud to mud with gastropod shells.
 - Sandy laminae between 224-231cm.
 - Gradational contact with Facies 2.
- **Facies 2, 220–154 cm:** Mud with minor bioturbation and organic rootlets (not in situ?).
 - Sharp disconformity with Facies 3.
- **Facies 3, 154–91cm:** V. well sorted fine to medium sand with faint heavy mineral planar laminations, clean at the bottom and grading into more organic-rich material.
 - Subfacies 1: Clean, planar laminated fine to medium sand; gradational contact with Sbf 2.
 - Subfacies 2: Bioturbated sand with rootlets and organics increasing up-core.
- **Facies 4, 91–51 cm:** Bioturbated, organic-rich, rooted, muddy fine sand with chunks of rafted(?) woody organics between 80–90 cm.
 - Vertical, in situ rooting, particularly at the top of the unit.
 - Sharp paleosol? contact with Facies 5.
- **Facies 5, 51–4 cm:** Massive to planar laminated, v. well sorted fine to medium sand.
 - Subfacies 1, 51–44 cm: Massive, cleaner, finer sand.
 - Subfacies 2, 44–27 cm: Massive, fine to medium sand with rooting and plant debris.
 - Subfacies 3, 27–10 cm: Planar and cross-cutting heavy mineral laminations in fine to medium sand with rootlets, plant debris, plant stains.
 - Subfacies 4, 10–4 cm: Bioturbated, organic-rich sand with rooting (directly underlies modern soil layer).
 - Energy levels change throughout.
 - Sharp contact with overlying layer.
- **Facies 6, 4 cm–TOP:** Black to v. dark brown, organic rich modern soil with rooting.

Interpretation:

Facies 1: Estuarine.

Facies 2: Marsh or mudflat.

Facies 3:

Sbf 1: Beach or overwash? Possible aeolian reworking? Physical processes dominate.

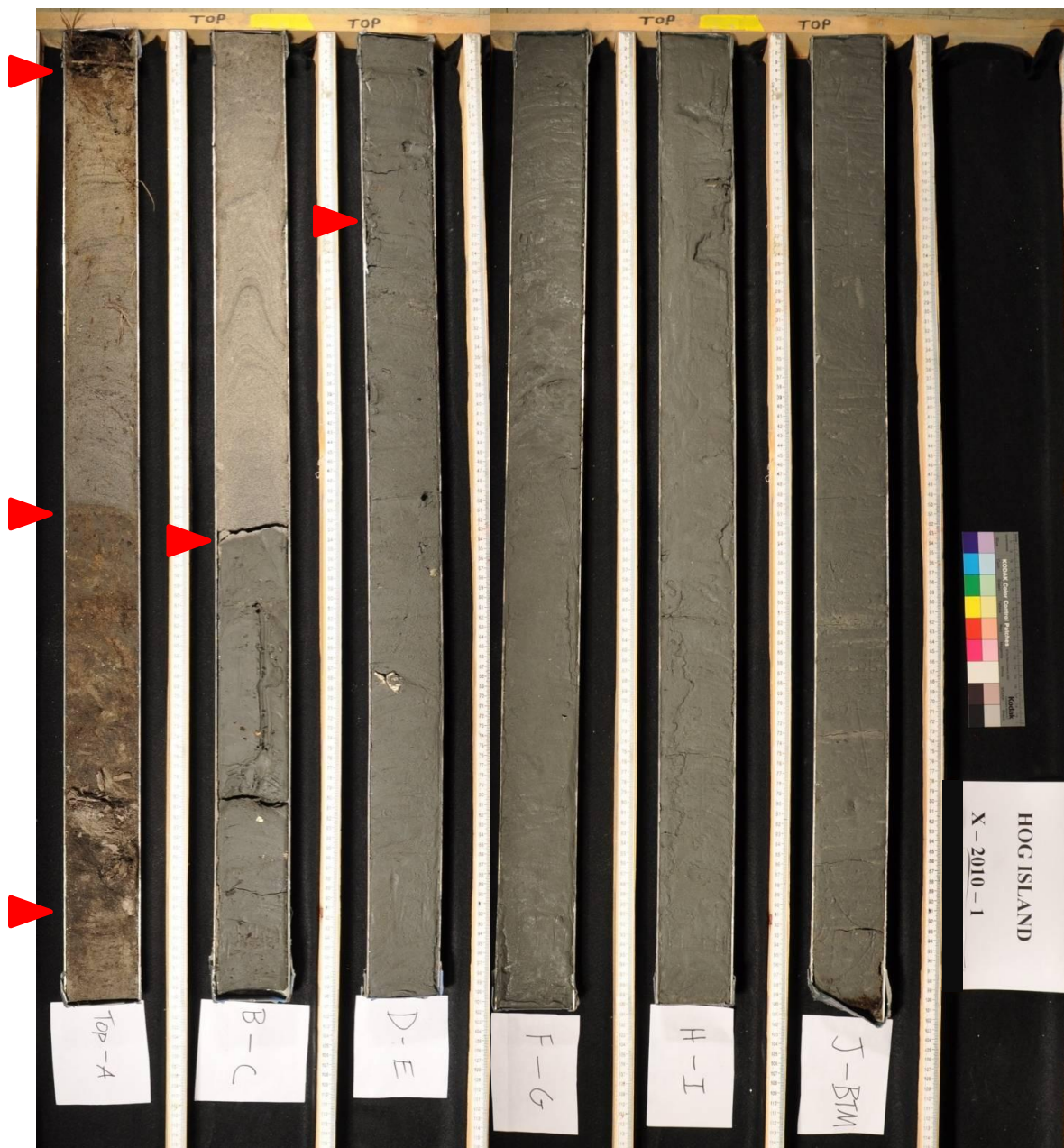
Sbf 2: Possible aeolian/upland? Lower energy level/sedimentation rates than Sbf 1. Biological processes dominate.

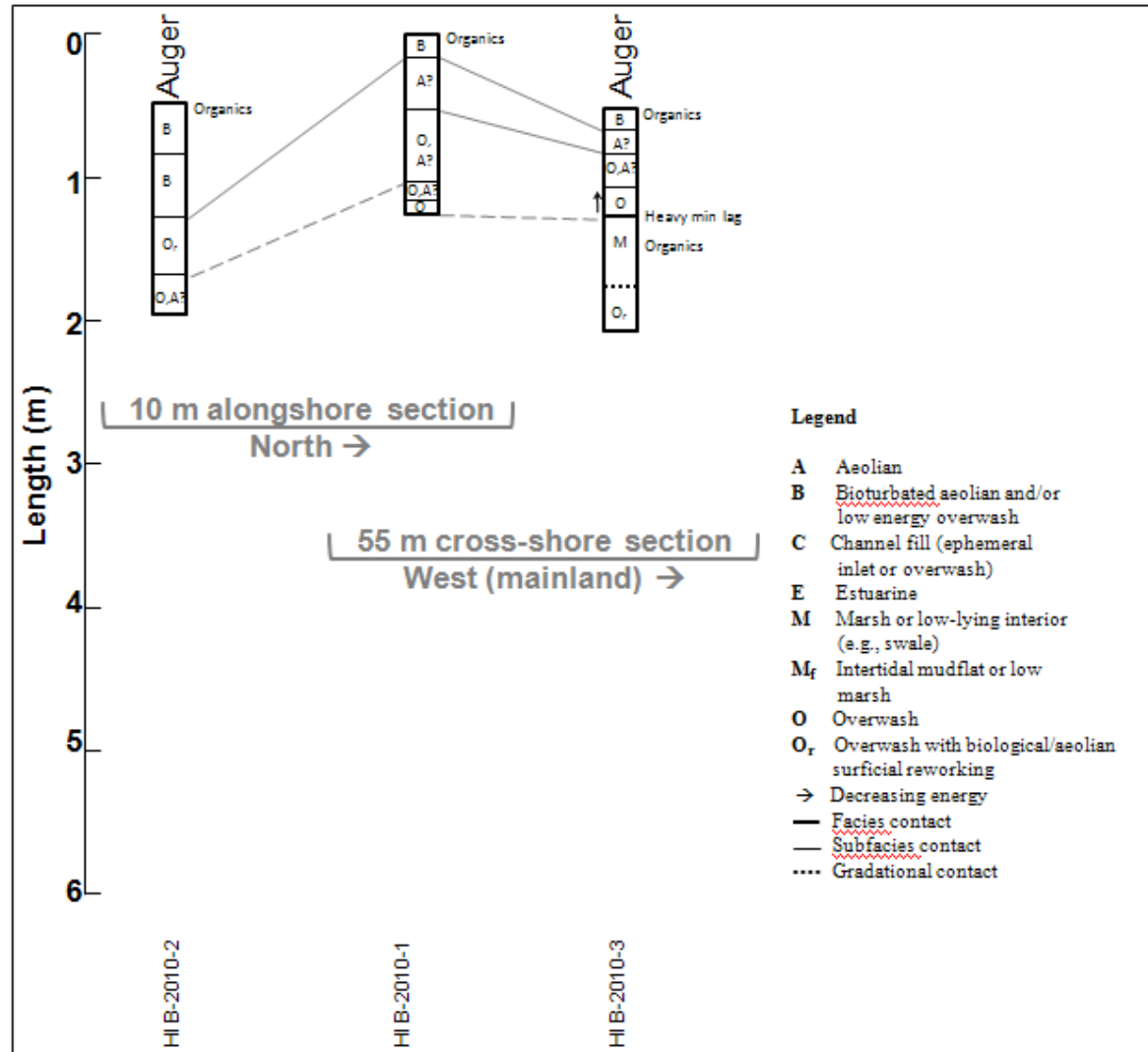
Facies 4: High marsh, shrub thicket, swale. Biological processes dominate.

Facies 5: Overwash intermingled with aeolian deposition and/or biological reworking?

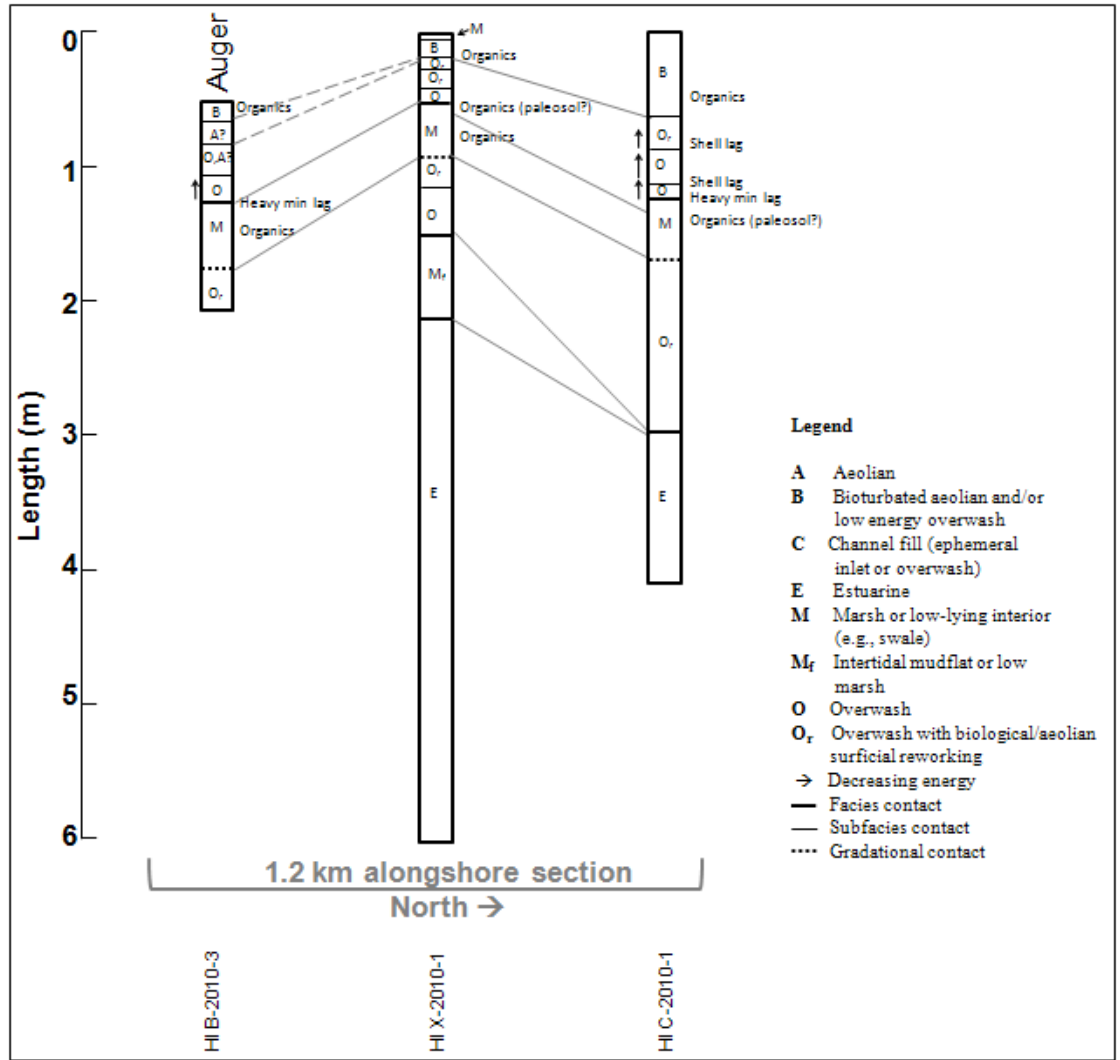
Overall pattern of overwash recovering into stable interior due to island rotation/shoreline accretion? Physical and biological processes both important.

Facies 6: Modern soil. Biological processes dominate.





Interpretation and stratigraphic correlation of adjacent cross- and alongshore sections on southern Hog Island. Lengths are not corrected for compaction.



Interpretation and stratigraphic correlation of an alongshore section on southern Hog Island. Lengths are not corrected for compaction.

Metompkin Island

MI C-2010-1

Coordinates (UTM 18N NAD83): N 4174157, E 449250

Total length (cm): 160
Compaction (cm): 199
Auger (cm): 0
Total Depth (cm): 359

- **Facies 1, BTM–133 cm:** Interlaminated mud, fine sandy/silty mud, and fine to medium sand with organic matter near the top of the unit.
 - Subfacies 1, BTM–137 cm: Interlaminated fine sandy/silty mud (clay drapes?) and fine to medium sand, with bioturbation increasing up-unit.
 - Subfacies 2, 137–133 cm: Grey, bioturbated, v. fine sandy/silty mud, with rooting and/or floated organic matter.
- Sharp disconformity with Facies 2.
- **Facies 2, 133 cm–TOP:** Well sorted, planar laminated to cross-cut laminated, fine to medium sand with large shells.
 - Subfacies 1, 133–120 cm: Grey, planar laminated, fine to medium sand with heavy mineral concentration at truncational surface.
 - Subfacies 2, 120–100 cm: Base is shells resting on/nestled into grey sands of Sbf 1. Grayish brown, planar laminated (thin, regular heavy mineral lams), fine to medium sand with large shell fragments throughout. Shell at top of unit = possible aeolian lag?
 - Subfacies 3, 100–40 cm: Light yellowish brown to grayish brown, moderately well sorted, fine to coarse sand with sometimes cross-cutting and discontinuous heavy mineral laminations of variable spacing and thickness (“Bengal tiger” pattern). Comparatively high percentages of quartz frosting. Brown organic matter at base of unit indicates a possible paleosol.
 - Subfacies 4, 40 cm–TOP: Bioturbated, massive, moderately well sorted, fine to coarse sand (fine to medium near top of unit) with rooting and plant debris. Organic matter appears to increase up-unit. One shell fragment near top of unit.

Interpretation:

Facies 1. Estuarine to marsh/mudflat.

Facies 2.

Sbf 1–2: Two pulses of overwash. Physical processes dominate.

Sbf 3: Aeolian deposition? A quiet, subaerial period may have led to the likely paleosol (possibly correlated with uppermost possible paleosol in MI C-2010-2 Facies 4_1), subsequently covered by aeolian deposits. Physical and biological processes both important.

Sbf 4: Bioturbated, aeolian or possible small-scale overwash. Physical processes dominate.



Top-A

B-BTM

METOMPKIN
ISLAND
C-2010-1



MI C-2010-2

Coordinates (UTM 18N NAD83): N 4174164, E 449406

Total length (cm): 265
Compaction (cm): 183
Auger (cm): 0
Total Depth (cm): 448

- **Facies 1, BTM–194 cm:** Mud to v. fine sandy mud to v. fine sand.
 - Subfacies 1, BTM–248 cm: Interbedded v. well sorted v. fine sand and v. fine sandy/silty mud.
 - Subfacies 2, 248–193 cm: Mud (mostly clay with subordinate silt).
 - Sharp disconformity with Facies 2.
- **Facies 2, 194–114 cm:** Medium to coarse sand with coarse shells and shell fragments
 - Subfacies 1, 194–148 cm: Medium to coarse sand with planar heavy mineral laminations.
 - Subfacies 2, 148–114 cm: Base is a coarse shell lag layer. Massive, medium to coarse sand with shell hash and large shell fragments throughout.
 - Gradational (bioturbated) contact with Facies 3.
- **Facies 3, 114–89 cm:** Muddy v. fine sand/silt with plant debris and rooting
 - Subfacies 1, 112–98 cm: Muddy v. fine sand/silt.
 - Subfacies 2, 98–89 cm: Mud and muddy v. fine sand/silt, bioturbated with roots and topped by a likely paleosol.
 - Sharp contact at the likely paleosol with Facies 4.
- **Facies 4, 89 cm–TOP:** Planar laminated medium to fine sand with heavy mineral laminations.
 - Subfacies 1, 89–61 cm: Planar laminated medium to fine sand with heavy mineral and organic laminations, plant debris and rooting. Possible organic rich paleosols throughout, including at the top of the subfacies.
 - Subfacies 61 cm–TOP: Moderately well to well sorted, fine to medium to lower coarse sand with heavy mineral laminations experiencing varying degrees of core-induced convolution and deformation. Faint organic layer at 2 cm. Alternation between heavy min lamination rich, coarser, moderately well-sorted sections (2) and finer, better sorted, non-laminated sections (2). Vague “Bengal tiger” appearance (core water deformation obscuring true appearance). Top 20 cm bioturbated.

Interpretation:

Facies 1: Estuarine with some storm beds and/or intertidal periods

Facies 2: High energy event: overwash or ephemeral inlet surge channel deposits?

Physical processes dominate.

Sbf 1: Sheet overwash reaching lagoon.

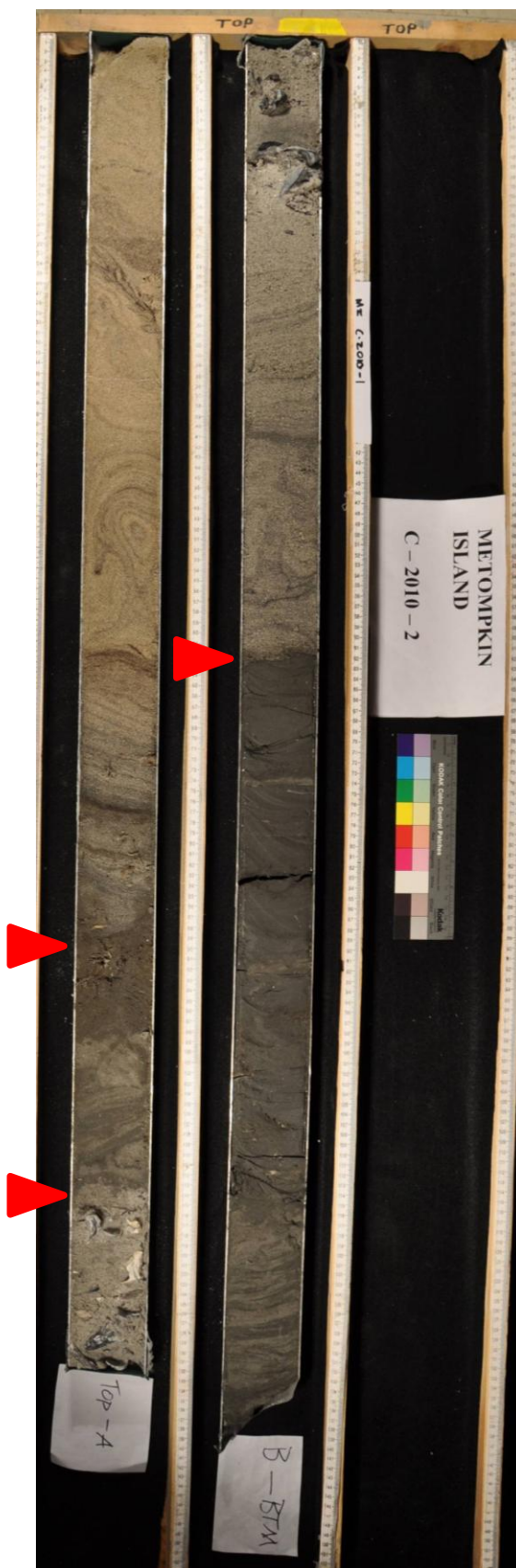
Sbf 2: Channel lag and infill.

Facies 3: Lower energy environment, allowing plant colonization, organic matter enrichment, bioturbation, and possible paleosol development—high/low marsh.

Facies 4:

Sbf 1: Transition from Facies 3 (truncated by higher flow regime); two overwash events (with slight aeolian reworking?), but with slow enough sedimentation rates that biological processes are evident, allowing plant colonization and possibly immature soil development.

Sbf 2: Overwash with aeolian reworking near the surface and/or between overwash deposits? Aeolian throughout? Physical processes dominate until upper 20 cm.



MI C-2010-3

Coordinates (UTM 18N NAD83): N 4174144, E 449442

Total length (cm): 132
Compaction (cm): 127
Auger (cm): 123
Total Depth (cm): 382

- **Facies 1, BTM–78 cm:** Interlaminated mud, fine sandy/silty mud, and fine to medium sand with organic matter near the top of the unit.
 - Subfacies 1, BTM–91 cm: Interlaminated fine sandy/silty mud (clay drapes?) and fine to medium sand, with bioturbation increasing up-unit
 - Subfacies 2, 91–78 cm: Grey bioturbated v. fine sandy/silty mud, with overlying fine sandy and muddy layers, including a possible rafted organic layer at 78–80 cm.
 - Sharp disconformity with Facies 2.
- **Facies 2, 78 cm–TOP:** Fine to medium sand and shell fragments.
 - Subfacies 1, 75–61 cm: Grey, massive to planar laminated, fine to medium sand with a piece of wrack near the top and a few muddy laminae near the bottom. Heavy mineral concentration at the truncational surface (underlying the muddy laminae).
 - Subfacies 2, 61–25 cm: Base is shell resting on clay and organic rich laminae surface (possible paleosol, or eroded clay drape?) which also appears to warp upward around shell. Greyish brown, massive, fine to medium sand with large shell fragments throughout.
 - Subfacies 3, 25 cm–TOP: Massive, fine to medium to lower coarse sand with sand- to granule-sized shell bits. Bioturbated.

Interpretation:

Facies 1:

Sbf 1: Estuarine with storm deposits, or intertidal mud flat.

Sbf 2: Intertidal mudflat. Muddy laminae at the top correlate in depth to a possible paleosol in MI C-2010-2, Facies 3_2.

Facies 2:

Sbf 1: Overwash (distal sheet?). Physical processes dominate.

Sbf 2: Higher energy overwash. Possible paleosol may correlate with lower possible paleosol in MI C-2010-2 Facies 4_1. Basal shell may represent hydraulic lag on the truncation surface. Physical processes dominate.

Sbf 3: Aeolian and/or biological reworking of overwash in Sbf 2? Lower energy overwash subsequently reworked?

***Upper facies closely resemble upper facies of MI E-2010-1.



MI E-2010-1

 Coordinates (UTM 18N NAD83): N 4179441, E 452144

Total length (cm): 326
Compaction (cm): 33
Auger (cm): 96
Total Depth (cm): 455

- **Facies 1, BTM–180 cm:** massive to finely laminated, bioturbated mud.
 - Gradational contact with Facies 2.
- **Facies 2, 180–110 cm:** Bioturbated (burrowed), rooted, plant debris-rich sand and sandy mud.
 - Sharp contact with Facies 3.
- **Facies 3, 110 cm–TOP:** Planar laminated to massive sand with shells.
 - Subfacies 1, 110 cm–66 cm: Fine to medium, planar laminated sand (heavy mineral laminations).
 - Subfacies 2, 66 cm–26 cm: Fine to medium massive sand matrix with large intact shells distributed throughout.
 - Subfacies 3, 26 cm –TOP: Massive to crudely stratified fine to medium sand with coarse shell hash, bioturbated.

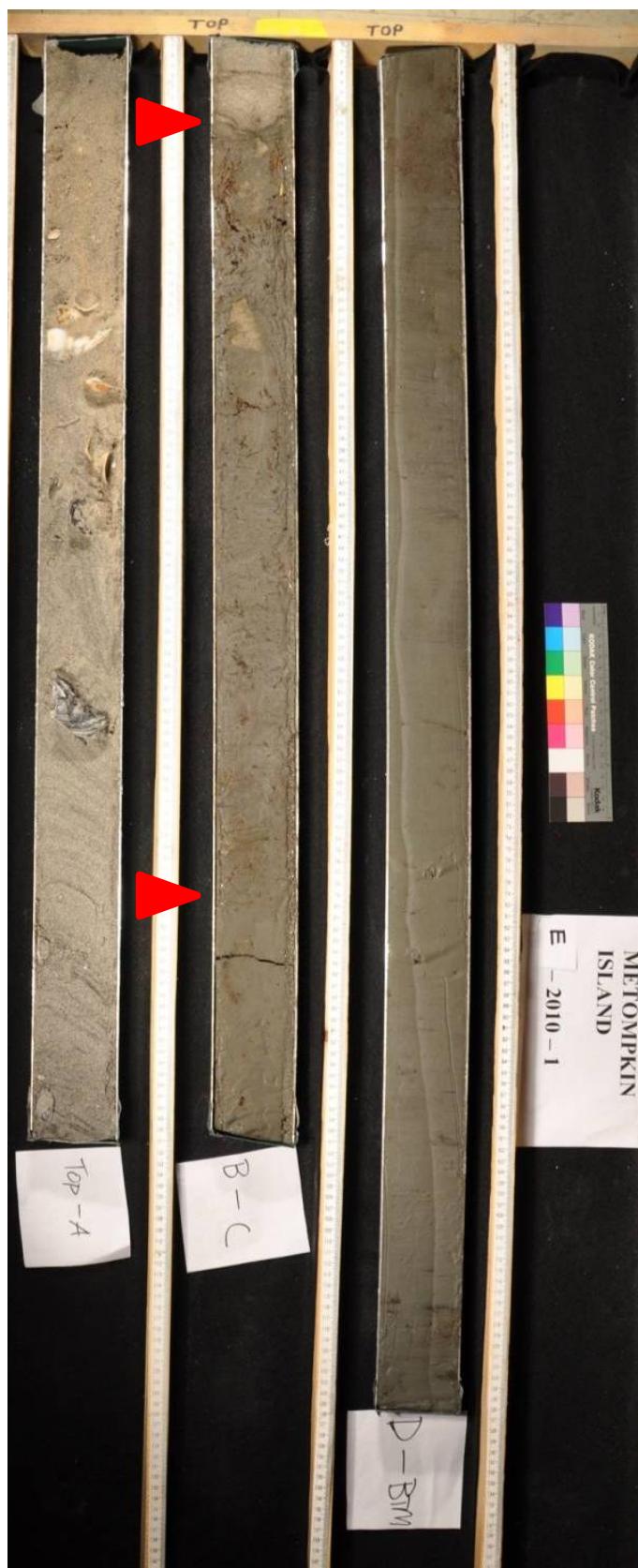
Interpretation:

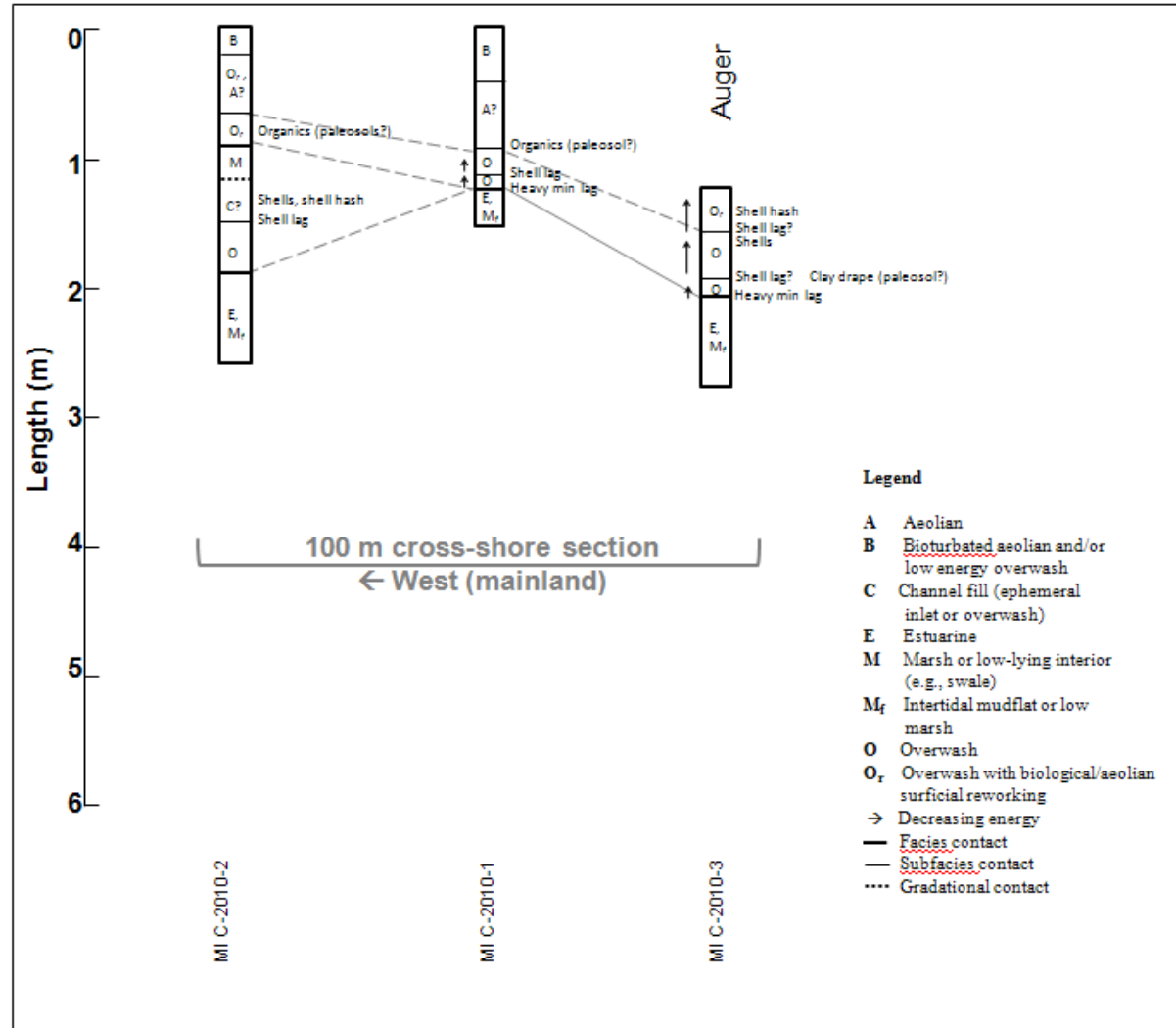
Facies 1. Estuarine.

Facies 2. Marsh or intertidal mudflat with burrowing activity and possibly periodic overwash sand deposition

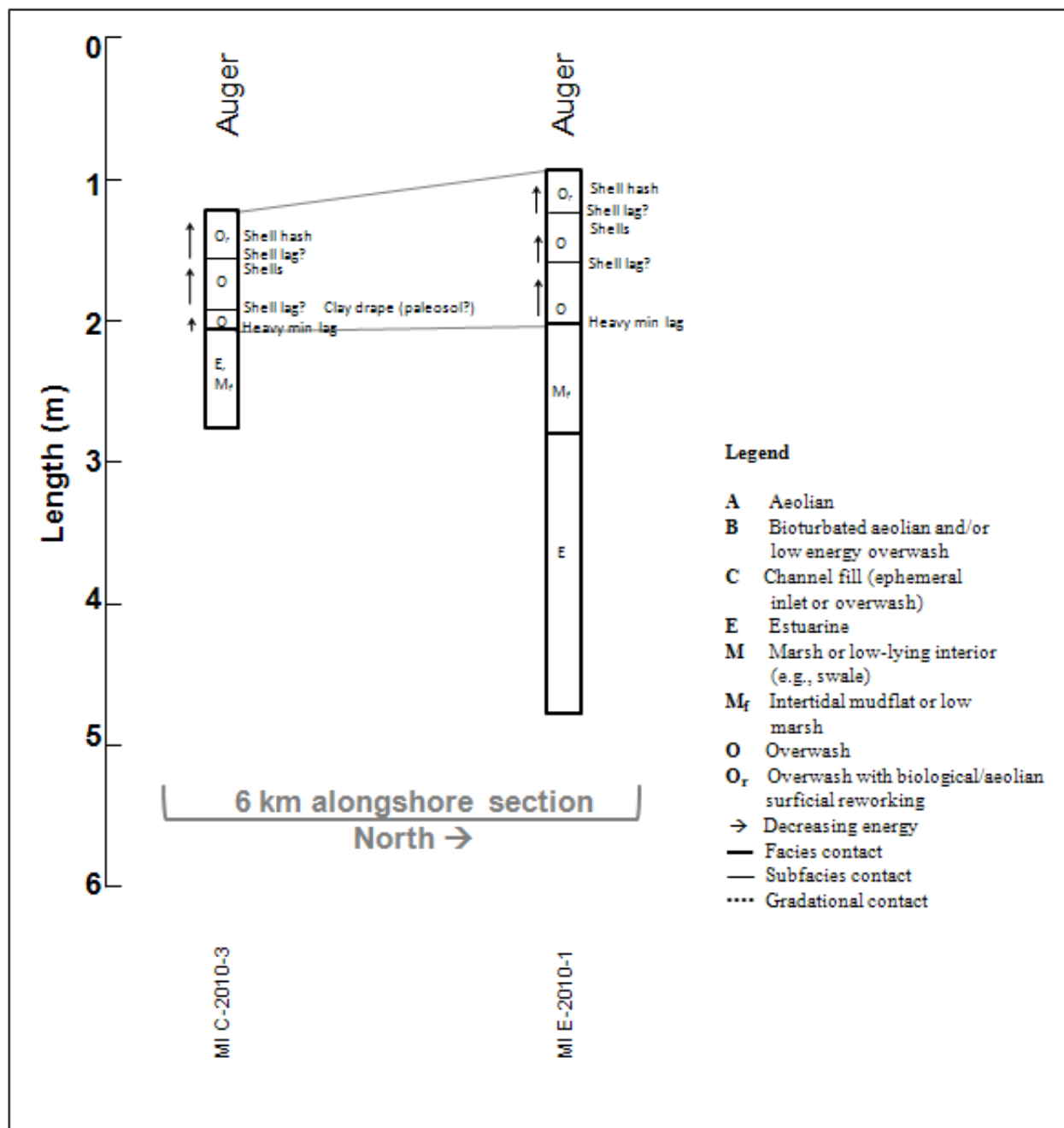
Facies 3. Overwash deposits grading from distal to proximal. Physical processes dominate.

***Entire core coarsens upwards (typical of a transgressive environment).





Interpretation and stratigraphic correlation of a cross-shore section on southern Metompkin Island. Lengths are not corrected for compaction.



Interpretation and stratigraphic correlation of an alongshore section from southern to northern Metompkin Island. Lengths are not corrected for compaction.

